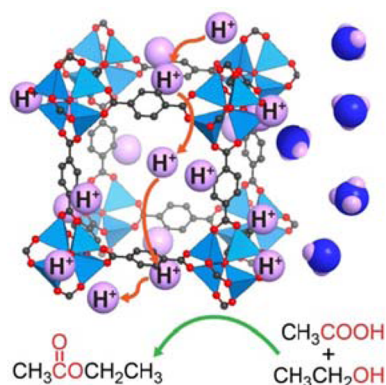


Brønsted Acidity in Metal–Organic Frameworks

Juncong Jiang^{*,†} and Omar M. Yaghi^{*,†,§}[†]Department of Chemistry, University of California—Berkeley, Materials Sciences Division, Lawrence Berkeley National Laboratory, and Kavli Energy NanoSciences Institute at Berkeley, Berkeley, California 94720, United States[§]King Fahd University of Petroleum and Minerals, Dhahran 34464, Saudi Arabia

S Supporting Information



CONTENTS

1. Introduction	6966
2. Preparation Methods	6967
2.1. Encapsulated Brønsted Acid Molecules	6967
2.2. Ligated Brønsted Acid Groups	6969
2.3. Covalently Bound Brønsted Acid Functional Groups of Organic Linking Units	6970
3. Characterization Methods	6973
3.1. Indicators and Titration Methods	6973
3.2. Test Reactions	6974
3.3. Gas Sorption Techniques	6976
3.4. Vibrational Spectroscopy Methods	6977
3.5. Solid-State Nuclear Magnetic Resonance (NMR) Methods	6978
3.6. Diffraction Techniques	6980
4. Applications	6980
4.1. Ammonia Capture	6980
4.2. Proton-Conducting Materials	6982
4.3. Catalysis	6986
5. Summary and Outlook	6989
Associated Content	6990
Supporting Information	6990
Author Information	6990
Corresponding Authors	6990
Notes	6990
Biographies	6990
Acknowledgments	6991
References	6991

1. INTRODUCTION

The past 20 years have witnessed rapid development of reticular chemistry,^{1,2} which is concerned with linking molecular building units with strong chemical bonds to form crystalline, extended structures. Joining metal-containing secondary building units (SBUs) with organic linkers using the principles of reticular chemistry has led to an extensive class of metal–organic frameworks (MOFs).^{3,4} Four distinct features figure prominently in MOF materials: (i) exceptional porosity and tunable pore size have led to a large variety and diversity of porous structures;⁵ (ii) structure design is achieved by consideration of preferred topologies and thus the most likely structures to result from the MOF synthesis;^{6,7} (iii) postsynthetic modification (PSM)^{8–10} has proven to be a powerful tool for altering the accessibility and reactivity of the pore interior, as well as changing the electronic and steric character of the active sites; and (iv) multivariate (MTV) functionalization,^{11,12} where multiple metals and/or organic linkers are incorporated within the MOF backbone while the original structure is retained, has made possible functional sites of different distribution within the pores. These unique aspects have contributed to the extensive study of MOFs in many fields of application, including catalysis,^{13–17} gas adsorption and separation,^{18–25} and energy storage devices.^{26–28}

Given such flexibility in MOF chemistry, it was, indeed, only a matter of time before the first example of a Lewis acidic MOF was reported for catalyzing the cyanosilylation reaction of aldehydes.²⁹ In successive years, coordinative unsaturation or open metal sites³⁰ on metal SBUs were made and found to be suitable as Lewis acid sites. In this case, several coordination positions of the metal center are occupied by solvent molecules, which can be removed by heating or evacuation during the activation process without framework collapse. In this group of MOFs, the metal center simultaneously acts as a structural building unit and a Lewis acid site for use as a catalytic site. Two examples involving HKUST-1 [$\text{Cu}_3(\text{BTC})_2$; BTC = benzene-1,3,5-tricarboxylate]³¹ and M-MIL-101 [$\text{M}_3\text{X}(\text{H}_2\text{O})_2\text{O}(\text{BDC})_3$; M = Al, Cr, Fe; X = F, OH; BDC = benzene-1,4-dicarboxylate] or functionalized MIL-101^{32–34} were found to be catalytically active in various reactions: aldehyde cyanosilylation,^{35,36} α -pinene oxide isomerization,³⁷ citronellal cyclization,^{37–39} Knoevenagel condensation,^{40,41} and selective oxidation of organic compounds.^{42–44} We note that MOFs without open-metal sites per se can act as Lewis acids because of accessibility to metal centers

Received: April 13, 2015

Published: June 19, 2015

within the SBUs. Several reviews on this property of MOFs are available in the literature.^{13–17,45,46}

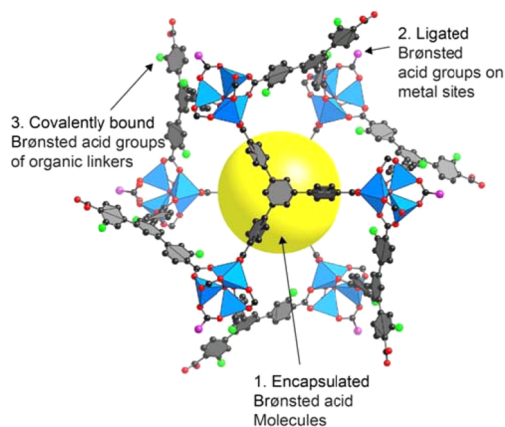
Compared to the relatively large body of work done on the Lewis acidic MOFs, Brønsted acid chemistry in MOFs is just beginning to emerge. This is mainly due to the combination of two factors: (i) the MOF has to withstand acidity up to and higher than that of sulfuric acid. Introduction of such acidic sites by either one-pot synthesis or postsynthetic modification is generally very difficult, because the activated acidic protons interfere with either the making or the stability of the framework, and (ii) there is an intrinsic difficulty in characterizing Brønsted acidity in many solid acids because of the inhomogeneity of acidic sites and the lack of an acid–base equilibrium state.^{47,48}

However, the molecular and well-defined nature of MOFs have brought new perspectives and opportunities for addressing these issues: the concept of heterogeneity within order,⁴⁹ the approaches of PSM^{8–10,50,51} and MTV,^{11,12} and MOFs' well-defined structure and functionality have led to progress in incorporating and understanding Brønsted acidity in MOFs. In this contribution, we provide a comprehensive review of MOF Brønsted acids, including their superacidity. We cover the different approaches used to introduce Brønsted acidity into MOF, with special focus on the design, synthesis, and characterization methods, keeping in mind the current opportunities and challenges in MOF-based solid acids. In addition, examples of potentially promising applications, including gas adsorption–separation, catalysis, and energy storage devices, are presented.

2. PREPARATION METHODS

As shown in Scheme 1, many methods for the preparation of Brønsted acidic MOFs have been reported. They can be classified

Scheme 1. Various Brønsted Acid Sites in MOFs



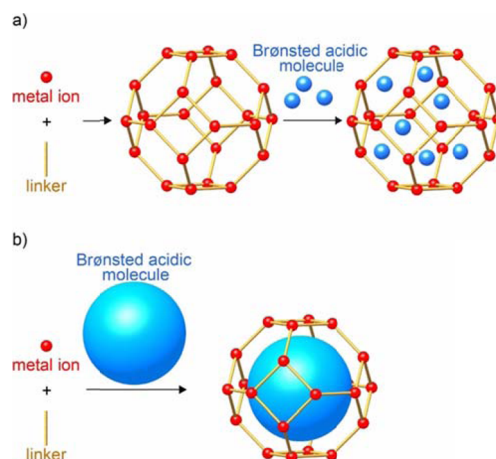
into three categories: (i) encapsulated Brønsted acid molecules within the MOF pores, (ii) ligated Brønsted acid groups onto metal sites of SBUs, and (iii) covalently bound Brønsted acid functional groups of organic linking units. In this section, specific examples are given for each of these categories.

2.1. Encapsulated Brønsted Acid Molecules

In this category, the Brønsted acidic guest molecules are included within the pores of MOFs, where they are interacting with the interior through weak intermolecular forces.

This can be done with a two-step synthesis approach (Scheme 2a). In the first step, the MOF is prepared, followed by the second step of impregnation of guest molecules into the MOF

Scheme 2. Schematic Illustration of Encapsulation of Brønsted Acidic Molecules within MOF: (a) Two-Step Method^a and (b) One-Step Method^b



^aIn the two-step method, Brønsted acidic molecules (blue spheres) are diffused into the pore after the MOF synthesis. ^bIn the one-step method, Brønsted acidic molecules (blue sphere) are encapsulated during the MOF synthesis using a mixture of metal ion and the prospective guest molecules.

pores by diffusing the guests into either solvent-filled or evacuated pores. An alternative way is the one-step synthesis (Scheme 2b), in which Brønsted acidic guest molecules are included at the same time when the MOF is formed. Typically, they are obtained from a mixture of the guest molecules and the molecular building units needed for MOF synthesis. The guest molecules can be acidified after their inclusion to further increase the amount or strength of their Brønsted acidity. This approach enlarges the scope of Brønsted acidic guest molecules (e.g., polyoxometalates, POMs), which will not pass through the narrow pore opening when using an impregnation method.⁵² Furthermore, large molecules included this way are less likely to leach out, resembling the “ship-in-a-bottle” approach. First introduced in the field of zeolite catalysis,⁵³ this term refers to encapsulated catalytic molecules larger than the pore aperture of the zeolite. This means that the molecules should be free to move around within the confinement of the cavities but prevented from leaching by restrictive pore openings. Hereafter, Brønsted acidic guest molecules included this way are noted as “encapsulated” molecules, to show the difference from “impregnated” molecules using the two-step approach.

In solution, the facile diffusion of small Brønsted acidic molecules in and out of MOF pores was reported using nonvolatile H_2SO_4 and H_3PO_4 as guests in MIL-101.⁵⁴ This was done by mixing the MIL-101 solid with a ca. 2.5 M acid aqueous solution followed by filtration and drying at 200 °C. The inclusion of acids is completed within 30 min, and not surprisingly, removal of 90% of the included acid could be done by washing with water for 10 min. It is worth noting that although the powder X-ray diffraction (XRD) patterns of the acid-impregnated samples showed no diffraction peaks in the low-angle region ($2\theta < 7^\circ$), they can be fully restored after washing away the acids in the pore, confirming the structural integrity of the MOF and that H_2SO_4 and H_3PO_4 are only impregnated guest molecules.

This facile diffusion of guest molecules that are solids at ambient temperature and pressure could also be achieved under

increased temperature and pressure. The Brønsted acidic CsHSO₄ was observed to penetrate into pores and fill the cavities of MIL-101 at 200–210 °C and 300–500 MPa for 10–20 min, conditions close to the melting point of CsHSO₄.⁵⁵

Another large group of Brønsted acidic guests to be incorporated into MOF pores are the POMs. When protonated, POMs with strong Brønsted acidity show promise as solid-acid catalysts for many acid-catalyzed organic transformations and industrial applications, such as the hydration of alkenes, esterification, and alkylation.^{56–58} However, when applying the aforementioned two-step diffusion method to POMs, due to their large molecular dimension (nanometer range), which exceeds the pore openings in normal MOFs, it is challenging to effectively utilize the high surface area MOF and thus to increase the loading of impregnated POMs without reducing the crystallinity or blocking the pores of the MOFs. Furthermore, when designing heterogeneous catalysts, reducing the catalyst leaching of impregnated POMs is another challenge to be seriously considered.

In MOFs, encapsulation of POMs was reported as early as 1999⁵⁹ and recently reviewed by several groups.^{60,61} The first example of a potentially Brønsted acidic proton in POM-encapsulated MOFs was reported 7 years later in a single crystal of [Co₄(DPDO)₁₂][H(H₂O)₂₇(CH₃CN)₁₂][PW₁₂O₄₀] (DPDO = 4,4'-bipyridine-*N,N'*-dioxide), in the form of protonated water cluster H⁺(H₂O)₂₇ to reach charge neutralization.⁶²

In 2009, the presence of acidic protons in POM-encapsulated HKUST-1 was reported for NENU-3a, [Cu₁₂(BTC)₈]-[H₃PW₁₂O₄₀] (Figure 1).⁶³ Here, Keggin-type POM-encapsu-

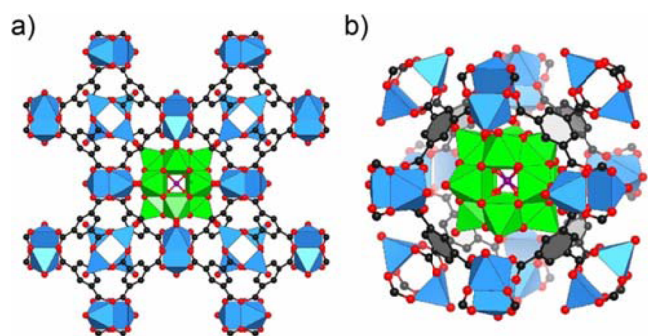


Figure 1. Crystal structure of NENU-3a: (a) a cube of five truncated-octahedral cages sharing square faces and (b) the pore accommodating the PW₁₂O₄₀³⁻ Keggin polyanion. Atom labeling scheme: Cu₂ paddlewheel cluster, blue polyhedra; W, green polyhedra; P, violet; C, black; and O, red. All H atoms are omitted for clarity.

lated HKUST-1 was first collected from a one-pot reaction of copper nitrate, H₃BTC, phosphotungstic acid (PTA, H₃PW₁₂O₄₀·*n*H₂O), (CH₃)₄NOH, and water, followed by heating at 200 °C under vacuum to remove all the water and ammonium ions, leaving behind acidic protons believed to be located on the PW₁₂O₄₀³⁻ anion. With the unequivocal confirmation of POMs encapsulated in the pores from single crystal XRD experiments, it is worth noting that no POM leaching was observed in the reaction solution after catalysis, demonstrating the successful application of the “ship-in-a-bottle” approach to confine large Brønsted acidic molecules inside MOF pores.

Similarly, Brønsted acidic POM-encapsulated MIL-101 was reported using the one-pot synthesis method.⁶⁴ It is worth noting that structural changes of POMs were observed during the

encapsulation process with Cr(III) substituting for one of the WO₆ units to form lacunary sites. Despite of the structural change, the partial integrity of the initial Brønsted acidic POM remained. Through analysis of nitrogen sorption isotherms measured at 77 K, it was shown that the distribution of included POMs in MIL-101 materials is highly dependent on the preparation methods: when the two-step method was used, only a small portion of the large cavities of MIL-101 (Figure 2a)

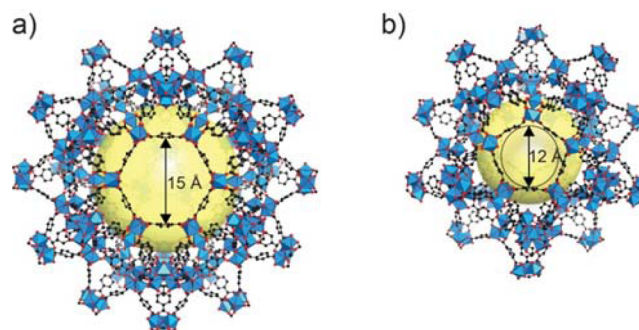


Figure 2. Two different pores in MIL-101: (a) the large pore (yellow sphere) with a hexagonal window of 15 Å in diameter and (b) the medium-size pore (yellow sphere) with a pentagonal window of 12 Å in diameter. Atom labeling scheme: Cr, blue polyhedra; C, black; and O, red. All H atoms are omitted for clarity.

was occupied by POM molecules, while the medium-sized pores (Figure 2b), which represent 60% of the total amount of pores, were not occupied due to a smaller pore opening than the size of the Keggin-type POM. Instead, blockage of the pore openings was observed. This indicates that a considerable number of molecules in these POM-impregnated MIL-101 samples are actually resting on the outside surface of the MOF crystals instead of being included within the pores. Alternatively, when the one-step method was used, better-dispersed POM moieties and catalytic activity were obtained in these POM-encapsulated MIL-101 samples. They were measured to have a nitrogen sorption isotherm similar to that of the pristine MIL-101 with all three steps observed in the profiles. This indicates a more even distribution of POMs in both the medium and the large cavities in MIL-101, with no significant blockage of the pore openings. Similar observations were also reported in MIL-100,^{65–67} indicating that the one-step encapsulation method could be the preferable method for the introduction of Brønsted acidic POM units into MOF pores in various systems.

The acidity of the POM-encapsulated MOF could be further strengthened through its reaction postsynthetically with a second kind of Brønsted acidic moiety.⁶⁸ Typically, PTA-encapsulated MIL-100, H₃PW₁₂O₄₀@MIL-100, was immersed in an ethanol solution of the ionic liquid 1-(propyl-3-sulfonate)imidazolium hydrogen sulfate {[SO₃H(CH₂)₃HIM][HSO₄]}⁻, where anion exchange took place to form [SO₃H(CH₂)₃HIM]₃PW₁₂O₄₀@MIL-100. A stronger catalytic activity of the latter in an acid-catalyzed reaction indicates that the sulfonic group in the ionic liquid cation either provided more Brønsted acidic sites or enhanced the acid strength. No leaching of ionic liquid or PTA was observed in the reaction solution.

We note here that despite of the growing number of reports on Brønsted acidic POM-encapsulated MOF materials and their catalytic performances, the interactions between POMs (especially those acidic protons) and the framework both during the synthesis and after the material activation remain unexplored.

A systematic characterization on the strength and environment of those protons will be valuable to understand, optimize, and exploit fully the potential of these materials.

2.2. Ligated Brønsted Acid Groups

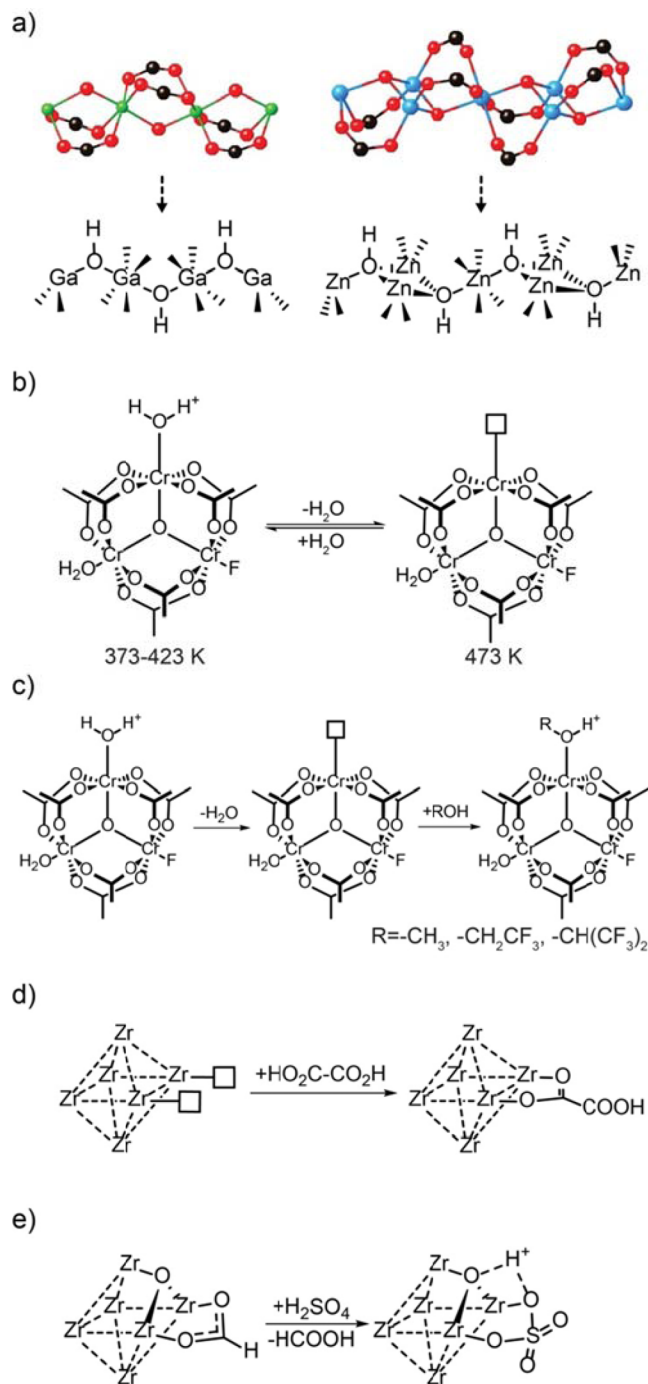
Brønsted acidity is found in ligands such as hydroxyl, water, alcohols, oxalic acid, and sulfuric acid when they are directly bound to metal sites (Scheme 3).

Hydroxyl-based Brønsted acidity in MOF systems is inspired by acidified zeolites in which hydroxyl groups bridge silicon and aluminum atoms.⁶⁹ MOFs with hydroxyl groups are known in which the hydroxyl groups are found bridging two or more metal ions in the SBU. For example, in MIL-53(Ga)⁷⁰ [$\text{Ga}(\mu_2\text{-OH})(\text{BDC})$] (also known as IM-19) and MOF-69C⁷¹ [$\text{Zn}_3(\mu_3\text{-OH})_2(\text{BDC})$], rod-shaped metal oxide units contain bridging hydroxyl groups that exhibit activity toward acid-catalyzed Friedel–Craft alkylation of aromatics.^{72–74} These acidic hydroxyl groups are well-known in MOFs and include SBUs of many metals (e.g., Al,⁷⁵ Cr,³² Cu,⁷⁶ Fe,⁷⁷ In,⁷⁸ Ni,⁷⁹ Sc,⁸⁰ Zn,⁷¹ and Zr⁸¹). However, the acid strength of these hydroxyls depends on the metal they are bound to,^{74,82} and the fact that these hydroxyls are bridging the same kind of metal, generally limits their acidity. A systematic study of mixed-metal MOFs containing several different kinds of metal ions within one SBU⁸³ is highly desirable for developing stronger Brønsted acids based on bridging hydroxyl groups.

Water molecules bound to metal sites could also result in Brønsted acidity, as exemplified by MIL-100.^{84,85} Medium-strength Brønsted acidic sites were located in samples activated at 373–423 K in which water coordinated to the Cr(III) sites that cannot be removed under activation conditions. The hydrogen atoms of these water ligands have stronger Brønsted acidity than noncoordinated water. The activation temperature plays an important role, as the number of water ligands and thus the concentration of Brønsted acid sites varies as guest molecules are removed from the Cr(III) sites at different temperatures. In such a case, as the number of Brønsted acid sites decreases, the number of Lewis acid [Cr(III)] sites increases.

Since the Brønsted acidity is generated from the interaction between a metal ion and a protic solvent ligand, strategies such as increasing the polarizing power of the metal ion and using ligands with stronger initial Brønsted acidity have proved useful. Preliminary results showed a much higher catalytic activity with the Fe(III) form of MIL-100 compared to Cr(III) in Friedel–Craft benzylation.⁸² However, one should be cautious interpreting this result, as Friedel–Craft benzylation is known to be catalyzed also by Lewis acids, especially Al(III) and Fe(III).⁸⁶ Therefore, this result remains inconclusive until it can be confirmed that the active species in the MOF catalysts have acidic protons. On the other hand, the use of protic coordinating ligands to enhance such acidity has been more carefully studied. A series of alcohols (methanol, trifluoroethanol, and hexafluoroisopropanol) with different pK_a values have been introduced to bind to the coordinatively unsaturated Cr(III) sites in MIL-100, and the Brønsted acidity of resulting complexes was measured and compared in the same way that was followed for the water complex.⁸⁷ Alcohol-complexed MIL-100 was prepared by first activating the MOF at 473 K to fully remove the adsorbed water molecules and expose the open chromium sites, followed by introduction of alcohol vapor to form the complex. Similar to the water case, due to the coordination, the hydroxyl groups of the coordinated alcohol are more acidic, as previously shown on BF_3 –alcohol complexes in solution.⁸⁸ As expected,

Scheme 3. Ligated Brønsted Acid Groups:^a (a) Brønsted Acidic Bridging Hydroxyl Groups in MIL-53(Ga) (left) and MOF-69C (right),^b Brønsted Acidity from Water Molecule Bound to Metal Sites in MIL-100, (c) Tuning of Brønsted Acidity through Coordinative Ligand Exchange in MIL-100, (d) Brønsted Acidity Generated through Oxalic Acid Group Bound to Missing Linker Defects in UiO-66, and (e) Sulfation of MOF-808



^aOrganic linkers are omitted for clarity. ^bAtom labeling scheme: Ga, green; Zn, blue; C, black; O, red. All H atoms are omitted for clarity.

(CF₃)₂CHOH coordination induces strong Brønsted acidity comparable to that of the protonated form of zeolite NaY, followed by CF₃CH₂OH, water, and methanol, in the same order of their pK_a values. Undoubtedly, this Lewis to Brønsted acid

approach enables the generation of a series of MOFs with a Brønsted acidity of different strengths. However, several drawbacks intrinsic to this approach could impede its application: (i) the reversible nature of this approach requires mild reaction conditions so as to prevent the dissociation of the Brønsted acidic complex; (ii) excessive amounts of water or alcohol in the system could undermine the Brønsted acidity of the complex by forming hydrogen bonds with the acidic protons, making it necessary to handle them under special conditions; and (iii) often the functioning acidic species is difficult to determine because of the complication involving the reversible conversion between Lewis and Brønsted acidity during the ligation process and the presence of Lewis base impurities and reaction byproducts.

Another approach to introduce Brønsted acidic species onto the metal sites demonstrated recently involves the introduction of acids by postsynthetic substitution of carboxyl units of the SBUs. These carboxyl units could be those from the organic linkers in a MOF crystal, as shown in a zirconium MOF, UiO-66 (Figure 3, left).⁸⁹ This could be achieved by first creating

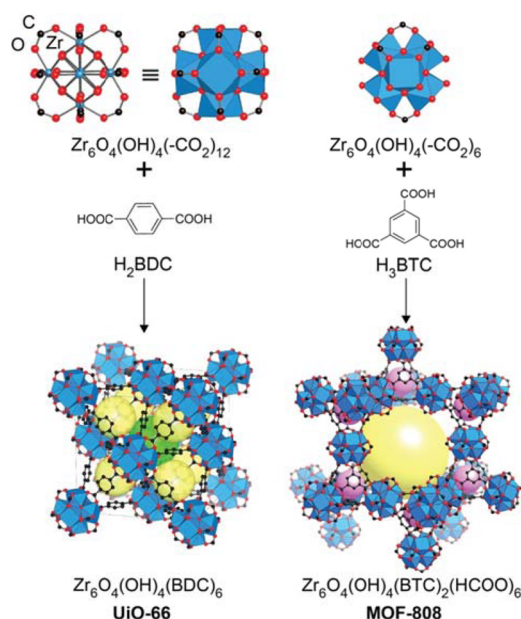


Figure 3. $Zr_6O_4(OH)_4(-CO_2)_n$ secondary building units (SBUs) with 12 and 6 coordination numbers are combined with organic linkers to form UiO-66 and MOF-808. Atom labeling scheme: Zr, blue polyhedra; C, black; O, red. All H atoms are omitted for clarity.

vacancies at metal SBU sites followed by solvent-assisted ligand incorporation. UiO-66 was first produced with missing BDC linkers,⁹⁰ leading to vacancies at the Zr SBUs. An *N,N*-dimethylformamide (DMF) solution of oxalic acid was later introduced, where oxalic acid was found to be bound to the SBUs on those vacant sites. As one carboxylate group from the oxalic acid coordinated to the SBU, the other free carboxylic acid group points inside the MOF's pore, creating a Brønsted acidic pore environment.

Controllable substitution was also reported for another zirconium MOF, MOF-808 (Figure 3)⁹¹ [$Zr_6O_5(OH)_3(BTC)_2(HCOO)_5(H_2O)_2$], with a stronger Brønsted acid, sulfuric acid, resulting in strong Brønsted acidity in sulfated MOF-808 [$Zr_6O_5(OH)_3(BTC)_2(SO_4)_{2.5}(H_2O)_{2.5}$].⁹² Controllable substitution of formates with sulfate groups was achieved by

submersion of MOF-808 in diluted aqueous sulfuric acid (0.005–0.1 M), where the degree of substitution was controlled by adjusting the amount of added sulfuric acid. Interestingly, this gradual sulfation process generates Brønsted acidity in the originally only Lewis acidic MOF-808, and the acid strength increases as more sulfates are incorporated, with the highest value reaching a Hammett acidity function⁹⁶ $H_0 \leq -14$ by Hammett indicator methods, serving as the first evidence of superacidity in MOFs. This strong acidity might be explained by considering the electron-withdrawing effect of the sulfate group, which greatly enhances the Brønsted acidity of the bridging or terminal hydroxyl, and the polarizing effect of the Zr(IV) makes the proton on the sulfate group more acidic.

In this section, we illustrated that bridging hydroxyl groups, protic ligands such as water or alcohols coordinated to the Lewis acidic metal sites, and sulfation of a Zr MOF through terminal ligand exchange are the state-of-the-art approaches for the introduction of Brønsted acidity onto the metal oxide SBUs of MOFs. Unlike previous approaches, where significant pore space is taken up by the large encapsulated POM and counterions, the change of pore volume is often negligible, due to the relatively small size of the protic ligands (i.e., methanol, water, and sulfate) used. The reactions involved in this preparative approach are simple substitution or addition coordination reactions; however, the resulting Brønsted acid sites could be quite hard to characterize, as often multiple non-Brønsted or weak Brønsted acidic hydroxyl groups are present in the structure, making it difficult to attribute the Brønsted acidity of the bulk to certain sites. In addition, Lewis acid sites are often generated, making the differentiation more difficult. Nevertheless, the well-developed acid–base chemistry in metal oxide SBUs could help in the study of these Brønsted acid sites. Clearly, the superacidity designed in MOF-808 by sulfation promises a new direction for Brønsted acidity in MOFs.

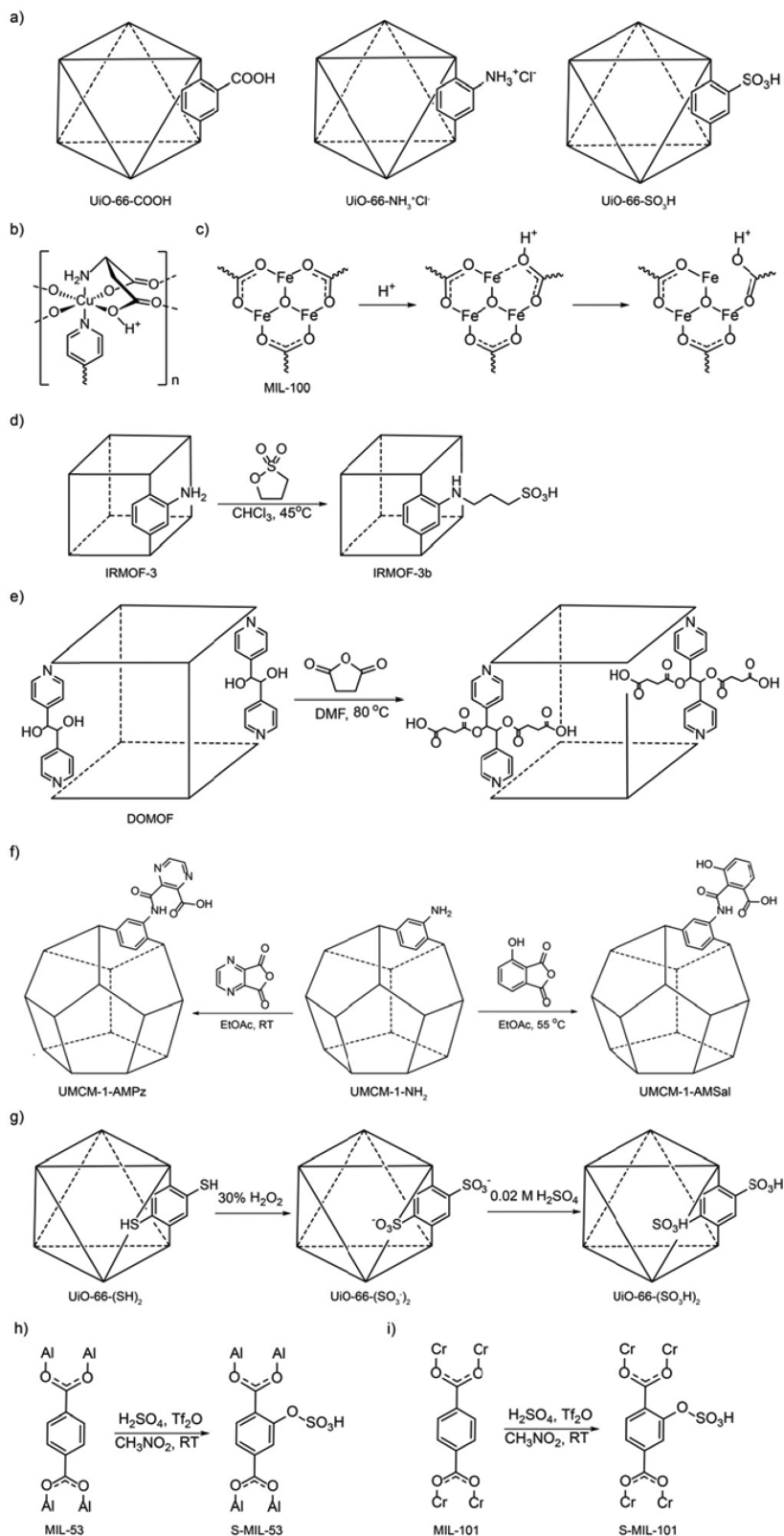
2.3. Covalently Bound Brønsted Acid Functional Groups of Organic Linking Units

This is so far the most extensively studied approach for introducing Brønsted acidity into MOFs. It takes advantage of the most distinguished difference between MOFs and other porous materials: their structurally well-defined organic functionalities within the framework. MOF pores decorated with Brønsted acid sites are achieved either directly from the acidic functional groups dangling on the organic linker or from sites that are introduced postsynthetically through protonation or organic reactions (Scheme 4). Several submethods covering these approaches will be discussed below.

Brønsted acidic groups can be dangled from the organic linkers (Scheme 4a). For example, a free carboxylic acid group was dangled in the pores of UiO-66 [$Zr_6O_4(OH)_4(BDC)_6$] by using $H_2BDC-COOH$ instead of H_2BDC in the preparation of UiO-66.⁹⁴ An excess amount of the linker with dangling units, plus a large amount of benzoic acid as modulator, was added to the reaction mixture to allow dangling carboxylic acid on the linker to stay protonated. Recently, the same MOF was reported to be synthesized from an environmentally friendly synthesis route in aqueous solution using $ZrCl_4$, $H_2BDC-COOH$, and H_3BTC as modulator.⁹⁵ Although several other MOFs with dangling carboxylic acid groups from $H_2BDC-COOH$ were reported,^{96–98} no Brønsted acidic properties were further investigated apart from their crystal structures.

Another UiO-66-type Zr MOF with Brønsted acid sites of a different strength was reported.⁹⁹ A mixture of $ZrCl_4$, H_2BDC-

Scheme 4. Covalently Bound Brønsted Acid Functional Groups of Organic Linking Units: (a) Brønsted Acidic Groups of Different Acid Strength Suspended from BDC Linkers in UiO-66; Brønsted Acidity Generated from Controlled Protonation in Copper Aspartate (b) and MIL-100 (c); and Brønsted Acidity Introduced through PSM in IRMOF-3 (d), DO-MOF (e), UCMC-1-NH₂ (f), UiO-66 (g), MIL-53 (h), and MIL-101 (i)^a



^aTf₂O = triflic anhydride; RT = room temperature.

NH₂, and DMF was heated at 120 °C to give an acid–base bifunctional MOF in which one-third of the amino-functionalized links are protonated to make an anilinium type of Brønsted acid, with the charge being balanced by chloride anions. This example clearly indicates the protonating ability of the proton generated from the formation of the carboxylate–metal bond. The efficiency of protonating the amino groups of the framework, however, is determined to be only ca. 17%. The other possible binding sites could be amino groups of the free linker or the basic DMF solvent molecules. This contributes to understanding the reason why excessive amounts of acid are needed to synthesize a carboxylic acid functionalized MOF: carboxylic acid groups are stronger acids than aniline-type ammonium groups, thus requiring a more acidic condition to have a highly protonated derivative of the functionalized MOF.

Alternatively, protonation of the aniline units in amino-functionalized UiO-66 produces weak Brønsted acidic anilinium groups. This is done postsynthetically by stoichiometric addition of anhydrous HCl solution in 1,4-dioxane.¹⁰⁰ The resulting MOF exhibited retention of crystallinity, with an estimated 3.35 mmol g⁻¹ of anilinium sites in the structure. This corresponds to a 2 times higher value than the reported anilinium site density in acidified amino-functionalized UiO-66 directly obtained from the one-pot synthesis approach (discussed earlier).

MOFs with stronger Brønsted acids were made by dangling sulfonic acid units in UiO-66.^{94,101} The fully sulfonic acid group functionalized UiO-66 was not porous, as its crystallinity and porosity were lost upon activation. However, by diluting the sulfonated linkers with nonsulfonated linkers (the original BDC linkers), it was possible to prepare UiO-66 with 25% sulfonated linkers and ca. 50% of the original porosity. Successful incorporation of sulfonic groups into MIL-101 was also achieved by using a combination of CrO₃, H₂BDC–SO₃Na, and concentrated hydrochloric acid in an aqueous system.¹⁰² Activation was reported without problem and two-thirds of the sulfonic groups in the framework are protonated. Recently, a facile postsynthetic HCl treatment applied subsequently was reported to afford 100% of sulfonic acid functionalized MIL-101.^{103,104}

Brønsted acidic protons are also present in a number of MOF structures made from organic linkers containing four, five, and six carboxylic acids.^{105–113} In the MOF structure, some of these carboxylic acids are noncoordinating and some are coordinating without being deprotonated. They are reported as crystal structures with no extensive study of Brønsted acidity. The combination of coordinating and noncoordinating carboxylic acid groups produces complex structures with low symmetry and porosity.

Similar to carboxylate-based organic linkers, organophosphonates can bond to metals in both deprotonated and protonated form, where in the latter case Brønsted acidity is present. For the preparation methods for this category of MOFs, interested readers are directed to several recent reviews on the topic.^{114,115}

Introduction of Brønsted acidic protons into the coordinating carboxylate group could also be achieved postsynthetically through controlled protonation, as exemplified in two Ni and Cu MOFs made with aspartic acid (ASP) and either 4,4'-bipyridine (BIPY) or 1,2-bis(4-pyridyl)ethylene (BPE) as linkers [M₂(ASP)₂(BIPY) and M₂(ASP)₂(BPE) (M = Ni, Cu)] (Scheme 4b).¹¹⁶ Controlled protonation on one of the aspartate carboxylate groups was achieved through addition of 1 M HCl ether solution to the MOF suspended in ether, resulting in the protonated phases M₂(ASP)₂(BIPY)(HCl)₂(guest)_x and

M₂(ASP)₂(BPE)(HCl)₂(guest)_x (M = Ni, Cu, guest = methanol, water), behaving as Brønsted acid catalysts. Absolute exclusion of moisture, acid stoichiometry, and reaction time are key factors to realize a controllable protonation. While the Ni-based compounds are marginally porous, on account of tiny channel dimensions, the copper versions are clearly porous.

MOFs that are more stable in acidic media could be handled in aqueous solution to produce Brønsted acidity. A predried Fe derivative of MIL-100 was immersed in an aqueous solutions of CF₃COOH or HClO₄ of varying concentration up to 0.078 M at 298 K.¹¹⁷ Alongside generation of protonated carboxylic acid that is Brønsted acidic, doubling of the Lewis acid sites is also evidenced (Scheme 4c). This indicates an acid-activation mechanism of the Fe₃-μ₃-oxo cluster by first protonation of the coordinating carboxylates, followed by breaking of the weakened Fe–O bond, resulting in Brønsted acidic carboxylic acids adjacent to newly formed open Fe sites. No significant porosity loss was found when the ratio of introduced acidic proton to coordinating carboxylates in the MOF was below 0.5.

Another strategy for introduction of Brønsted acidity is to use PSM to bind the Brønsted acid group or its precursor covalently onto the organic linker. This was first illustrated through a ring-opening reaction between the amine-bearing IRMOF-3 and 1,3-propanesulfone to generate a sulfonic acid group, which is a strong Brønsted acidic group (Scheme 4d).¹¹⁸ For the reaction, 57% of the amine sites in IRMOF-3 were converted to sulfonates, as found by elemental analysis. Similarly, DO-MOF, a Zn(II) paddlewheel MOF with TCPB [H₄TCPB = 1,2,4,5-tetrakis(4-carboxyphenyl)benzene] and DPG [*meso*-1,2-bis(4-pyridyl)-1,2-ethanediol] with diol groups,¹¹⁹ readily undergoes modification with succinic anhydride, resulting in a ring-opened product with free Brønsted acidic carboxylic acid groups (Scheme 4e). In a related example, modifying UMCM-1-NH₂ with cyclic anhydrides also produced salicylic acid and pyrazine carboxylic acid groups.¹²⁰ Reaction of UMCM-1-NH₂ with 3-hydroxyphthalic anhydride or 2,3-pyrazinedicarboxylic anhydride resulted in acid-functionalized UMCM-1 with percent conversions of 35% and 50%, respectively (Scheme 4f).

Other chemical reactions have also been tried to incorporate strongly acidic sulfo-type functionalities postsynthetically. While traditional sulfonation or sulfation methods¹²¹ are clear dead-ends, as MOFs cannot be exposed to high concentrations of sulfuric acid due to their limited chemical stability, pioneering work has been done to incorporate secondary sulfone moieties by using thiol-tagged linkers followed by a postsynthetic oxidation.¹²² Recently, direct oxidation of thiol-tagged UiO-66 [UiO-66-(SH)₂] into sulfuric acid functionalized UiO-66 was reported (Scheme 4g).¹²³ Air-dried UiO-66-(SH)₂ was oxidized at room temperature with 30% H₂O₂ solution, followed by acidification with 0.02 M sulfuric acid solution. Complete conversion of –SH to –SO₃H was observed using this method. However, the resulted Brønsted acidic MOF did not show high surface area (<20 cm³ g⁻¹ N₂ uptake at 77 K and 1 bar), indicating that the pores might be blocked by either bulky –SO₃H groups or other moieties inside the pore.

A harsher and more direct PSM strategy was later reported to successfully incorporate the bisulfate groups through a direct treatment of chemically stable MOF structures MIL-53 and MIL-101 with a mixture of triflic anhydride and sulfuric acid in nitromethane (Scheme 4h,i).¹²⁴ Strongly Brønsted acidic organo-bisulfate groups are found to attach to up to 50% of the aromatic BDC linkers of the structures, a yield comparable to that achieved through the milder conditions. Triflic acid is

generated as a byproduct of the reaction; thus, it is necessary to check the integrity of the MOF. While MIL-101 exhibits almost no change in its powder XRD pattern with a slight decrease of BET specific surface area (from ca. 2700 to 2200 m² g⁻¹), sulfated MIL-53 is not accessible for N₂ at 77 K. Instead, water adsorption is measured to prove the retained intrinsic porosity in the MOF. The large decrease in the pore size of MIL-53 is believed to be caused by the volume of the bisulfate groups and their stacking after dehydration, as well as the presence of residual water within the framework.

Postsynthetic linker exchange was another feasible strategy reported for the introduction of Brønsted acidity into MOFs. This approach takes advantage of the dynamic equilibrium between MOFs and the solution that they are immersed in, where examples of solvent-assisted metal or linker exchanges were reported.^{125,126} Free carboxylic acid groups on a BTC linker were introduced in NU-125 (Figure 4a), a Cu MOF with 5,5',5''-(4,4',4''-(benzene-1,3,5-triyl)tris(1*H*-1,2,3-triazole-4,1-diyl))-

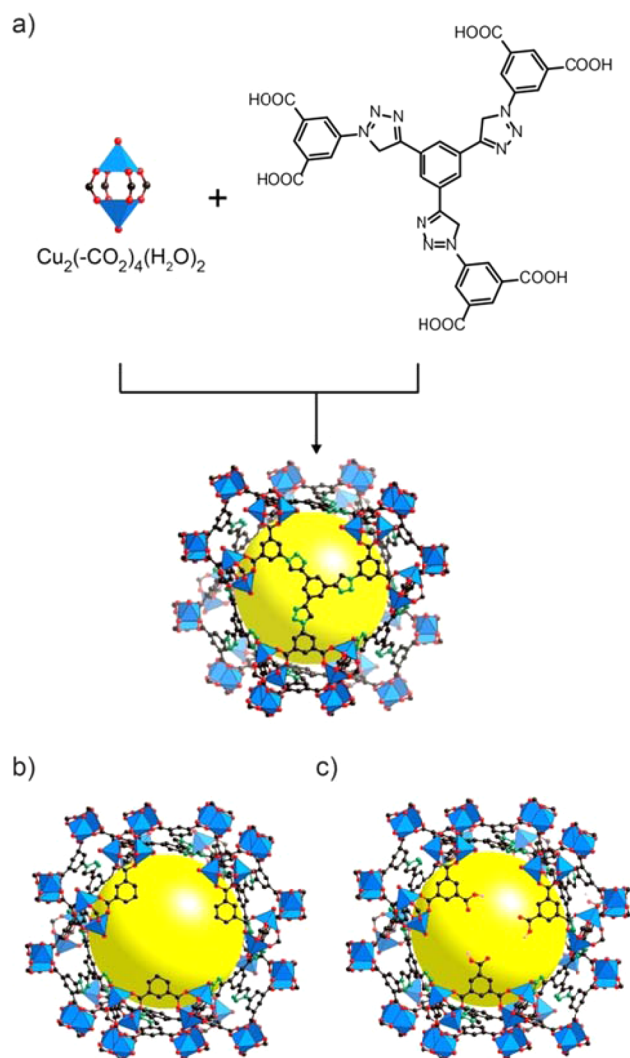


Figure 4. (a) $\text{Cu}_2(-\text{CO}_2)_4(\text{H}_2\text{O})_2$ SBUs are combined with a deprotonated organic linker to form NU-125. (b) Schematic representation of NU-125 with terminal isophthalate ligands and (c) Brønsted acidic NU-125 with terminal BTC ligands and acidic protons (pink spheres). Atom labeling scheme: Cu₂ paddlewheel cluster, blue polyhedra; C, black; N, dark green; and O, red. All H atoms except for acidic protons are omitted for clarity.

triisophthalate,¹²⁷ in this manner.¹²⁸ To facilitate the substitution, NU-125 samples featuring terminal isophthalate (IPA) defects were first synthesized (Figure 4b).¹²⁹ The MOF was then immersed in a DMF solution of 3 equiv of H₃BTC overnight at 80 °C. The target groups for substitution are the terminal IPA located on the Cu SBU of NU-125, which are generally more reactive than the hexatopic linkers, since they are connected to only two as opposed to six Cu₂ paddlewheel clusters. Complete substitution was observed in this case, and the resulting MOF has been shown to possess Brønsted acidic pores (Figure 4c).

As described in this section, anilinium cations, protonated phosphonates, carboxylic acids, and sulfo-type groups are the most common state-of-the-art Brønsted acidic groups on organic linkers of MOFs. Unlike the previous two approaches shown in sections 2.1 and 2.2, acidic solutions are generally necessary to avoid deprotonation of the acid group in the final MOFs or actually to create Brønsted acidity in the MOFs. This has raised a requirement for the chemical stability of the targeted MOFs, which should be resistant to the strength of the acid that it bears itself; Zr, Al, Cr, and Fe are the most common metals satisfying this requirement. When Brønsted acidity is to be introduced to MOFs with metals that are known to be nonresistant to acidic environments (e.g., Zn), special care needs to be taken by either strictly controlling the degree of defect generation or selecting a strategy in which no harmful free protons are involved. However, these MOFs may encounter problems in real practical conditions. Given the above-mentioned points, retention of the framework and porosity is not always guaranteed, even if “stable MOFs” are used; therefore, meticulous examination of the framework integrity is never an unnecessary move.

3. CHARACTERIZATION METHODS

Characterization of acidity in solid acid materials requires the answer to the following questions: (i) What type of acid sites are present, Brønsted, Lewis, or both? (ii) What is the acid strength? (iii) What is the acid concentration? In order to answer these questions, a number of techniques have been developed to characterize the surface acidity, which will be described below.

3.1. Indicators and Titration Methods

The acidity of a material is defined relative to the base used in the acid–base interaction. Therefore, the solid Brønsted acid is defined as a solid that protonates or at least partially transfers protons to a base. By use of an appropriate series of bases, in other words, indicators, the acidity scale is given by the Hammett acidity function H_0 .⁹³ The H_0 scale can be understood as an extrapolation of the pH scale from diluted aqueous media to all media, with a similar written definition of the form

$$H_0 = \text{p}K_a + \log[\text{B}]/[\text{HB}^+]$$

where [B] and [HB⁺] are the concentrations of the indicator in its base and acid form, respectively.

The acid strength of a solid acid can be qualitatively estimated using a series of indicators, known as Hammett indicators,¹³⁰ which will have a bright color in their conjugated acid form that is intense enough to mask the color of their base form.¹³¹ Typically, if immersion of a solid in a specific indicator solution changes the color of the solid to that of the acid form of the indicator, the H_0 value of the solid is the same as or is lower than the $\text{p}K_a$ value of the conjugate acid of the indicator.⁴⁸

This method was first used in the case of sulfonic acid group functionalized UiO-66, with a single Hammett indicator, 4-*o*-tolylazo-*o*-toluidine (Table 1), to confirm the MOF’s possession

Table 1. Hammett Indicators Used for the Measurement of Acid Strength in MOFs

Indicators	Structure of Base Form	Color		pK_a
		Base Form	Acid Form	
4-Phenylazoaniline		Orange	Red	+2.8
4- <i>o</i> -Tolylazo- <i>o</i> -toluidine		Orange	Red	+2.0
2-Nitroaniline		Yellow	Red	-0.2
4-Nitrodiphenylamine		Yellow	Red	-2.4
2,4-Dichloro-6-nitroaniline		Yellow	Red	-3.2
2,4-Dinitroaniline		Yellow	Red	-4.4
2-Benzoylnaphthalene		Colorless	Yellow	-5.9
2-Bromo-4,6-dinitroaniline		Yellow	Red	-6.6
Anthraquinone		Colorless	Yellow	-8.1
4-Nitrotoluene		Colorless	Yellow	-11.4
4-Nitrofluorobenzene		Colorless	Yellow	-12.4
2,4-Dinitrotoluene		Colorless	Yellow	-13.8
2,4-Dinitrofluorobenzene		Colorless	Yellow	-14.5

of acidic protons.¹⁰¹ A positive test with the solid exhibiting a dark brown color upon addition of the indicator solution in cyclohexanone proves the presence of acidic protons in the MOF structure, as nonfunctionalized UiO-66 failed to change the color of physically adsorbed indicator molecules (orange).

A more recent use of Hammett indicators in a Brønsted acidic MOF appeared in 2014, when the Brønsted acid strength of sulfated MOF-808 was studied with a series of 12 Hammett indicators with pK_a values ranging from 2.8 to -14.5 (Table 1).⁹² It was determined through this test that the gradual sulfation of MOF-808 had promoted its acidity from low acidity ($H_0 \geq 2.8$, no color change observed for any of the indicators used) to moderate acidity ($-4.4 \geq H_0 \geq -5.9$) and finally to very strong acidity ($H_0 \leq -14.5$, color change observed for all indicators, including three that have pK_a values lower than -12), in the superacid region ($H_0 \leq -12$) by this criterion. It is also shown by the Hammett method that this superacidity readily undergoes neutralization by atmospheric moisture, as no change of color of the Hammett indicators was observed under these conditions.

The two examples mentioned above show the potential of using these indicators for estimating the range of acid strength in Brønsted acidic MOFs. However, despite of its simple experimental setup, the indicator method only qualitatively determines the strongest acid present in MOFs, but there may exist at least limitations: (i) Visual determination of the color change is subjective when colored samples are to be measured with this method. These are MOFs consisting of generally colored metal ions, such as Cu(II), Cr(III), and Fe(III), or

colored organic linkers. The majority of MOFs made with Zr(IV) and Al(III) and BDC and BTC types of linkers are often white or have light color, making them more amenable to this method. (ii) Difficulties for those indicator molecules to diffuse to the interior of MOF pores exist when samples with small pores or narrow pore apertures are to be measured,¹³² which leads to the characterization of the surface acidity of the outside of the particle. (iii) There is an inconsistency between the estimated acidity and the catalytic performance of the solids, especially in the superacidity region.¹³³

Quantitative determination of the Brønsted acid concentration in MOFs could be carried out using liquid–solid acid–base titration methods. The first example was reported in 2009, with the concentration of acidic protons in HKUST-1 encapsulated Brønsted acidic polyoxometalates determined using the back-titration method.⁶³ The MOF was placed in a diluted solution (0.0085 M) of a known amount of NaOH under a CO₂-free atmosphere for 10 h at room temperature to complete the acid–base neutralization. Then, the solids were filtered off and the base was back-titrated with HCl solution to determine the amount of base consumed, which is equal to the amount of acidic protons in the MOF acid. The direct acid–base titration method was used in the system of sulfonic acid functionalized MIL-101.^{102,134} In both cases, the titration was carried out using a saturated NaCl solution as an ion-exchange agent¹³⁵ to release the acidic protons from the MOF to the solution, which was later titrated using NaOH directly after filtration of the MOF.

We note that these titrations were carefully designed with regard to the following aspects to achieve accurate results: (i) Only one kind of Brønsted acid site that will be titrated in the given condition is present in the above-mentioned MOF-based Brønsted acids, i.e., protons on polyoxometalates in the former example and sulfonic acid groups on the BDC linker in the latter. Although stepwise titration of acid sites of different strength using a series of Hammett indicators in nonaqueous media was reported in zeolites,¹³⁶ questions concerning its validity persist.^{47,48} (ii) Titrations were carried out in aqueous media to remove errors that could be caused by interfering Lewis acid sites (open metal sites) if any. (iii) The integrity of the parent MOF structure was kept during the whole titration procedure. The decomposition of MOF will consume acid for the protonation of the carboxylates on the organic linker and also base for complexation with the metal ion, which will introduce errors to the analysis result. Thus, only very diluted NaOH solution was added to HKUST-1, and the MOFs were always filtrated before addition of the HCl titrant. (iv) The equilibrium time should be left long enough (10 h and above) to achieve a complete exchange of protons, even though the MOF pores are large enough, to guarantee a precise quantification.

Overall, the indicator method is still valuable as a quick and simple method to estimate the acid strength present in MOFs, although the surface acidity function H_0 does not have an explicit physical meaning in the case of heterogeneous acids.⁴⁷ In practical use, tests carried out with Hammett indicator sets are preferred over single indicators, and it is always encouraged to combine results from the indicator method with other characterization methods to reach a comprehensive judgment.

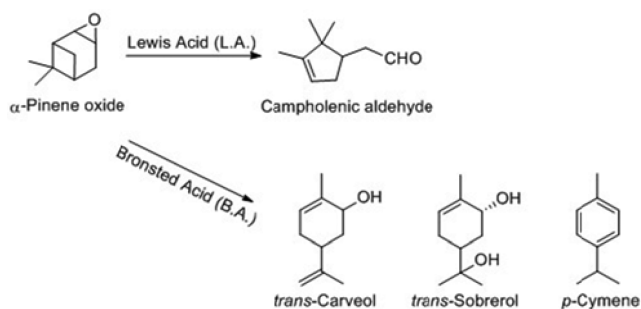
3.2. Test Reactions

Unlike in the field of acidic zeolites and sulfated metal oxides, where test reactions are often of industrial interest,^{137–139} until now, test reactions in acidic MOFs are merely used for fundamental studies and understanding the nature of the acidic

sites (Lewis acidity or Brønsted acidity). For this purpose, each test run typically requires 50–100 mg of MOF samples often in their microcrystalline powder form with particle sizes in the range of a few hundred nanometers to one hundred micrometers. These samples are preferred over large single crystals due to easier diffusion of reactants and products. Besides, a careful check of the condition of MOF crystals before and after catalyst activation and reaction is also necessary to avoid misjudgements.

Isomerization of α -pinene oxide to campholenic aldehyde is one of the two most frequently used catalytic test reactions for differentiating Brønsted and Lewis acidity in MOFs (Scheme 5).³⁷ Campholenic aldehyde is an important fragrance

Scheme 5. Isomerization of α -Pinene Oxide



compound; it can only be prepared in high yield when a suitable Lewis acid is used. Brønsted acids tend to also produce a mixture of compounds in low yields, *trans*-carveol, *p*-cymene, *trans*-sobrerol, and dimerization products. The selectivity toward campholenic aldehyde is usually less than 55% with Brønsted acids, while with Lewis acids selectivities as high as 85% can be reached.^{140,141} HKUST-1 samples were prepared under different conditions using this reaction to study the potential for opportunistic catalysis at defect Brønsted sites (e.g., exposed carboxylic acids). On the basis of experimental data, it was concluded that the HKUST-1 samples prepared indeed function primarily as a Lewis acid catalyst.

Cyclization of citronellal to isopulegol (Scheme 6) is another example. The product distribution of this reaction is also known to be sensitive to the nature of the acid sites: with Lewis acids only, high selectivity ($\geq 75\%$) toward (\pm)-isopulegol is obtained, while, with Brønsted acids, the selectivity is significantly lower.^{37–39,142,143} A lot of work has used this reaction to prove the existence of primarily Lewis acidic sites inside the MOFs. Semiquantitative conclusions about the acid strength and concentration were also drawn from the catalytic activity of

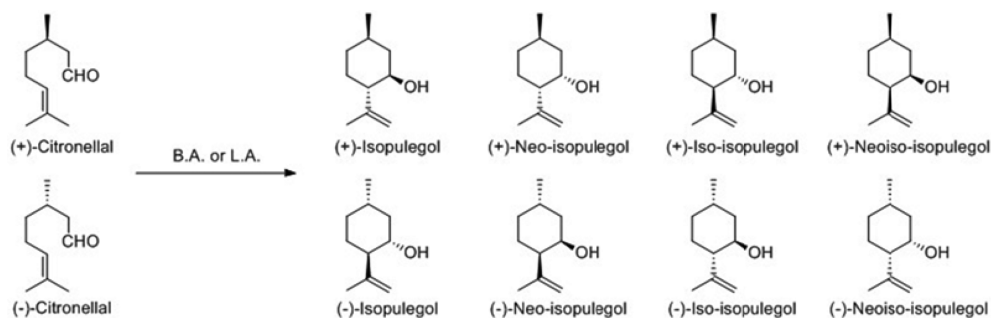
MOF. This same reaction was also employed to support the presence of Brønsted acidity in sulfated MOF-808.⁹² It was observed that MOF-808 materials, despite their nearly identical structural frameworks and porosities, displayed selectivity toward (\pm)-isopulegol that decreased monotonically with an increasing amount of sulfate incorporated from 85% in MOF-808 to 55% in MOF-808 treated with 0.1 M sulfuric acid. This result indicates that only weak Lewis acidity was present in MOF-808, while Brønsted acidity was introduced into MOF-808 during sulfuric acid treatment, leading to decreased product selectivity.

When combined with other techniques, test reactions could also serve as probes for mapping the Brønsted acidity in MOFs. Confocal fluorescence microscopy was used for three-dimensional visualization of Brønsted acidic sites in HKUST-1.¹⁴⁴ The test reaction used is the selectively Brønsted acid catalyzed oligomerization of furfuryl alcohol, an approach for catalytic fluorescence generation. This reaction is also preferable due to the fact that the small size of furfuryl alcohol permits easy diffusion and its weak interaction with MOF structures minimizes the risk of structural changes during the experiment. As shown in Figure 5a,b, very weak and homogeneous fluorescence intensity was observed for HKUST-1 crystals obtained after a short crystallization time. However, when the crystallization time was elongated, intense fluorescence was displayed at well-defined zones of the crystal (Figure 5c–f). This result pointed to the important role of crystallization time in the density and distribution of Brønsted acidic sites in the previously thought Lewis acidity of HKUST-1. The microscopic observation was later evidenced by checking the product distribution of the bulk catalyzed α -pinene oxide isomerization.

Aside from distinguishing Brønsted acidity from Lewis acidity, test reactions could also help to assess qualitatively the strength of Brønsted acid sites in MOFs. α -Pinene isomerization, which is carried out in the presence of strong acid catalysts (Scheme 7),^{145–148} was used to probe the same system. The authors reported that no conversion of α -pinene was observed when only Lewis acidic MOF-808 was used. Yet, α -pinene conversion was quantitative using MOF-808 treated with 0.1 M sulfuric acid, where selectivity toward camphene and limonene was similar to that observed for sulfated zirconia. These findings indicate the presence of strongly acidic sites in sulfated MOF-808.

Another aspect of these test reactions is that they are used to prove that the decoration of the pores with active sites is in the interior of the pores rather than on the outside surface of the particle.⁶³ This is usually done by applying substrates of similar reacting groups but different sizes to the catalytic reaction. Substrates having sizes larger than the pore aperture will not be

Scheme 6. Cyclization of Citronellal to Isopulegol^a



^aB.A. = Brønsted acid; L.A. = Lewis acid.

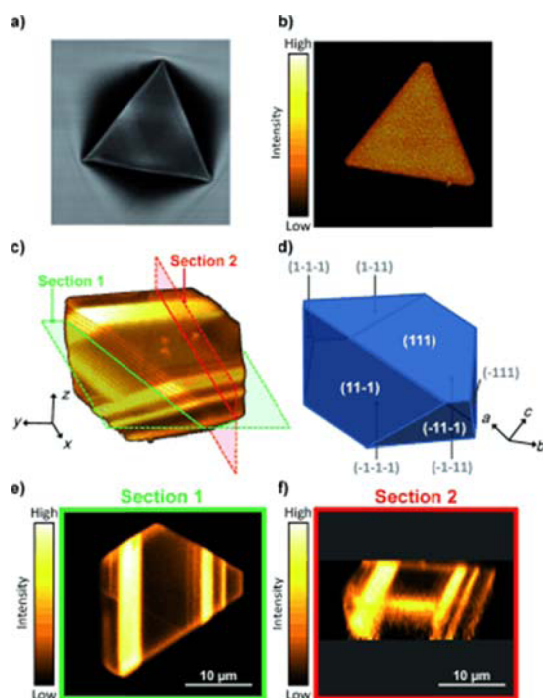
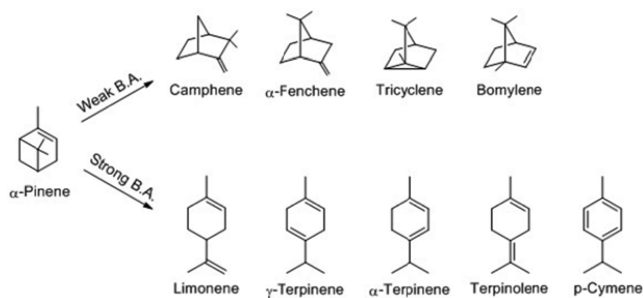


Figure 5. Confocal fluorescence images of HKUST-1 single crystals demonstrating the introduction of defects upon extending crystallization time. (a) Transmission micrograph of a HKUST-1 crystal obtained after a short crystallization time. (b) Fluorescence micrograph of the surface of the same crystal illustrating the absence of defects. (c) Fluorescence data recorded for a HKUST-1 crystal obtained after extended crystallization time. Semitransparent three-dimensional representation of the fluorescence data obtained as a series of xy -scans along the z -axis. Positions of xy - and xz -sections shown in panels e and f, respectively, are indicated. (d) Schematic representation of the single crystal shown in panel c with indication of the limiting crystal planes and crystallographic axes. (e) As-recorded xy -section. The crystal boundaries in this two-dimensional section are all parallel to the $\langle 110 \rangle$ directions. (f) The xz -section reconstructed from the data shown in panel c and visualizing the angles between the crystal's exterior surface and defect planes propagating in the crystal's interior. Reprinted with permission from ref 144. Copyright 2013 John Wiley & Sons Inc.

Scheme 7. Isomerization of α -Pinene^a



^aB.A. = Brønsted acid.

able to access the active sites inside and, thus, are only catalyzed by functional groups exposed to the outside surface. By comparing the turnover frequency of different substrates, one could have an idea whether the active sites have been successfully incorporated inside the pores.

3.3. Gas Sorption Techniques

Adsorption of volatile amines such as NH_3 , pyridine, and n -butylamine, to mention a few, can be used to determine the number of acid sites on solid acid materials. Typically, this is done by exposing solid acid materials to an excess amount of basic molecules followed by removal of those physisorbed ones by long time evacuation. Whatever is left on the surface is considered as chemisorbed, with the amount equal to that of the acid sites in the solids and acid strength related to the heat of adsorption or the temperature required for desorption, measured by calorimetry^{149,150} and temperature-programmed desorption (TPD)^{151,152} using a commercially available calorimeter and chemisorption analyzer, respectively.

Although the development of stable MOFs has enabled the exploration of the adsorption chemistry of basic gas molecules such as NH_3 , previously considered to be too reactive for MOFs,^{153,154} to date, no measurement of Brønsted acidity in MOFs is carried out intentionally. An increase of NH_3 uptake, especially at low pressure, was shown in Brønsted acidic UiO-66- NH_3Cl compared to the parent framework nonacidic UiO-66- NH_2 .¹⁰⁰ The improvement was attributed to the presence of weakly Brønsted acidic anilinium groups, calculation results showed that each site absorbs ca. 0.5 NH_3 molecules, and the adsorption is reversible, probably due to only weak Brønsted acidity present. The Lewis acid sites may also interfere, as shown in the case of MIL-101- SO_3H . With the calculated number of total acidic sites distributed between the protic sulfonic acids (2.19 mmol g^{-1}) and the Lewis acidic unsaturated metal centers (3.28 mmol g^{-1}), the measured NH_3 uptake at low pressure (510 ppm) was 3.52 mmol g^{-1} , larger than the total amount of Brønsted acid sites but smaller than the total acid sites. This has raised a need to further confirm the amount of chemisorbed ammonia exclusively on Brønsted acidic sites and also per Brønsted acidic site. Possible approaches to address the latter include combined in situ or ex situ diffraction and spectroscopic characterization of the adsorbates and also theoretical calculations. The former could be roughly estimated by evaluating the cyclic performance after carefully choosing activation conditions between consecutive runs so that all adsorbed ammonia molecules except for those chemisorbed on strong Brønsted acidic sites will be removed. However, to obtain a quantitative result, desorption characterizations of the adsorbates are indispensable.

While in the field of inorganic solid acids, where desorption of the chemisorbed basic molecules can be done by programmed ramping of temperature to further measure the acid strength hop-by-hop, this is so far not applicable in Brønsted acidic MOFs, since the desorption temperature of protonated NH_3 or pyridine are generally above 400 °C, a temperature believed to decompose the MOFs. However, preliminary TPD experiments have been carried out on stable lanthanide MOFs with Lewis acidity and pyridine as the base.¹⁵⁵ The desorption spectrum with an obvious band at 500 K indicates that Lewis acid metal sites are available, giving the evidence that, if thermally stable enough, acidity in MOFs can be probed by TPD measurements.

Overall, probing Brønsted acidity in MOFs using sorption techniques is so far quite undeveloped, with the major concerns being (i) the stability of MOFs toward those basic molecules, (ii) the lack of knowledge of the existing form of probe molecules in MOF pores, and (iii) the thermal stability of MOFs, if TPD is to be used. However, the use of less basic molecules (e.g., acetone, Ar) has been or is being developed in the field of inorganic solid

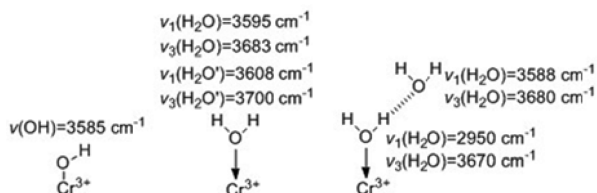
acids,^{156,157} which might be a viable method for probing the acidity in MOFs.

3.4. Vibrational Spectroscopy Methods

Infrared (IR) spectroscopy has been used to characterize the successful incorporation of acid moieties inside the framework and, more importantly, to determine the acidity of solid acids by studying adsorbed probe molecules.^{158,159} Besides, it allows one to see the vibrational frequencies of hydroxyl groups, which are not readily identified by other techniques. Since hydroxyl bands have characteristic frequencies in the IR, one can determine their mode of interaction with other molecules,¹⁶⁰ which renders this a good means of characterization for the presence of Brønsted acidity.

Terminal and bridging hydroxyl groups are quite common in MOFs. Attempts have been made to measure the surface concentration of different hydroxyl groups on the basis of assigned O–H stretching frequencies to specific types of hydroxyl groups. A systematic study was carried out on the system of MIL-100(Cr), where multiple species of hydroxyl groups could be present, depending on the degree of hydration.⁸⁴ Three main species were identified (Scheme 8): (i) Cr–OH

Scheme 8. Brønsted Acidic Hydroxyl- and Water Functionalities in MIL-100 and Their Characteristic Infrared Bands



groups, with a single sharp $\nu(\text{OH})$ band appearing at 3585 cm^{-1} and its $\nu + \delta(\text{OH})$ combination band at 4295 cm^{-1} ; (ii) water molecules coordinated to two different unsaturated Cr sites, showing their heterogeneity with two bands of $\nu_1(\nu_3)$ vibrational mode at 3595 and 3608 cm^{-1} , respectively; and (iii) additional adsorbed water molecules, not bound to chromium atoms but in strong interaction with the terminal water molecules aforementioned. It is noticed that the IR band corresponding to Cr–OH groups was lacking in samples activated at temperature below 473 K , perturbed by hydrogen-bonded water molecules, a sign of Brønsted acidity. Similar behavior was also observed in the Al version of MIL-100.⁸⁵

The Brønsted acidity could furthermore be observed by IR studies on adsorbed probe molecules. Two major types of probe molecules are used for solid acids: (i) strong bases, such as pyridine and NH_3 , and (ii) weak bases involving CO, acetone, acetonitrile, benzene, olefins, H_2S , and H_2 . The use of the former type of probe molecules and IR spectroscopy for MOF-based acids could be problematic, as their characteristic IR absorption bands overlap with those of the frameworks. To be more specific, reported pyridine molecules adsorbed on Brønsted and Lewis acid sites normally give rise to IR absorption bands in the $1450\text{--}1650\text{ cm}^{-1}$ region, which overlaps with the IR absorption bands from the carboxylate groups, phenyl units, bipyridines, phosphonates, and sulfonates commonly existing as building blocks or functional groups of interest in MOF structures. In contrast, in the latter type, CO and acetonitrile are promising probe molecules, as their characteristic IR absorption band will

appear in the triple bond region ($2000\text{--}2300\text{ cm}^{-1}$),¹⁶¹ a normally empty region for MOF spectra.

CO is a weak soft Lewis base that has a small molecular size (almost no steric hindrance) and is unreactive at low temperatures. IR spectroscopy of adsorbed CO at low temperatures (77 or 100 K) can probe both Lewis and Brønsted acid sites.¹⁶² When probing the hydroxyl type of Brønsted sites, it gives rise to H-bonded CO molecules,¹⁶³ and both $\Delta\nu(\text{OH})$ (shift of the acidic O–H stretching frequency after CO adsorption) and $\Delta\nu(\text{CO})$ (shift of the C–O stretching frequency of adsorbed CO compared to free CO) depend on the strength of the acid sites: the larger the shifts, the stronger the acidity. At 100 K , three main $\nu(\text{CO})$ bands were observed in outgassed MIL-100(Cr) (Figure 6): (i) CO interacting with

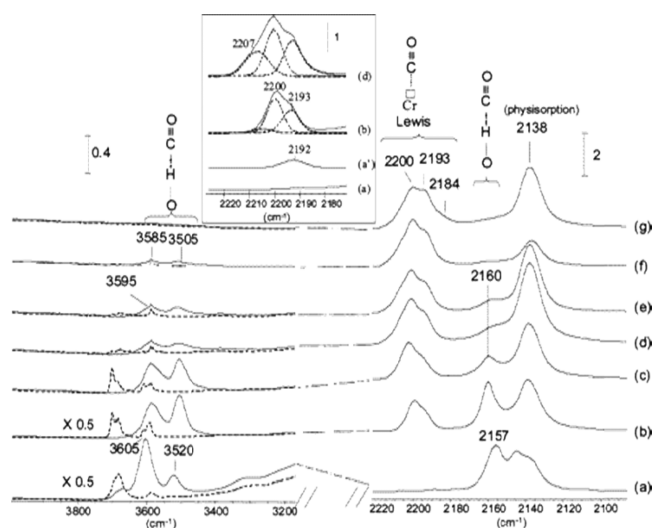


Figure 6. Infrared spectra of CO loaded in MIL-100 samples outgassed for 2 h (a) and 12 h (a') at room temperature and 2 h at 373 K (b), 423 K (c), 473 K (d), 523 K (e), 573 K (f), and 623 K (g) (dotted line, before CO adsorption; solid line, after introduction into the IR cell of an equilibrium pressure of CO equal to 266 Pa). Reprinted with permission from ref 84. Copyright 2006 American Chemical Society.

Brønsted acid sites centered at 2160 cm^{-1} , (ii) CO coordinating to Cr(III) sites at $2215\text{--}2280\text{ cm}^{-1}$, and (iii) physisorbed CO at 2138 cm^{-1} . On the other hand, information from the $\nu(\text{OH})$ region revealed that the Cr–OH groups are slightly acidic, with a $\Delta\nu(\text{OH})$ value of 90 cm^{-1} , acidity close to that of silanol groups in silicalite [$\Delta\nu(\text{OH}) = 100\text{ cm}^{-1}$];¹⁶⁴ the water molecules coordinated to the Cr(III) sites are more acidic, with a $\Delta\nu(\text{OH}) = 160\text{ cm}^{-1}$, comparable to P–OH groups of phosphate silica [$\Delta\nu(\text{OH}) = 180\text{ cm}^{-1}$].¹⁶⁵ Furthermore, MIL-100 samples with a different kind of alcohol molecule coordinated to the Cr(III) sites were studied in the same way.⁸⁷ The largest perturbation of the $\Delta\nu(\text{OH}) = 235\text{ cm}^{-1}$ band was observed for $(\text{CF}_3)_2\text{CHOH}$ coordinated to the Cr(III) sites (Figure 7). From an empirical relationship between the $\Delta\nu(\text{OH})$ shift and the Hammett acidity function H_0 drawn from data for silica, some phosphate materials, and zeolites (Figure 8),^{166–168} the strongest Brønsted acidity of these alcohol-coordinated MIL-100 materials is that of $(\text{CF}_3)_2\text{CHOH}$ -coordinated MIL-100. This gives H_0 equal to -7.7 , a value comparable to that of HNaY .

Apart from evaluating the strength of the Brønsted acidity in MOFs, IR studies of CO adsorption are also employed for semiquantification or quantification (if the extinction coefficients are known for each kind of acid site) of Lewis and Brønsted acid

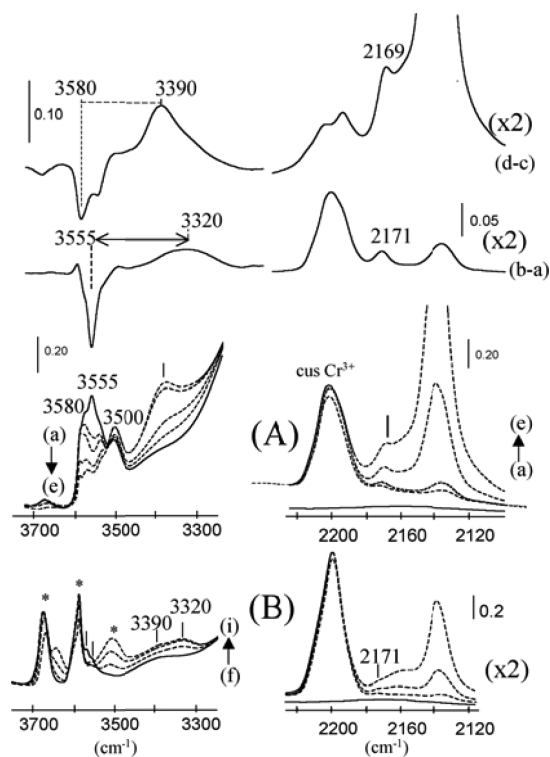


Figure 7. Infrared spectra of MIL-100 samples exposed to excess $(\text{CF}_3)_2\text{CHOH}$, evacuated at room temperature (A) or 373 K (B), and then loaded with CO at 100 K. Spectra a–e and f–i are recorded with no CO and increasing dosage of CO. Subtracted spectra are used to compare the shift of the $\nu(\text{OH})$ band. Reprinted with permission from ref 87. Copyright 2007 American Chemical Society.

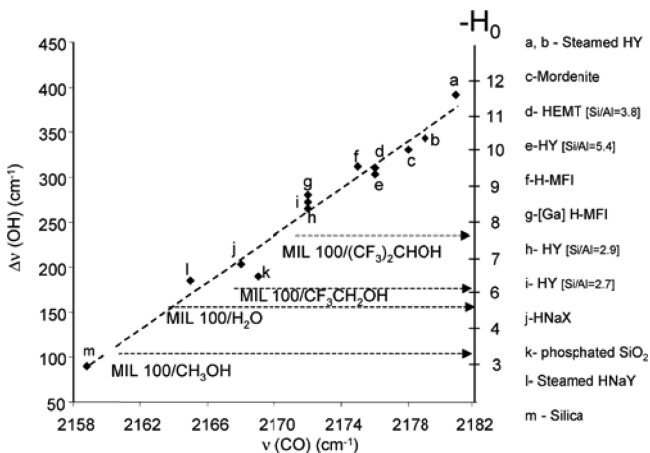


Figure 8. Correlation between the Hammett acidity function H_0 and the $\Delta\nu(\text{OH})$ shift measured by CO adsorption. Reprinted with permission from ref 87. Copyright 2007 American Chemical Society.

sites in MOFs. The change of the distribution of acid sites in MIL-100 with different degrees of hydration was semi-quantitatively monitored.^{84,87} The introduction of Brønsted acidity and an increase of Lewis acid sites in CF_3COOH - or HClO_4 -treated MIL-100 were also studied using this method.¹¹⁷

Although not as commonly used as CO, acetonitrile, also a small molecule with low basicity ($\text{p}K_b = 24$), shows great potential for utility in determining strong Brønsted acid sites in MOFs. It is even better when deuterated acetonitrile (CD_3CN) is used to give a less complex spectrum.¹⁶⁹ Characteristic IR

bands for protonated CD_3CN in solid acids usually appear in the region of 3650–2800, 2300, and 2150–2200 cm^{-1} .¹⁷⁰

A more routine function for IR spectra in studying the Brønsted acidic MOFs involves confirming the incorporation of those Brønsted acidic moieties or functionalities by their characteristic absorption bands. This is normally done by comparing the IR spectra of MOF before and after functionality encapsulation or PSM. Regions of interest include 900–1400 cm^{-1} , for all kind of sulfate, sulfonate, sulfonic acid groups;¹⁷¹ ca. 1720 cm^{-1} , for protonated carboxylates;¹⁷² and 800–1000 cm^{-1} , for those metal–oxo stretching frequencies if polyoxometalates are encapsulated into the framework.¹⁷³ Compared to the aforementioned direct measurement of acidity from IR spectra of CO adsorbed samples, these results are indirect evidence, and it is necessary to include chemical knowledge and other characterization techniques to reach a definitive conclusion.

3.5. Solid-State Nuclear Magnetic Resonance (NMR) Methods

Another powerful tool to study solid acids is solid-state NMR. Thanks to the development of milestone techniques such as cross-polarization (CP), magic-angle spinning (MAS) of solids, and high-resolution and pulse-field-gradient magnetic resonance, the significant improvements in resolution for solids have led to a steady increase of the popularity of this technique.¹⁷⁴ The application of NMR techniques in MOF chemistry is also constantly evolving from simple characterization of the existence of free DMF molecules in the as-synthesized MOF pores¹⁷⁵ to a technique for monitoring the encapsulation of moieties^{176,177} and characterizing the complex processes that take place within the pores of MOFs. NMR techniques have also been used to help in the structure determination of MOFs¹⁷⁸ and to study luminescence properties,¹⁷⁹ diffusion and relaxation of molecules within the pores,^{180,181} apportionation of functionalities,¹⁸² and gas sorption.^{183,184} Thus, we are also expecting this technique to be very powerful in characterizing the Brønsted acidity in all these systems.

Direct characterization of Brønsted acidic protons is commonly achieved using ^1H MAS NMR of solid samples. Using this technique, successful detection of Brønsted acidic protons was achieved in sulfonic acid functionalized MIL-53.¹²³ The ^1H NMR spectrum exhibited a new signal at 13–14 ppm in the sulfonic acid functionalized MIL-53, which is not seen in the pristine MOF. A critical issue about this result is to confirm that this proton is attached to the sulfonate, making it a strong Brønsted acidic proton, rather than attached to nonreacted linkers (H_2BDC) in the pore or protonated linkers on the framework during the PSM. To address this point, ^{13}C CPMAS NMR and ^1H – ^{13}C heteronuclear shift correlation (HETCOR) NMR experiments were carried out to confirm the absence of any H_2BDC species in the pore or on the framework, thus finally confirming the position of this acidic proton on the sulfonic acid group and it being a strong Brønsted acid site.

Further estimation of the framework-bearing Brønsted acid strength could be achieved through direct observation of changes of the ^1H resonance position after introduction of bases. As shown by the ^1H MAS NMR spectra of MIL-53 samples (dehydrated at 473 K), a change of the resonance position of the signal of bridging Al–OH groups from 2.3 ppm for the pristine MIL-53 to 3.5, 5.3, and 4.5 ppm (Figure 9a), after adsorption of acetonitrile, ammonia, and pyridine, respectively, was observed (Figure 9b–d).¹⁸⁵ This indicates an existing interaction between these nitrogen bases and the hydroxyl protons of bridging Al–

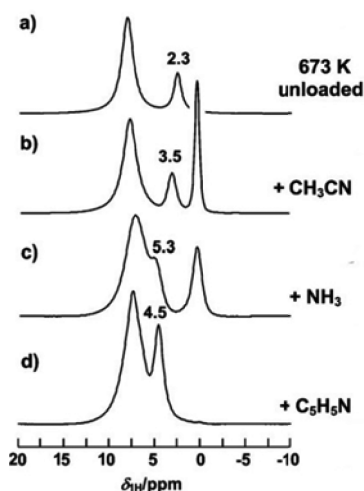


Figure 9. Recorded ^1H MAS NMR of MIL-53 samples activated at 473 K (a) and subsequently loaded with acetonitrile (b), ammonia (c), and pyridine (d). Adapted with permission from ref 185. Copyright 2010 American Chemical Society.

OH groups, and the low-field shift of $\Delta\delta_{\text{1H}} = 1.2$ ppm, after loading of acetonitrile, points to a low Brønsted acid strength compared to those found for bridging $\text{Si}-(\text{OH})-\text{Al}$ hydroxyl groups in zeolites H-Y, H-MOR, and H-ZSM-5.^{186,187}

However, more often the ^1H NMR signals of interest are obscured due to the relatively narrow window of the ^1H NMR spectra plus the presence of large amounts of hydrogen atoms from the organic linkers or solvent molecules in the MOF. This might be solved by indirect characterization of those acidic protons. One way to achieve this is through characterization of the change of chemical environment of other nuclei linked to the proton. A weakly Brønsted acidic anilinium-functionalized UiO-66(Zr) framework⁹⁹ was studied using this method. In this MOF, the acidic protons, if any, will be residing on the N atoms of the amino groups on the organic linker. This will change the chemical environment of the nitrogen atoms, which will be reflected by a chemical shift change in the ^{15}N CP-MAS NMR spectra. As shown in Figure 10, a clean spectrum was obtained with two distinct resonances at 56 and 137 ppm (referenced to

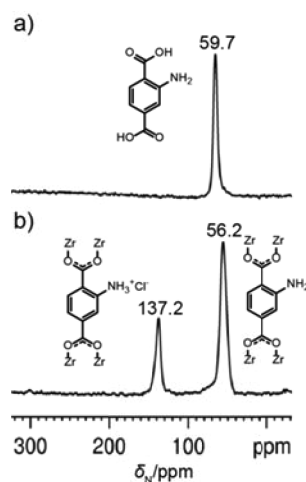


Figure 10. Recorded ^{15}N CP-MAS NMR of (a) $\text{H}_2\text{BDC-NH}_2$ and (b) anilinium-functionalized UiO-66. Adapted with permission from ref 99. Copyright 2011 American Chemical Society.

liquid N_2 at 0 ppm and glycine at 36.2 ppm), assigned to N atoms on BDC-NH_2 and $\text{BDC-NH}_3\text{Cl}$, respectively, further supported by solution ^{15}N NMR experiments performed on a 1:1 mixture of $\text{H}_2\text{BDC-NH}_2$ and HCl . Integration of direct-excitation NMR with a relaxation time of 45 s gave ca. 33% of protonated amine. Although the method was found to be successful in quantification of the acid protons, two limitations were pointed out by this example: (i) synthetic difficulty for ^{15}N -labeled linkers and (ii) the limited variety of acidic protons that can be characterized in this way, as NMR active isotopes have to be present adjacent to the acid sites.

The second approach of indirect characterization of acidic protons is more versatile. Instead of studying the interaction between protons and framework-bearing acceptors, proton acceptors are introduced into the solid acids. This facilitates the measurement and lowers the cost, providing that only isotope-labeled small molecules are needed now. Similarly to those used in IR spectroscopy, probe molecules include strong bases, such as pyridine and amines, and also weak bases, including alcohol, acetone, and acetonitrile.¹⁸⁸ The significant difference in the spectra of the protonated and unprotonated forms of these probe molecules will be used to characterize the interaction with acid sites, providing information including quantification as well as the acid strength. Moreover, the use of phosphorus-containing probe molecules such as trialkylphosphines and trialkylphosphine oxides further helps in the quantification of acid sites on solid acids by means of ^{31}P MAS NMR and CPMAS NMR, as ^{31}P has an isotopic abundance of 100%, a relatively high magnetogyric ratio, and a spin of $1/2$, making spectra relatively easy to interpret.¹⁸⁹ With complementary data from elemental analyses or solution NMR of the digested sample, the exact amount of each type of acid site can be determined. Recently, the use of trimethylphosphine oxide (TMPO) as probe molecules in a superacidic MOF was reported.⁹² TMPO is chosen because of its suitable size for diffusion in MOF pores. As shown in Figure 11, a downfield-shifted resonance at 69 ppm (reference to 98% H_3PO_4 at 0 ppm) was found in sulfated MOF, indicating a strongly acidic site

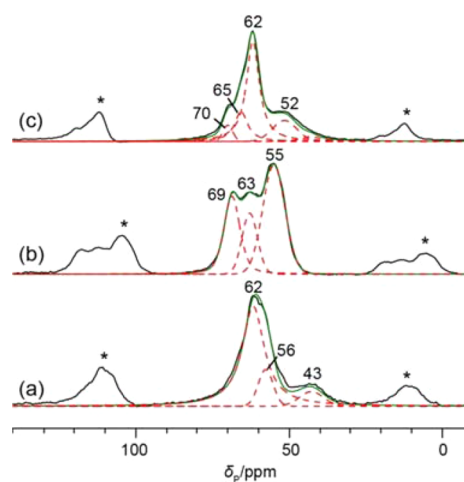


Figure 11. ^{31}P MAS NMR spectra of TMPO loaded on MOF-808 (a), sulfated MOF-808 (b), and sulfated MOF-808 exposed to atmosphere moisture (c). Experimental spectra are shown in black, deconvoluted peaks in red dashes, and the sum of the deconvoluted peaks in green. The asterisks denote spinning sidebands. Adapted with permission from ref 92. Copyright 2014 American Chemical Society.

generated from the sulfuric acid treatment, which is consistent with the results from other characterization methods. The neutralization of this strong acidity by atmospheric moisture is also observed when the 69 ppm resonance loses almost all of its intensity after exposure to atmospheric moisture.

3.6. Diffraction Techniques

Diffraction techniques (including X-ray, electron, and neutron diffractions) are typically used for interpreting the solid structures. Compared to other Brønsted acidic polymers, which are always amorphous, or metal oxides and zeolites large crystals, which are hard to obtain, the highly crystalline MOFs render an excellent platform to study the detailed structure of the acidic sites. Preliminary trials have been carried out by successfully harvesting single crystals of sulfuric acid solution treated MOF-808.⁹² Zr-bound sulfate groups on the SBU were unequivocally determined through a single crystal X-ray diffraction measurement (Figure 12), which serves as a good starting point to understand the sulfate promotion effect in this material.

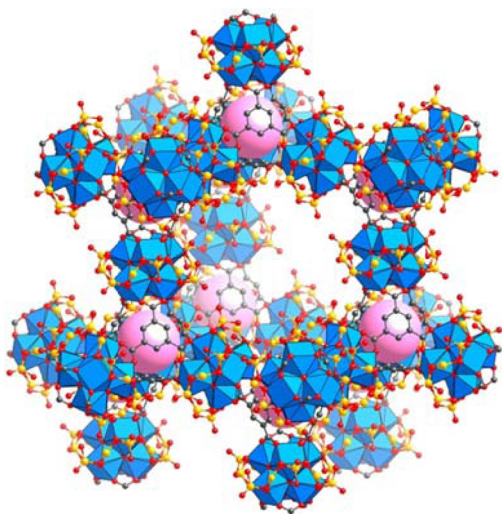


Figure 12. Structure representation of sulfated MOF-808 single crystal. Atom color scheme: Zr, blue polyhedra; C, gray; O, red; and S, orange. All H atoms are omitted for clarity. Violet spheres indicate the space in the tetrahedral cage of the framework.

To better apply such techniques in characterizing Brønsted acidic MOFs, the following prerequisites are highly recommended: (i) Obtain highly crystalline materials and, if possible, single crystals with a suitable size for diffraction experiments. Typically, single crystals with all three dimensions larger than 50 μm are needed for single-crystal XRD, while a crystal of a few millimeters is preferred for single-crystal neutron diffraction experiments. For Brønsted acidic MOFs that are not able to be grown into single crystals, a single-crystal structure for nonacidic pristine MOF could also be valuable to ease the refinement of powder data. (ii) Increase the occupancy of target atoms or atom groups and reduce the degree of disorder. This greatly helps to obtain high-resolution structure solutions. (iii) Reduce the noise. This could be done, for example, by careful removal of guest molecules inside the pores. It is recommended that during this process, the condition of the crystal is frequently checked, and if acidic protons in the solid acids will be studied using neutron diffraction techniques, deuterated MOF are preferred to reduce the noise.

4. APPLICATIONS

4.1. Ammonia Capture

Ammonia is one of the unpleasant chemicals related to life, contributing to a number of environmental problems, including atmospheric particulate matter,¹⁹⁰ acidification of soil, and alteration of the global greenhouse balance.¹⁹¹ The atmospheric ammonia level, from contributors including the agricultural sector (fertilizer and livestock operations), losses from ammonia refrigeration systems, and oxidative degradation of amine-based solvents in CO_2 capture plants, is predicted to keep rising.¹⁹² Therefore, safe removal of ammonia is needed for a pleasant environment and better human health.

Under the big scope of ammonia capture applications, there are two main categories, each requiring materials that bear specific merits. One is irreversible ammonia removal. This direction targets toxic gas removal applications, like gas masks. Two criteria are prominent here. First, the absorption or adsorption of ammonia occurs at low ammonia concentration. This is important because the capturing agent should still be able to remove ammonia from the environment where it is present at low concentration to make sure the concentration afterward is below the harmful level, for example, 25 ppm, the recommended CAL-OSHA permissible ammonia exposure limit.¹⁹³ The second criterion is the competitive ammonia removal under moist conditions due to the presence of significant amounts of moisture in real world applications (for example, exhaled gas from humans). The other direction aims at reversible capture of ammonia in applications such as ammonia transportation and recycling. It is beneficial to use solid adsorbents to replace the toxic, corrosive, and difficult-to-handle compressed liquid ammonia. For this purpose, criteria of the material such as high ammonia uptake capacity at 1 bar or even higher pressure, high cycling performance, and stability in the presence of ammonia are important.

MOFs have attracted tremendous attention in the fields of gas storage and gas separation over the past 20 years.^{18–25} Preliminary investigations have proved MOFs and also related MOF/graphite oxide composite materials as potentially promising materials for ammonia capture.²² A series of MOFs have been surveyed, including MOFs with Lewis acidic open metal sites (MOF-74, HKUST-1) and MOFs without acidic sites per se (MOF-177, IRMOF-3 and IRMOF-62) for capture of ammonia in kinetic breakthrough measurements.^{194–196} The good performance of MOF-74 and HKUST-1 indicates that Lewis acidic open metal sites are promising capturing sites for ammonia under dry conditions.

The contribution of Brønsted acidic centers in MOFs for ammonia capture was observed alongside with Lewis acidic open metal sites in MIL-100.¹⁹⁷ As mentioned before, water molecules bound to Fe(III) centers that cannot be removed under the given activation conditions exhibit Brønsted acidity.^{84,85} Not surprisingly, excess moisture in ammonia was found to be detrimental to its capacity when Lewis acidic sites are primarily responsible for ammonia capture, as water molecules compete for open metal sites, a lethal problem for irreversible ammonia removal applications like gas masks. However, since the ratio of Brønsted acidic center to its Lewis acidic counterpart in this MOF was not determined and is highly dependent on activation conditions, the effectiveness of Brønsted acids under moist conditions toward ammonia removal in this material is yet to be determined.

The competitive strength of Brønsted acidic centers in MOFs as alternatives to those Lewis acidic sites for potential ammonia

removal was later confirmed. Excellent low- and ambient-pressure ammonia capacity were observed in a primarily Brønsted acidic MOF-205 analogue (MOF-205-OH) made of free phenolic $-OH$ groups containing linkers under dry conditions (Figure 13a).¹⁹⁸ Comparison of ammonia uptake

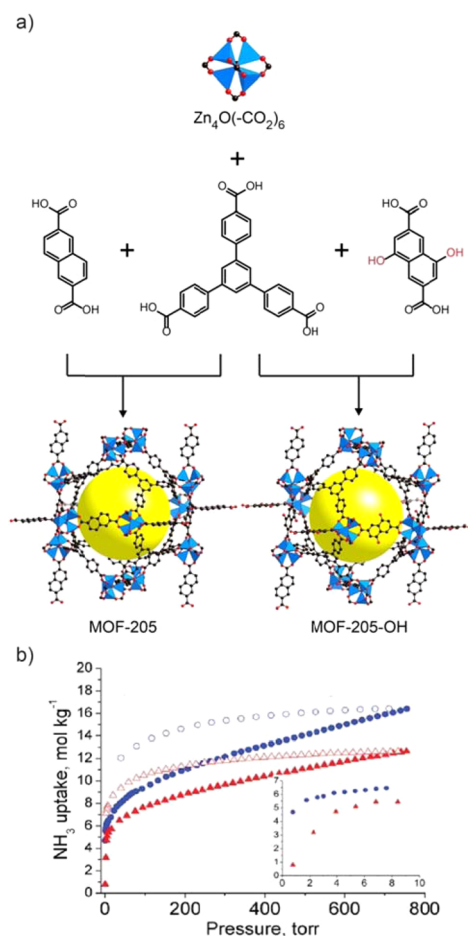


Figure 13. (a) Structure representation of MOF-205 and MOF-205-OH. Atom color scheme: Zn, blue polyhedra; C, black; and O, red. All H atoms are omitted for clarity. (b) NH_3 adsorption (solid symbols)/desorption (open symbols) isotherm for MOF-205 (red) and MOF-205-OH (blue) up to 1 bar at 298 K. The inset shows an expansion of the low-pressure region. Panel b is adapted with permission from ref 198. Copyright 2013 American Chemical Society.

between pristine MOF-205 (DUT-6) and Brønsted acidic MOF-205 has shown that the functionalized MOF exhibits an extra uptake of ca. 4 mmol g^{-1} at 1 mbar (Figure 13b), corresponding to two ammonia molecules per acidic sites, clearly demonstrating the beneficial effect of Brønsted acidic sites on ammonia capacity at low relative pressure. However, the lack of ammonia uptake data under wet conditions makes it difficult to judge whether this material could be promising for irreversible ammonia removal applications. On the other hand, due to its ultrahigh surface area (BET surface area $4354 \text{ m}^2 \text{ g}^{-1}$), the observed ammonia uptake at 1 bar is 16.4 mmol g^{-1} , surpassing all other reported values in Lewis acidic MOFs at that time. However, the MOF was found to lose its crystallinity after ammonia exposure, as indicated by the nonreversible ammonia isotherm as well as loss of the sharp powder XRD patterns after ammonia capture. This is in line with the observation for MOF-5 and MOF-177,¹⁵³ two other MOFs bearing the $Zn_4O(-CO_2)_6$ -type SBU. A rational explanation

points to guest-induced framework destruction by strong interactions (hydrogen bond) between ammonia and the Zn_4O cluster.

An ammonia-stable, thus potentially reusable, zirconium-based $UiO-66-(NH_3Cl)_{0.33}(NH_2)_{0.67}$ featuring anilinium cations as the Brønsted acid source, was reported for ammonia capture studies.⁹⁹ Ammonia uptake at 1 mbar is below 1.5 mmol g^{-1} , indicating a weaker interaction, compared to phenolic $-OH$ groups, between ammonia and anilinium groups on the organic linkers. However, in this material, only one-third of the amino groups on the BDC- NH_2 linkers are protonated; thus, the uptake of ammonia could be further improved if complete protonation of the amino groups is achieved. As expected, double of the total ammonia uptake to ca. 3 mmol g^{-1} at 1 mbar was observed for 100% protonated $UiO-66-NH_3Cl$,¹⁰⁰ corresponding to a contribution of approximately 0.7 molecules of ammonia per anilinium site. The capacity at 1 bar was also improved from ca. 7 mmol g^{-1} in $UiO-66-(NH_3Cl)_{0.33}(NH_2)_{0.67}$ to ca. 11 mmol g^{-1} in $UiO-66-NH_3Cl$ (Figure 14). Most impressively, this material

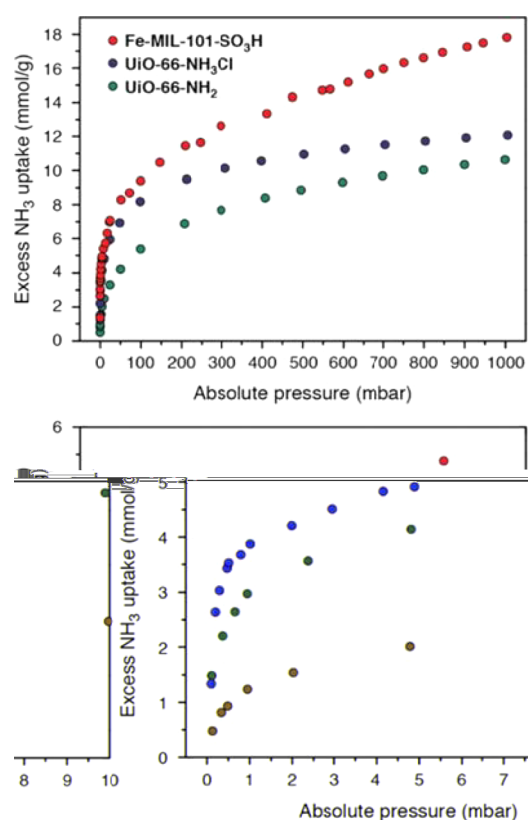


Figure 14. Ammonia adsorption at 298 K in selected MOFs (MIL-101- SO_3H , red; $UiO-66-NH_3Cl$, blue; and nonacidic $UiO-66-NH_2$, green for comparison). Reprinted with permission from ref 100. Copyright 2014 American Chemical Society.

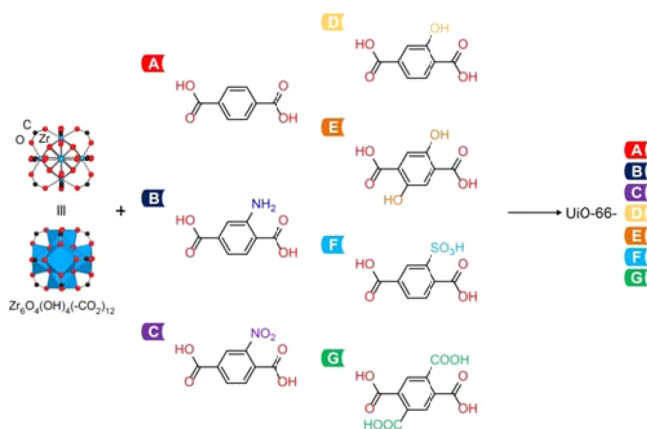
survived exposure up to 1 bar of ammonia, as evidenced by the reversible uptake of ammonia and retention of both crystallinity and porosity, probably due to the framework stability of Zr MOFs as well as the weak interaction between ammonia and weakly Brønsted acidic anilinium sites.

Grand canonical Monte Carlo (GCMC) simulations using a developed force field describing the interactions between NH_3 and the functional groups were carried out to study the adsorption behavior of NH_3 in MOFs functionalized with phenolic $-OH$, $-C=O$, $-Cl$, and $-COOH$.¹⁹⁹ In all four MOF

systems examined, Brønsted acidic functional groups (i.e., phenolic –OH and –COOH) were found to increase the ammonia capture capacity in the low-pressure region. This was explained with an increased acidity and dielectric constant from Brønsted acid functional groups in MOFs, which can promote protonation of ammonia, thus leading to a better uptake performance at low pressure.

This conclusion was later experimentally tested using a series of functionalized UiO-66,²⁰⁰ among which four were Brønsted acidic (UiO-66-D, UiO-66-E, UiO-66-F, and UiO-66-G) (Scheme 9). Breakthrough measurements under dry conditions

Scheme 9. UiO-66 with Various Functional Groups for Ammonia Capture



and 2000 mg m⁻³ ammonia concentration have shown the superior performance of these Brønsted acidic MOFs compared to pristine UiO-66 and nonacidic UiO-66-C. UiO-66-D was identified with the highest capacity of 5.69 mmol g⁻¹, surpassing those with an increased density of –OH groups, as in UiO-66-E, or an increased Brønsted acid strength, as in UiO-66-F/G. (Table 2). This was explained due to the decreased surface area

Table 2. Ammonia Capacity of UiO-66 with Various Functional Groups at 293 K^a

sample	surface area (m ² g ⁻¹)	capacity for ammonia			
		mmol g ⁻¹		μmol m ⁻²	
		dry ^b	wet ^c	dry ^b	wet ^c
UiO-66-A	1100	1.79 ^d	2.75 ^d	1.63 ^d	2.50 ^d
UiO-66-B	1096	3.56 ^d	3.01 ^d	3.25 ^d	2.75 ^d
UiO-66-C	729	1.98 ^d	1.60 ^d	2.72 ^d	2.19 ^d
UiO-66-D	946	5.69 ^e	2.77 ^e	6.01 ^e	2.93 ^e
UiO-66-E	814	2.29 ^e	2.16 ^e	2.81 ^e	2.65 ^e
UiO-66-F	323	2.24 ^e	1.45 ^e	6.93 ^e	4.49 ^e
UiO-66-G	221	2.83 ^e	1.83 ^e	12.8 ^e	8.28 ^e

^aAll data are from ref 200. ^b0% relative humidity (RH). ^cBefore being fed with ammonia, the sample was pre-equilibrated at 80% RH for 2 h. ^dAmmonia feed concentration of 1000 mg m⁻³; ^eAmmonia feed concentration of 2000 mg m⁻³.

in latter case, due to bulkier functional groups or potential activation problems. To examine the influence of a low specific surface area for Brønsted acidic UiO-66-F and -G, the ammonia removal capacity per surface area is calculated in Table 2. In this comparison, under both dry and wet conditions, Brønsted acidic MOFs outperform their nonacidic counterparts. Although the

benefit could be overestimated, it is clear that Brønsted acidic sites are beneficial for ammonia removal at low concentration. Also, stronger Brønsted acidic sites (–SO₃H and –COOH) exhibited higher ammonia capture capacity than weak Brønsted acidic sites (phenolic –OH).

Thus, MIL-101-SO₃H was studied as a representative for high surface area MOFs with strong Brønsted acidic sites. Not surprisingly, compared to anilinium groups in UiO-66, the more acidic framework of MIL-101-SO₃H yielded an exceptional adsorbent, which displayed better uptake both at low pressure (3.9 mmol g⁻¹ at 1 mbar) and, owing to its significantly higher specific surface area, at higher pressure as well (17.80 mmol g⁻¹ at 1 bar) (Figure 14).¹⁰⁰ This value at 1 bar also surpassed the record in Brønsted acidic MOFs kept by MOF-205 with phenolic groups. Although it has not been done yet, it would be worth checking its performance under wet conditions, as well as in the following cycles.

Another interesting related topic would be the nature of interactions between adsorbed ammonia and the MOF interior. This is important as it determines whether this adsorption will be a reversible or irreversible process. When ammonia interacts with a Brønsted acid, it forms an ammonium cation and becomes an integral part of the functional group, and thus, it is irreversibly bound. This could be important when irreversible ammonia capture is required for an application. Quantum chemical methods were used to calculate the interactions between ammonia and Brønsted acidic functional groups, including –OH, –COOH, –HSO₄, and –SO₃H connected to aromatic rings (Table 3).²⁰¹ All these model clusters, when in the gaseous phase, were found to be unable to transfer the acidic proton to ammonia molecules. However, if these functional groups are incorporated into MOFs, the surrounding atoms can create a dielectric polarization in the pores, and this dielectric polarization could affect whether or not ammonia will be protonated. Computed results have shown that protonation of ammonia will take place if strong Brønsted acidic functional groups such as –HSO₄ and –SO₃H are present, even if the dielectric constant is small; however, in weaker Brønsted acids, such as carboxylic acid, the protonation will only happen when strong polarization is felt within the MOF pore.

As described in this section, we have identified two types of applications for ammonia capture: reversible and irreversible capture. Important judging criteria are uptake at ambient pressure (1 bar) and recyclability of the material for the former and uptake at low pressure (1 mbar) and competitive uptake under moist condition for the latter. MOFs featuring Brønsted acid sites have been evaluated in the context of ammonia uptake according to these criteria. Studies have shown that Brønsted acidic MOFs can display excellent ammonia adsorption characteristics. Weaker Brønsted acid sites are preferred for reversible capture applications due to the ease of recycling, while strong Brønsted acidic sites, which are tightly bound to adsorbed ammonia molecules, are ideal for irreversible ammonia removal applications. For both cases, MOFs should bear specific surface areas higher than 1000 m² g⁻¹ to take advantage of these Brønsted acidic sites.

4.2. Proton-Conducting Materials

Proton conductivity plays a crucial role in processes as diverse as the chemical energy production (hydrocarbon) in plants and the electric energy production in fuel cells, both of which figure prominently as alternatives to the depleting fossil fuels. Consequently, proton transport and transfer phenomena have

Table 3. Observation of the Protonation of Ammonia (Yes or No) on Selected Brønsted Acidic Groups under Various Dielectric Values^a

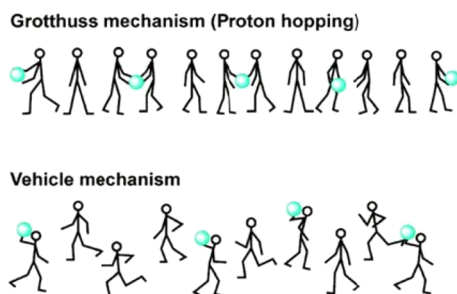
solvent ^b	dielectric constant	NH ₃ protonation ^c			
		R-SO ₃ H (pK _a = 0.27)	R-HSO ₄ (pK _a = 1.92)	R-COOH (pK _a = 4.17)	R-OH (pK _a = 9.51)
gaseous phase	0	no	no	no	no
		-52.1	-65.9	-41.8	-34.3
chloroform	4.7113	yes	yes	no	no
		-104.6	-142.6	-58.1	-50.8
pentanal	10	yes	yes	no	no
		-114.0	-151.5	-58.1	-50.8
2-hexanone	14.136	yes	yes	yes	no
		-116.4	-155.9	-54.3	-50.6
acetone	20.493	yes	yes	yes	no
		-118.3	-151.5	-55.3	-50.4
nitroethane	28.29	yes	yes	yes	no
		-119.3	-151.5	-56.0	-50.3

^aAll data are from ref 201. ^bThe name of the solvent corresponds to each dielectric constant in the second row. ^cThe binding energy (kJ/mol) of ammonia with each functional group at different dielectric constant is given in the second row of each cell.

been studied extensively, with focus placed on both understanding the mechanism and developing materials with good proton-conducting properties.

As the only ion that has no electron shell of its own, the proton strongly interacts with the electron density of its environment and, thus, normally cannot be transported on its own. Two principal mechanisms are used to describe proton conductivity in materials without direct translational motion of protons (Scheme 10). The first case is the assistance of proton migration by the

Scheme 10. Illustration of Proton Transportation Mechanisms^a



^aAdapted with permission from ref 204. Copyright 2008 American Chemical Society.

translational dynamics of bigger protogenic species (vehicle mechanism), e.g., H₃O⁺ (Scheme 10, bottom).²⁰² In the other case, the proton carriers, like swings, show pronounced local dynamics but reside on their sites, while the proton can hop through hydrogen bonds when two “swings” are close enough, also known as the “Grotthuss mechanism” (Scheme 10, top).²⁰³

Brønsted acids or solid materials with Brønsted acidic sites have long been studied in this field for their good proton-conducting performance. Nafion, the first exploited proton-conducting material for fuel cell applications, is a Brønsted acidic sulfonated perfluoro polymer.²⁰⁵ Other Brønsted acidic systems include oxo acids and their salts, polymer-embedded sulfuric acid, polymer with ammonium salts, and supported heteropolyacids, exhibiting high proton conductivity at various temperatures and humidities.²⁰⁶ With the rapid development

of MOFs since the 1990s, great attention has been focused on new opportunities in these inorganic–organic hybrid materials.^{207,208} Unique properties are expected from their designable structure, modifiable pore surface functionality and/or included guest molecules, and crystalline nature for intermediate characterization by diffraction techniques.

Use of Brønsted acidic MOFs as proton-conducting materials is categorized into two types, based on two rational ways to introduce proton carrier moieties. The simplest approach would be to use the MOF pores to encapsulate acidic moieties, both as ions such as NH₄⁺, H₃O⁺, and HSO₄⁻ and neutral molecules. The second approach would be fixing Brønsted acidic groups (for example, sulfonic acid and phosphonic acid groups) on the framework, which could be achieved by functionalization of the organic linkers.

Studies on a highly proton-conductive MOF, (NH₄)₂(ADP)-[Zn₂(OX)₃].3H₂O (OX = oxalate, ADP = adipic acid), appeared in 2009, with the proton conductivity found to be 8 × 10⁻³ S cm⁻¹ at 25 °C under 98% RH conditions,²⁰⁹ comparable to that of Nafion. Synthesized by a hydrothermal method, this MOF successfully employed two approaches to incorporate the proton carriers. Ammonium ions were introduced as cations using the anionic framework [Zn₂(OX)₃]²⁻, while Brønsted acidic adipic acid was successfully incorporated inside the honeycomb-shaped pore. Single X-ray diffraction experiments showed that water molecules are necessary to form hydrogen-bonded networks for effective proton transportation. This was experimentally demonstrated 5 years later when a series of three phases of this MOF—anhydrate, dehydrate, and trihydrate—was obtained as single crystals.²¹⁰ A careful examination of these crystal structures by X-ray crystallography has identified water's role in triggering hydrogen-bonding-network rearrangements, a key factor for MOF's proton conductivity (Figure 15a–c). Proton conductivity was measured to vary from ca. 10⁻¹² S cm⁻¹ in anhydrous MOF to ca. 10⁻⁴ S cm⁻¹ in the dihydrate phase and to ca. 10⁻² S cm⁻¹ in the trihydrate phase. As these polymorphs of MOF can be reversibly transformed through water adsorption/desorption processes, this discovery served as the first example of controllable crystalline proton-conducting pathways using MOFs. Furthermore, the proton conductivity of this MOF could also be controlled through cation exchange of NH₄⁺ with K⁺.²¹¹ Similarly, the substitution of NH₄⁺ with non-hydrogen-

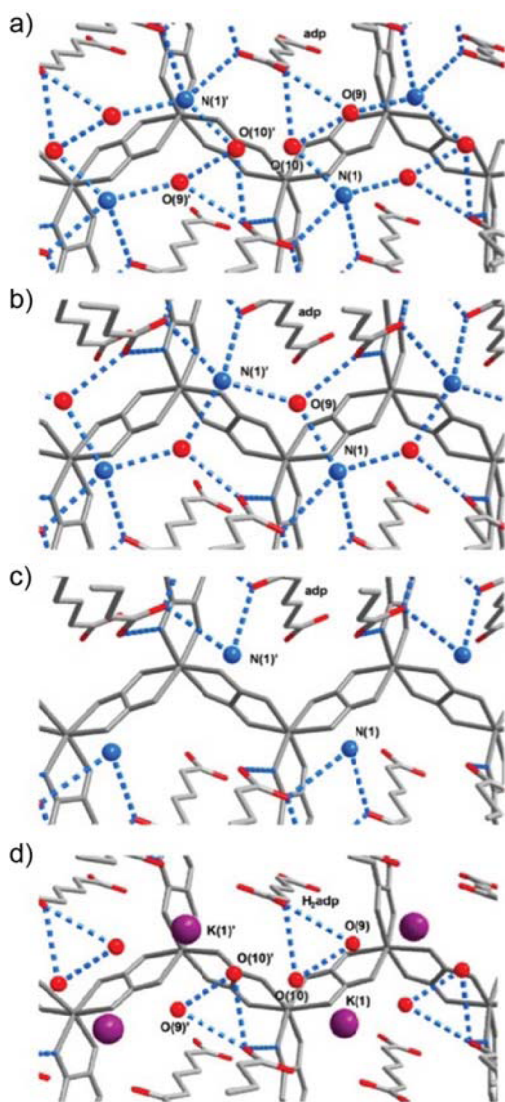


Figure 15. Representation of hydrogen-bonding network (blue dotted line) in (a) $(\text{NH}_4)_2(\text{ADP})[\text{Zn}_2(\text{OX})_3] \cdot 3\text{H}_2\text{O}$, (b) $(\text{NH}_4)_2(\text{ADP})[\text{Zn}_2(\text{OX})_3] \cdot 2\text{H}_2\text{O}$, (c) $(\text{NH}_4)_2(\text{ADP})[\text{Zn}_2(\text{OX})_3]$, and (d) $\text{K}_2(\text{ADP})[\text{Zn}_2(\text{OX})_3] \cdot 3\text{H}_2\text{O}$. The MOF backbones are shown as gray sticks. Adapted with permission from refs 210 and 211. Copyright 2014 American Chemical Society.

bonding species K^+ re-formed the hydrogen-bonded network (Figure 15d), which reduced the MOF's conductivity by 2 orders of magnitude under 98% RH at 25 °C.

Impregnation of the MOF with adipic acid already showed large promotion of proton conductivity in MOFs. It is thus reasonable to assume a better result from a stronger Brønsted acid. Recently, sulfuric acid soaked MOF-74(Ni) achieved a proton conductivity of $1.1 \times 10^{-2} \text{ S cm}^{-1}$ at 25 °C and 95% RH,²¹² higher than that of adipic acid impregnated zinc oxalate. One would expect the promoted proton conductivity due to hydrogen-bonded networks built with sulfuric acids and water molecules in these 1D hexagonal channels. Unexpectedly, both EDX and elemental analysis data indicated no traces of sulfur in the framework, excluding this possibility. It turned out that proton conductivity is achieved through a water-based hydrogen-bond system in the acidified MOF, $\text{H}^+@ \text{MOF-74}(\text{Ni})$. Here, protons bind to associated water molecules, forming protonated water clusters [mainly $\text{H}_3\text{O}^+ \cdots (\text{H}_2\text{O})_3$ and $\text{H}_2\text{O} \cdots \text{H}^+ \cdots \text{OH}_2$]

within 1D channels, thus giving rise to high conductivity and low energy barrier.

Strong organic Brønsted acids, toluenesulfonic acid (TsOH) and triflic acid (TfOH), were also incorporated in a similar manner to a more acid-stable MIL-101.²¹³ Unlike in the previous case of MOF-74(Ni), the existence of both acids together with water molecules was unequivocally confirmed by elemental analyses ($\text{TsOH}@ \text{MIL-101}$, $\text{MIL-101} \cdot 1.1 \text{ TsOH} \cdot 2\text{H}_2\text{O}$; $\text{TfOH}@ \text{MIL-101}$, $\text{MIL-101} \cdot 6.7 \text{ TfOH} \cdot 15\text{H}_2\text{O}$). $\text{TsOH}@ \text{MIL-101}$ only exhibited moderate proton conducting ability ($8.0 \times 10^{-6} \text{ S cm}^{-1}$ at 66 °C and 100% RH), probably due to their weaker acidity, larger non-hydrogen-bonded phenyl groups, and small loading of both acid and water molecules. The highest measured conductivity for $\text{TfOH}@ \text{MIL-101}$ reached 0.08 S cm^{-1} at 60 °C and 100% RH, comparable to that of fully hydrated Nafion.²¹⁴

Although quite high values were achieved in above examples under high RH, obvious limitations were still present regarding the proton conductivity at higher temperature and lower RH, which is highly desirable for fuel cell proton-exchange membranes. To deal with this problem, instead of building hydrogen-bonded networks in MOFs involving water molecules, which are sensitive to temperature and RH fluctuations, nonvolatile Brønsted acids, sulfuric acid and phosphoric acid, were introduced into acid-resisting mesoporous MIL-101 frameworks.⁵⁴ This was done by first impregnating the MOFs by diluted acid aqueous solution, followed by dehydration at various temperatures. It was determined that after dehydration at 150 °C, the targeted working temperature, acid concentration confined in the MOF pores reached 10 M, indicating water-deficient hydrogen bond systems. Such a simple approach affords solid materials with potent proton-conducting properties ($1 \times 10^{-2} \text{ S cm}^{-1}$ for $\text{H}_2\text{SO}_4@ \text{MIL-101}$, $3 \times 10^{-3} \text{ S cm}^{-1}$ for $\text{H}_3\text{PO}_4@ \text{MIL-101}$) at moderate temperatures (150 °C) and low RH (0.13%), ranking among the highest values achieved by MOF-based compounds.

With the above-mentioned examples exclusively involving proton conductivity introduced by acidic guest molecules in MOF pores, studies have also been done using MOF with Brønsted acidic functional groups covalently bound to the organic linker, type III in the aforementioned categories. Proton conductivity of a series of functionalized MIL-53 was examined (Table 4).²¹⁵ Phenolic $-\text{OH}$ and carboxylic acid groups were found to increase the proton conductivity by 1–2 orders of magnitude under 95% RH and different temperatures, alongside with decreased activation energy due to their stronger Brønsted acidity. More importantly, the proton conductivity of this material was further shown to be controllable by varying the ratio between different linkers in the MTV system.²¹⁶

Table 4. Proton Conductivities at 298 and 353 K under 95% RH and Activation Energies for MIL-53 with Various Functional Groups^a

sample	σ (S cm^{-1})		E_a (eV)
	298 K	353 K	
$\text{Al}(\text{OH})(\text{BDC})(\text{H}_2\text{O})$	2.3×10^{-8}	3.6×10^{-7}	0.47
$\text{Al}(\text{OH})(\text{BDC-NH}_2)(\text{H}_2\text{O})$	2.3×10^{-9}	4.1×10^{-8}	0.45
$\text{Al}(\text{OH})(\text{BDC-OH})(\text{H}_2\text{O})$	4.2×10^{-7}	1.9×10^{-6}	0.27
$\text{Fe}(\text{OH})(\text{BDC}(\text{COOH})_2)(\text{H}_2\text{O})$	2.0×10^{-6}	0.7×10^{-5}	0.21

^aAll data are from ref 215.

Table 5. List of Known Catalytic Brønsted Acidic MOFs and Summary of Reactions Catalyzed

MOF materials ^a	substrate(s)	reaction(s) catalyzed	ref
H ₃ PW ₁₂ O ₄₀ @[Cr ₃ F(H ₂ O) ₂ O(BDC) ₃]	styrene oxide and methanol	alcoholysis	227
	resorcinol and ethyl acetate; acetic acid and <i>n</i> -butanol	Pechmann reaction; esterification	228
	acetaldehyde; acetaldehyde and phenol; acetaldehyde and methanol	aldol condensation; Baeyer condensation; acetalization	229
	glucose; fructose	carbohydrate dehydration	230
H ₃ PW ₁₂ O ₄₀ @[Cu ₃ (BTC) ₂]	acetic acid and <i>n</i> -propanol	esterification	231
H ₄ SiW ₁₂ O ₄₀ @[Cu ₃ (BTC) ₂]	methanol; acetic acid and ethylene	etherification; esterification	232
H ₃ PW ₁₂ O ₄₀ @[Al ₃ F(H ₂ O) ₂ O(BDC-NH ₂) ₃]	acetaldehyde	aldol condensation	233
Pt/H ₃ PW ₁₂ O ₄₀ @[Cr ₃ F(H ₂ O) ₂ O(BDC-NH ₂) ₃]	hydrogen and toluene; carbon monoxide and oxygen	hydrogenation; oxidation	234
Ru/H ₃ PW ₁₂ O ₄₀ @[Cr ₃ F(H ₂ O) ₂ O(BTC) ₂]	cellulose and hydrogen	cellulose conversion	235
Ru/H ₃ PW ₁₂ O ₄₀ @[Cu ₃ (BTC) ₂]	cellulose and hydrogen	cellulose conversion	236
[SO ₃ H(CH ₂) ₄ IM][HSO ₄] and [SO ₃ H(CH ₂) ₄ TEDA][HSO ₄] @ [Cr ₃ F(H ₂ O) ₂ O(BDC) ₃]	benzaldehyde and glycol	acetalization	237
[SO ₃ H(CH ₂) ₃ HIM] ₃ PW ₁₂ O ₄₀ @ Fe ₃ F(H ₂ O) ₂ O(BDC) ₃]	oleic acid and ethanol	esterification	68
Zn ₃ (OH) ₂ (BDC) ₂ (DEF) ₂ , Zn ₄ O(BDC) ₃ , and Zn ₄ O(NDC) ₃	toluene, biphenyl, and <i>tert</i> -butyl chloride	Friedel–Craft alkylation	73, 238, 239
Cu ₃ (BTC) ₂	furfuryl alcohol; benzaldehyde and malononitrile	Knoevenagel reaction; oligomerization	37, 240
V(OH)(BDC-NH ₂)	styrene oxide and carbon dioxide	carbonation reaction	241
Fe ₃ F(H ₂ O) ₂ O(BTC) ₂	1,3-cyclohexadiene and dimethyl fumarate; α -pinene oxide; citronellal	Diels–Alder reaction; isomerization	117
Cr ₃ F(H ₂ O) ₂ O(BDC) ₃ , Cr ₃ F(H ₂ O) ₂ O(BDC-NO ₂) ₃ and Cr ₃ F(H ₂ O) ₂ O(BDC-NH ₂) ₃	benzaldehyde and methanol	acetalization	242
Al ₃ F(H ₂ O) ₂ O(BDC-NH ₂) ₃	benzaldehyde dimethylacetal and malononitrile	deacetalization–Knoevenagel condensation	243
Zr ₆ O ₃ (OH) ₃ (BTC) ₂ (SO ₄) _{2.5} (H ₂ O) _{2.5}	anisole and benzoic acid; oleic acid and methanol; methylcyclopentane; α -pinene	Friedel–Craft acylation; esterification; isomerization	92
Cr ₃ F(H ₂ O) ₂ O(BDC) _x (BDC-OSO ₃ H) _{3-x}	acetic acid and <i>n</i> -butanol	esterification	124
Cr ₃ F(H ₂ O) ₂ O(BDC-SO ₃ H) ₃	acetic acid and <i>n</i> -hexanol	esterification	134
	2-butanol	dehydration	244
	fructose	carbohydrate dehydration	245
	cellulose	hydrolysis	102
Al(OH)(BDC-AMMal) and Al(OH)(BDC-AMSuc)	<i>cis</i> -2,3-epoxybutane and methanol	alcoholysis	246
Zr ₆ O ₄ (OH) ₄ (BPDC) _x (BPDC-Squar) _{6-x}	indole and β -nitrostyrene	Friedel–Craft alkylation	247
Zr ₆ O ₄ (OH) ₄ [BDC-(COOH) ₂] ₆	methyl benzylidene carbamate and nitromethane	Mannich reaction	248
Zr ₆ O ₄ (OH) ₄ (BDC-NH ₂) _x (BDC-NHCH ₂ CH ₂ CH ₂ SO ₃ H) _{6-x}	benzaldehyde and methanol; benzaldehyde and <i>o</i> -phenylenediamine	acetalization; condensation	249
Al(III)@Cr ₃ F(H ₂ O) ₂ O(BDC-SO ₃ H) ₃	mesitylene and benzyl alcohol	Friedel–Craft alkylation	250
[Ln(H ₂ DBBP)(H ₃ DBBP)(H ₂ O) ₄](H ₂ O) _x Ln = La, Ce, Pr, Nd, Sm, Gd	benzaldehyde and cyanotrimethylsilane	cyanosilylation of aldehydes	251
Cu(L-ASP)(BPE) _{0.5} (HCl)(H ₂ O) and Cu(D-ASP)(BPE) _{0.5} (HCl)(H ₂ O)	<i>cis</i> -2,3-epoxybutane and methanol	alcoholysis	116
[(R)-TBBP-1]Cu ₂ (H ₂ O) ₂ and [(R)-TBBP-2]Cu ₂ (H ₂ O) ₂	indole and <i>N</i> -sulfonyl aldimines	Friedel–Craft alkylation	252

^aIM = imidazole; TEDA = triethylenediamine; H₂NDC = naphthalene-2,6-dicarboxylic acid; H₂BDC-AMMal = 4-((2,5-bis(carboxylate)phenyl)amino)-4-oxobut-2-enoic acid; H₂BDC-AMSuc = 4-((2,5-bis(carboxylate)phenyl)amino)-4-oxobutanoic acid; H₂BPDC = biphenyl-4,4'-dicarboxylate; H₂BPDC-Squar = 3-((3,5-bis(trifluoromethyl)phenyl)amino)-4-(2-(4'-carboxylphenyl)-5-carboxylphenyl)-cyclobut-3-ene-1,2-dione; H₄DBBP = 2,2'-diethoxy-1,1'-binaphthalene-6,6'-bisphosphonic acid; H₄(R)-TBBP-1 = (R)-3,3',6,6'-tetrakis(4-benzoic acid)-1,1'-binaphthyl phosphate; H₄(R)-TBBP-2 = (R)-4,4',6,6'-tetrakis(4-benzoic acid)-1,1'-binaphthyl phosphate.

Brønsted acidic MOFs with acid functional groups introduced postsynthetically could also be candidates for proton-conducting materials, as shown in sulfated MIL-53¹²³ and MIL-101.²¹⁷ Proton conductivity of both MOFs functionalized with phenyl-bisulfate group lies in the order of magnitude of that of Nafion (10⁰ S cm⁻¹ at 20 °C and 98% RH). However, the conductivity dropped significantly above 80 °C, suggesting the necessity of water to link the bisulfates, which are dangling in the 1D channels, for efficient proton transportation. A better example was shown by –SO₃H-functionalized UiO-66.¹²³ The material

exhibited a proton conductivity of 8.4 × 10⁻² S cm⁻¹ at 80 °C and 90% RH and, more importantly, a long-term stability for 100 h. Again, this value is among the highest values reported to date for MOF materials and proves the applicability of Brønsted acidic MOFs as competitive proton conductors.

The scope of work could also be extended to sulfonate- and phosphonate-based MOFs. β -PCMOF-2 [Na₃(2,4,6-trihydroxy-1,3,5-benzenetrisulfonate)] was reported to conduct protons in its regular one-dimensional pores lined with partially protonated sulfonate groups, with the structure confirmed from single crystal

XRD experiments.²¹⁸ Although the conductivity of hydrated β -PCMOF-2(H_2O)_{0.5} is not very high ($5.0 \times 10^{-6} \text{ S cm}^{-1}$) compared to that of the compounds mentioned above, controlled loading of 1*H*-1,2,4-triazole (Tz) guests within the pore raised the conductivity by 3 orders of magnitude and also improved the stability at moderate temperature (150 °C).

As mentioned before, phosphonates can coordinate to metals in multiple protonation states. This not only leads to a large number of structures with phosphonates, hydrogen phosphonates, and dihydrogen phosphonates but also to a number of proton-conducting materials with the differently protonated phosphonates. In 2010, a proton conductivity of $3.5 \times 10^{-5} \text{ S cm}^{-1}$ at 25 °C and 98% RH was achieved in a zinc organophosphonate, enabled by ordered water molecules anchored by both Zn centers and phosphonate oxygens.²¹⁹ When monohydrogen phosphonate MOFs are used, the highest proton conductivity achieved so far lies in a magnesium MOF reported in 2012,²²⁰ with a value of $1.6 \times 10^{-3} \text{ S cm}^{-1}$ at 19 °C and ca. 100% RH. In the same year, a dihydrogen phosphonate (phosphonic acid) based MOF, PCMOF-5, was also reported,²²¹ based on La and the 1,2,4,5-tetrakisphosphonomethylbenzene linker. It conducts protons above $10^{-3} \text{ S cm}^{-1}$ at 60 °C and 98% RH through channels filled with crystallographically located water and the Brønsted acidic groups. The aforementioned β -PCMOF-2 was also later modified by isomorphous ligand replacement of 2,4,6-trihydroxy-1,3,5-trisulfonate benzene with 1,3,5-benzenetriphosphonic acid.²²² The resulting PCMOF-2^{1/2} gave a conductivity value of $2.1 \times 10^{-2} \text{ S cm}^{-1}$ at 90% RH and 85 °C, more than 10 times the value for β -PCMOF-2, exceeding even the value of H_2SO_4 @MIL-101. Examples of MOFs consisting of organophosphonic acid and other transitional metals (Ce, Pr, Sm, Eu, Gd, Tb, Dy, and Zr) were also reported to show moderate proton-conducting properties.^{223,224}

Another approach, combining MOFs and original proton-conducting materials, was also proposed and successfully realized. Hybrid compounds consist of CsHSO_4 , the proton-conducting $\text{M}_m\text{H}_n(\text{XO}_4)_p$ family, and MIL-101, formulated as $(1-x)\text{CsHSO}_4 \cdot x\text{MIL-101}$ ($x = 0-0.07$), where x stands for the mole fraction of MIL-101 in the nanocomposite system.⁵⁵ The addition of the MOF was found to decrease the superionic phase transition²²⁵ of CsHSO_4 by 15 K while at the same time considerably increasing the proton conductivity up to 2 orders of magnitude in the low-temperature phase. In another example, phytic acid loaded in MIL-101 (phytic acid@MIL-101) was successfully incorporated into a Nafion hybrid membrane.²²⁶ The measured proton conductivity for the resulting hybrid membranes was 0.06 and $7.63 \times 10^{-3} \text{ S cm}^{-1}$ at 57% and 11% RH, respectively, 3 and 11 times higher than that of pristine Nafion membrane. This observed improvement in proton conductivity at different RHs especially under low RHs was ascribed to the high mobility of phosphate groups in MIL-101's mesopores as well as the better mechanical and swelling resistance properties of the hybrid membrane.

Brønsted acidic MOFs are competitive candidates for proton-conducting materials. For most of the Brønsted acidic MOFs the conductivity depends on water-based hydrogen-bonding arrays or networks, which offer a proton-conduction pathway. These water-mediated-type materials could face problems under anhydrous conditions or higher temperature (e.g., 150 °C). Emerging efforts were also made to replace water with nonvolatile molecules, including mineral acids and N-heterocyclic aromatic compounds. Composite materials of MOF and

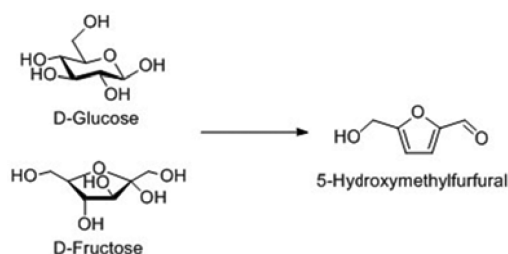
original proton-conducting materials also offer new perspectives for applications of MOFs in the field.

4.3. Catalysis

Brønsted acidic MOFs are emerging as a new aspect of MOF applications. Catalogued in Table 5 are the majority of the known catalytically active Brønsted acidic MOFs. Recently, Brønsted acidic MOFs have been attracting more and more attention due to their increasing versatility in diverse organic reactions.

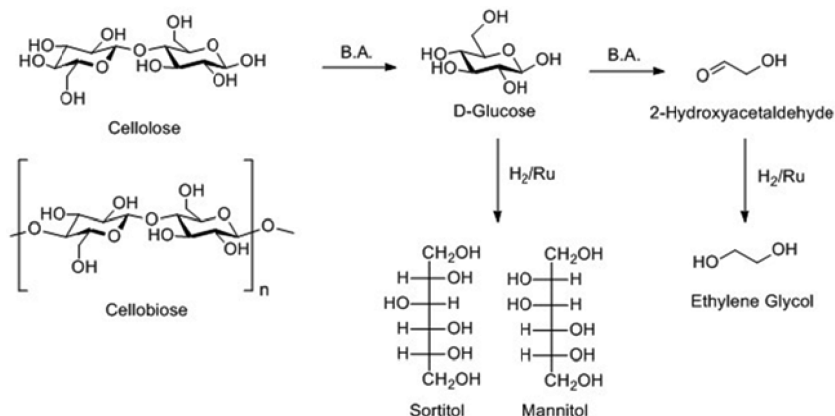
The possibility of encapsulating large Brønsted acidic molecules into MOF pores has enabled the first group of important catalytically active Brønsted acidic MOFs. Brønsted acidic Keggin-type POM and phosphotungstic acid (PTA) and its analogues, when encapsulated in MOF pores, were shown to exhibit activity comparable to those free acids.²²⁷⁻²³² For example, PTA encapsulated in MIL-101 is effective and recyclable for production of 5-hydroxymethylfurfural (HMF),²³⁰ a renewable chemical platform, from biomass-derived glucose or fructose (Scheme 11), serving as the first example of use of a Brønsted acidic MOF material in carbohydrate dehydration reactions.

Scheme 11. Production of 5-Hydroxymethylfurfural from Carbohydrate Dehydration Reactions



More importantly, acid–base and acid–metal binary systems were reported for these PTA loaded in various MOFs, including MIL-101,^{233,234} MIL-100,²³⁵ and HKUST-1.²³⁶ In the acid–metal binary system, the highly dispersed PTA molecules in the MOF pores were reported to function as molecular anchors or Pt precursors.²³⁴ Besides, proposed formation of intermetallic Pt–W(V) species also resulted in a higher selectivity than Pt/alumina toward CO_2 production in CO oxidation, a synergistic effect of metal and support. Another advantage of these multifunctional systems is their ability to catalyze tandem reactions. Catalytic conversion of cellulose to sorbitol, mannitol, and other simple alcohols requires a first step of acid-catalyzed hydrolysis to glucose, followed by hydrogenation on metallic sites (Scheme 12).^{235,236} Ru supported on Keggin-type polyacids@MIL-100 has exhibited complete conversion of cellulose after 10 h at 150 °C and more than 70% selectivity toward sorbitol, while MIL-100 or PTA@MIL-100 only showed 40% conversion and the major product as glucose under the same conditions. A screening of reaction conditions has identified parameters that can affect the conversion and product selectivity, including Ru loading, acid loading, and the strength of the loaded Brønsted acid.

Apart from Keggin-type polyacids, Brønsted acidic ionic liquids (BAILs) are another type of acidic moiety that has been encapsulated in MOF pores for catalysis. A tandem procedure was adopted to incorporate BAILs into MIL-101's mesopores.²³⁷ When catalyzing the acetalization of benzaldehyde with glycol, the resulted Brønsted acidic catalysts achieved comparable catalytic performance with that of TsOH, the benchmark homogeneous catalyst, and also a high reusability. Recently, BAIL was also

Scheme 12. Catalytic Conversion of Cellulose to Sorbitol, Mannitol, and Other Simple Alcohols^a

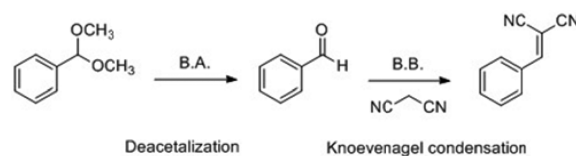
^aB.A. = Brønsted acid.

reported to be encapsulated in PTA@MIL-100 materials, and the resulting solid acid was shown to be effective in production of biodiesels.⁶⁸

The second major group of Brønsted acidic MOF catalysts is less clear with regard to its catalytically active sites, as they are often coexisting with Lewis acidic sites. Typically, this type of MOF acid will have Brønsted acidic sites located on or near their SBUs, which, as stated beforehand, are difficult to characterize. MOFs in this category could be nonacidic or only Lewis acidic when they are “perfect” structures. The former case includes MOF-5, IRMOF-8, and Zn₄O(NDC)₃. Although no acidic sites are expected from the coordinatively saturated Zn₄O(−COO)₆ SBU, catalytic activity toward Friedel–Craft alkylation reactions was observed in both MOFs.^{238,239} It is widely accepted now that the presence of defects in these MOFs should be counted for their acidity, and Brønsted acidity is believed to be generated from uncoordinated carboxylic acid groups of the linker, especially considering the formation of HCl as a byproduct in these reactions. In the latter case, previously considered “pure Lewis acidic” HKUST-1 is also examined for existence of Brønsted acidic components from protonated carboxylates when used as acid catalyst.^{144,240}

Brønsted acidity generated from the interaction between a metal ion and a protic solvent ligand, often water molecules, in MIL-100 and MIL-101 is also capable of catalyzing reactions, including Diels–Alder reactions,¹¹⁷ acetalizations,²⁴² and isomerization of pinene oxide and citronellal.¹¹⁷ A nitro group functionalized MIL-101 was found to acetalize benzaldehyde effectively with 99% conversion within 90 min with turnover numbers of 114. An activity comparison was also carried out for pristine MIL-101 and amino group functionalized MIL-101. Not surprisingly, the electron withdrawing group (nitro group) functionalized materials gave the most acidic pH (1.9) and the highest activity in the reaction, confirming the benefits of having strong Brønsted acidic sites in the catalysts. On the other hand, the coexisting Brønsted acidic and Brønsted basic sites in amino-functionalized MIL-101 open a new approach to a one-pot acid–base reaction.¹⁷² In this case, sequential deacetalization–Knoevenagel condensation between benzaldehyde dimethylacetal and malononitrile (Scheme 13) could be achieved in one-pot with amino-functionalized MIL-101 as the only catalyst with superior activity over HY, MgO, and alumina.

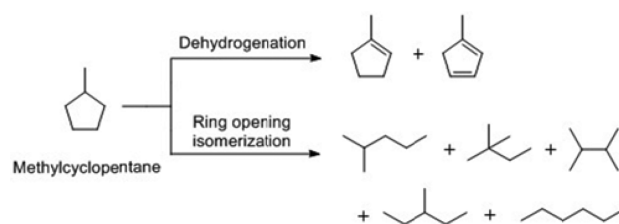
In several cases, Lewis acidity is created alongside when preparing the Brønsted acidic MOF catalyst.^{92,117} One example

Scheme 13. Sequential Deacetalization–Knoevenagel Condensation^a

^aB.A. = Brønsted acid; B.B. = Brønsted base.

involves the superacidic sulfated MOF-808.⁹² A 2:1 reaction stoichiometry for formate substituted by sulfate groups created a significant amount of Lewis acidic sites together with the appearing strong Brønsted acidity. More importantly, this MOF, for the first time, showed activity in the isomerization of a saturated hydrocarbon (methylcyclopentane) at 150 °C (Scheme 14), serving as the benchmark for MOF-based solid

Scheme 14. Reforming of Methylcyclopentane by Sulfated MOF-808



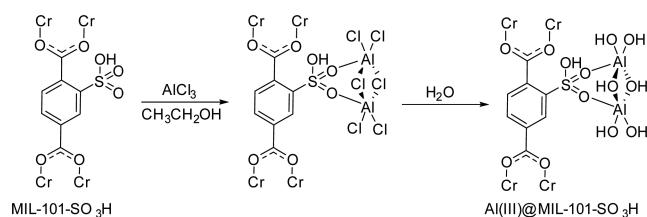
acid catalysts. Although the reaction mechanism remains unknown, it is believed that both Lewis and Brønsted acidic sites contribute to this material’s catalytic activity.

As the third major group of Brønsted acidic MOF catalysts, MOFs with strong Brønsted acid groups covalently bound to organic linkers have been shown to catalyze esterification reactions effectively. Organo-bisulfate functionalized MIL-53 and MIL-101 exhibit activity comparable to that of Nafion in the liquid-phase stoichiometric esterification of *n*-butanol and acetic acid at 70 °C.¹²⁴ The measured turnover frequency (TOF) in MIL-53 (0.72–1.04 min^{−1}) in four consecutive runs was all higher than that of Nafion NR50 (TOF = 0.63 min^{−1}). In the case of MIL-101, although similar substrate conversion to MIL-53 was obtained using the same weight of catalysts, the calculated TOF is lower due to its higher acid density.

This group of Brønsted acidic MOFs also exhibits activity toward the hydrolysis of cellulose, an important nonfood source for bioethanol production.¹⁰² Sulfonic acid functionalized MIL-101 was reported to convert cellulose to only mono- or disaccharides (xylose, glucose, and cellulose) at 120 °C. Although the conversion is higher when strong homogeneous Brønsted acids (e.g., sulfuric acid) are used, unfavorable side products, such as 5-hydroxymethylfurfural, levulinic acid, and formic acid are produced. The stability of this Brønsted acidic MOF was further tested by conducting 13 consecutive runs, showing no activity loss. Compared to the loss of 80% of activity in standard solid acid catalyst SBA-15, sulfonic acid functionalized MIL-101 proved to be a quite stable and reusable catalyst for this reaction.

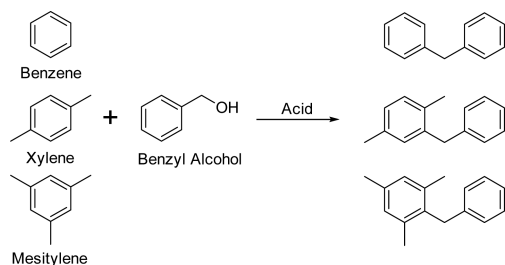
Recently, synergistic effects between postsynthetically introduced catalytic active Lewis acidic Al(III) moieties and framework-bearing Brønsted acidic $-\text{SO}_3\text{H}$ groups were reported for MIL-101,²⁵⁰ hereafter Al(III)@MIL-101- SO_3H . As shown in Scheme 15, the proposed coordination environment

Scheme 15. Proposed Active Site in Al(III)@MIL-101- SO_3H



of Al(III) indicates a very close geometric position between Al(III) and $-\text{SO}_3\text{H}$, prerequisite for this synergistic effect. This catalyst was shown to effectively conduct benzylation of aromatic hydrocarbons (benzene, xylene, and mesitylene) with benzyl alcohol on a fixed-bed reactor (Scheme 16). In all cases, the

Scheme 16. Benzylation of Aromatic Hydrocarbons with Benzyl Alcohol



catalytic performance of the bifunctional MOF catalyst is comparable to benchmark H-mordenite and H- β , if not surpassing them, with excellent stability also. Given the inferior performance of Brønsted acidic MIL-101- SO_3H and AlCl_3 , it is undoubted that the synergy between the two kind of acidic sites renders this Lewis acid@Brønsted acid MOF a promising new approach toward highly active MOF-based acid catalysts.

Apart from multifunctioning systems, enantio- and stereoselective catalysis is another focus for MOF catalysis to impart unique catalytic performances that are not possible in other materials. This also applies to MOF-based Brønsted acid catalysis. In 2001, a chiral porous MOF with Brønsted acid catalytic sites based on lamellar lanthanide phosphonates was reported.²⁵¹ A series of homochiral lanthanide bisphosphonates

were prepared by slow evaporation of an acidic mixture of nitrate or perchlorate salts of Ln(III) and H_4DBBP in methanol at room temperature (Figure 16). The resulting MOFs exhibited

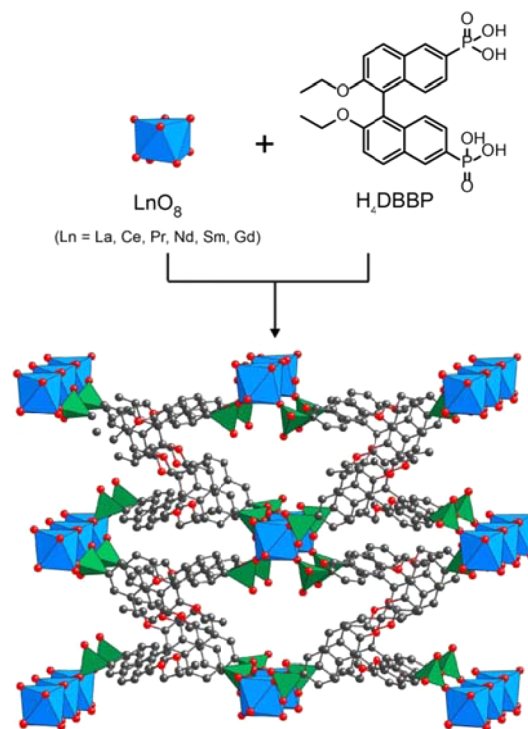


Figure 16. LnO_8 SBUs are combined with deprotonated H_4DBBP linkers to form $[\text{Ln}(\text{H}_2\text{DBBP})(\text{H}_3\text{DBBP})(\text{H}_2\text{O})_4](\text{H}_2\text{O})_x$. Atom labeling scheme: Ln, blue polyhedral; P, green polyhedra; C, gray; and O, red. All H atoms and water molecules are omitted for clarity.

Brønsted acidic sites from the protonated phosphonates and Lewis acidity from the open lanthanide sites. Good framework stability toward water molecules has enabled the study of this acidic MOF as enantioselective acid catalyst in several organic transformations, including cyanosilylation of benzaldehyde and ring opening of *meso*-carboxylic anhydrides. However, in both cases, the products were essentially racemic (*ee* < 5%). Despite the limited enantioselectivity, these MOFs represent a new generation of chiral porous solid acids capable of chiral separation and heterogeneous catalysis.

In 2007, Brønsted acidic sites were made by postsynthetically treating a homochiral copper MOF, $\text{Cu}_2(\text{ASP})_2(\text{BPE})(\text{guests})_x$ (Figure 17a), with HCl .¹¹⁶ The resulting Brønsted acidic MOFs, $\text{Cu}_2(\text{L-ASP})_2(\text{BPE})(\text{HCl})_2(\text{H}_2\text{O})_2$ and $\text{Cu}_2(\text{D-ASP})_2(\text{BPE})(\text{HCl})_2(\text{H}_2\text{O})_2$, were found to be capable of methanolizing *meso*-compound *cis*-2,3-epoxybutane, to give (*R,R*)- and (*S,S*)-3-methoxybutan-2-ol with modest *ee* (Figure 17b). As expected, the MOF with opposite chirality gave the opposite enantiomer dominating in the product. It was also found that the *ee* was higher when the catalytic reaction was carried out under a lower temperature with a slower conversion, which is also seen in other chiral catalysts.

The year of 2012 witnessed another pair of highly porous Brønsted acidic chiral metal–organic frameworks, $[(R)\text{-TBBP-1}]\text{Cu}_2(\text{H}_2\text{O})_2$ and $[(R)\text{-TBBP-2}]\text{Cu}_2(\text{H}_2\text{O})_2$ (CMOF-1 and CMOF-2) (Figure 18).²⁵² Both MOFs showed good activity for Friedel–Craft alkylation of indole with imines (Scheme 17). Interestingly, CMOF-1 gave the major reaction product with chirality opposite to that afforded by the corresponding

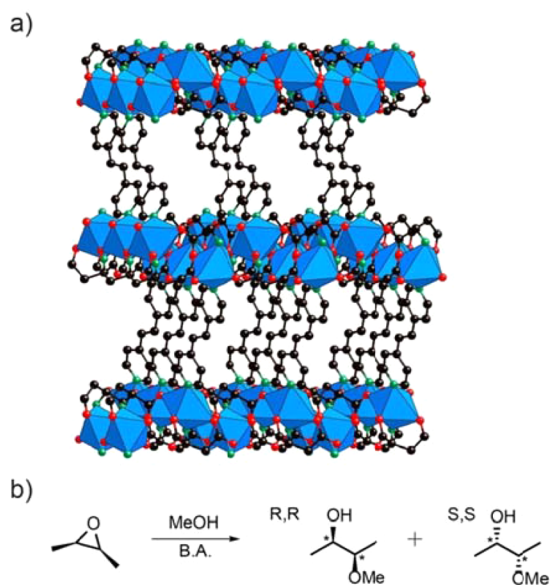


Figure 17. (a) Structural representation for $\text{Cu}(\text{L-ASP})\text{-(BPE)}_{0.5}(\text{guests})$. Atom labeling scheme: Cu, blue polyhedra; C, gray; O, red; and N, green. All H atoms and guest molecules are omitted for clarity. (b) Reaction scheme for methoxylation of *cis*-2,3-epoxybutane.

homogeneous catalyst. A theoretical calculation has pointed to an altered reaction pathway in MOF compared to the homogeneous catalyst due to the interaction between substrates and MOF pores, resulting in a totally different enantioselectivity in the MOF catalysts.

Overall, it is obvious that compared to the large number of Lewis acidic MOF-based catalysts employing various metallic

sites, the field of Brønsted acidic MOF-based catalysis is still only focused on a limited number of MOFs, raising the demand for further development of acid-stable MOFs. Regarding the term “stability”, two aspects are involved. First, stability toward acidic protons: Brønsted acid catalyzed reactions involve the transfer of protons from the catalyst acidic sites to substrates for the activation of the reactant, which, however, could lead to the slow destruction of the framework if those protons migrate to the carboxylates in the framework instead of returning to their origin. Second, stability toward reactivation: the MOF has to be stable toward conditions to regenerate the acidic sites or to dredge the tunnels, which nowadays are typically done through high-temperature calcination or use of strong chemicals. The need exists for developing MOFs in which the metal-link binding units are not carboxylates but other more acid resistant linkages.

5. SUMMARY AND OUTLOOK

In this contribution we have comprehensively reviewed the various strategies by which Brønsted acidity can be designed and produced in MOFs. The different characterization tools used to identify the nature of the acidic sites and their strength are also reviewed. Although, design of Brønsted acidity of moderate strength can be readily achieved in MOFs, the ability to produce superacidity remains a challenge, with only few successful examples reported.⁹² Here, the metal oxide SBUs can be sulfated by replacing formate units acting as termini in an otherwise thermally and chemically stable MOFs. It remains difficult to characterize superacids in general; however, since MOFs maintain their porosity and crystallinity, superacidity in MOFs is far better characterized than in traditional solid superacids, such as zeolites and sulfated zirconia. The importance of Brønsted acidity in accessing various properties is gleaned from

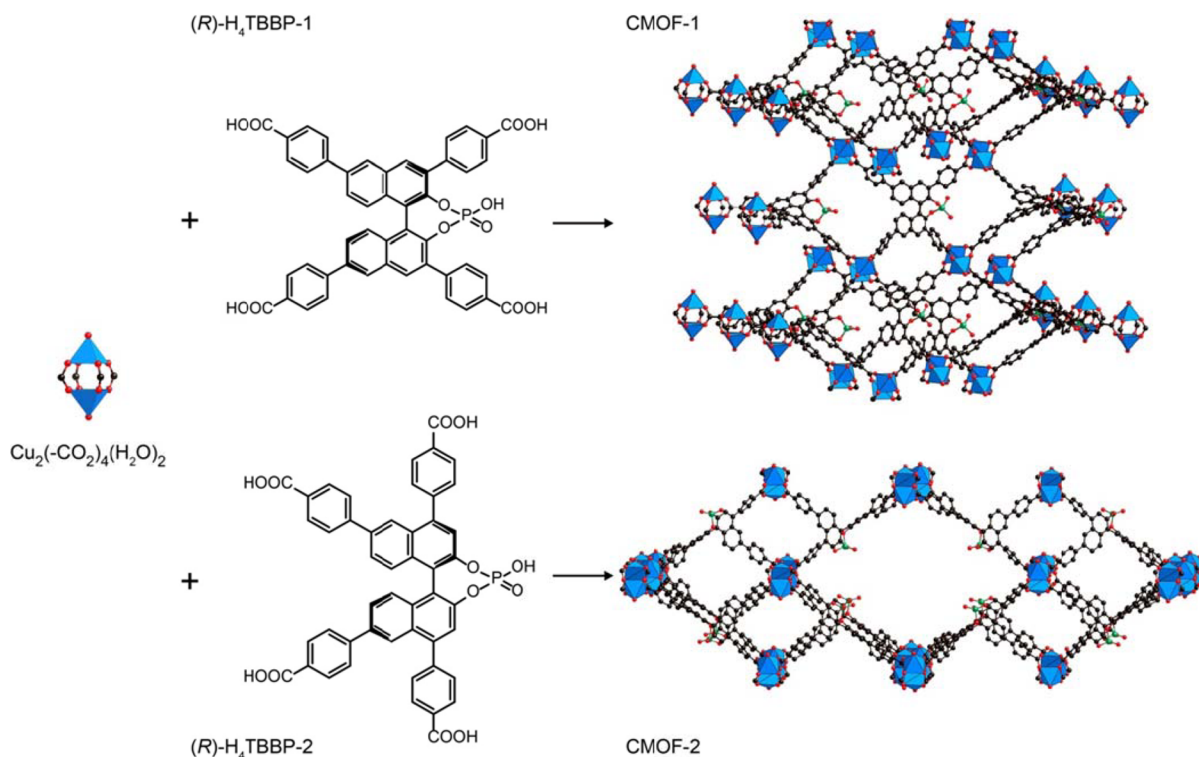
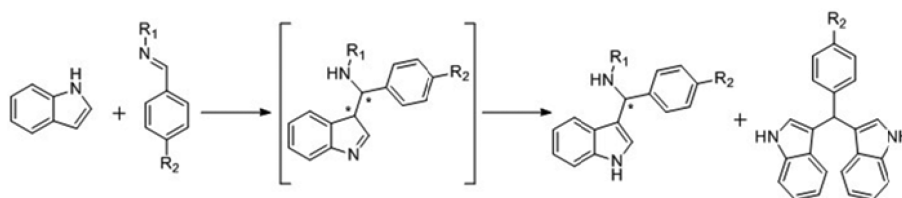


Figure 18. $\text{Cu}_2(-\text{CO}_2)_4(\text{H}_2\text{O})_2$ SBUs are combined with $(R)\text{-H}_4\text{TBBP-1}$ and $(R)\text{-H}_4\text{TBBP-2}$ linkers to form CMOF-1 and CMOF-2, respectively. Atom labeling scheme: Cu_2 paddlewheel clusters, blue polyhedra; C, black; O, red; and P, green. All H atoms are omitted for clarity.

Scheme 17. Friedel–Craft Alkylation of Indole with Imines



its increasing application in catalysis, proton conductivity, and ammonia capture, all of which are summarized in this review.

Given the flexibility with which MOF constituents can be varied and the ability to prepare bulk MOFs as nanocrystals without changing their underlying chemical connectivity, we anticipate exciting opportunities for Brønsted acidic MOFs to be incorporated in mesoscopic systems. For example, enclosing a typical metal catalysts with Brønsted acidic MOFs is expected to alter the catalyst activity and selectivity. In a way, the MOF in this case acts as a complex “ligand” enclosure for metal nanoparticles, where it is possible to impart the MOF designable attributes onto the metal catalyst. This includes variation of the organic linker’s length and functional groups as well as incorporation of multiple metal ions into the MOF enclosures. It is clear that Brønsted acidity, both of moderate and superacidic strength, should be another likely avenue of modifying the enclosures and accessing completely different kinds of reactivity for these traditional catalyst systems.

Indeed, the interfacing of Brønsted acidic MOFs with metal nanoparticles in the way we envision here provides even a more powerful means of making mesoscopic systems when coupled with multivariable MOFs. Here, nanometer regions replete with superacidic sites can be intermingled with regions of moderate acidity or even basic sites. Thus, one can potentially design the interior of the MOF to have compartments of different scales of acidity that are linked but which potentially can operate differently, aspects very common in biology but that remain uncommon in synthetic systems.

ASSOCIATED CONTENT

Supporting Information

Complete refs 65, 95, 113, 143, 220, 223, and 250. The Supporting Information is available free of charge on the ACS Publications website at DOI: 10.1021/acs.chemrev.5b00221.

AUTHOR INFORMATION

Corresponding Authors

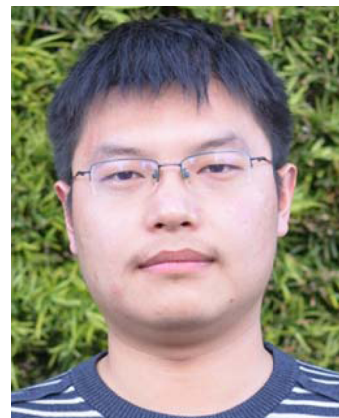
*J.J. e-mail: jcjiang@berkeley.edu .

*O.M.Y e-mail: yaghi@berkeley.edu.

Notes

The authors declare no competing financial interests.

Biographies



Juncong Jiang was born in Wuhan, Hubei, China, in 1990. He received his B.Sc. in chemistry from Peking University in 2012. He then joined Prof. Omar M. Yaghi’s research group in the same year at University of California, Berkeley. He is now a Ph.D. candidate at University of California, Berkeley. His research interests include the development of new porous materials and their use in catalysis and energy-related applications.



Omar M. Yaghi received his Ph.D. from the University of Illinois—Urbana (1990) with Prof. Walter G. Klemperer. He was an NSF Postdoctoral Fellow at Harvard University (1990–1992) with Prof. Richard H. Holm. He has been on the faculties of Arizona State University (1992–1998), University of Michigan (1999–2006), and University of California, Los Angeles (2007–2012). His current position is the James and Neeltje Tretter Professor of Chemistry, University of California, Berkeley, and Faculty Scientist at Lawrence Berkeley National Laboratory. His work encompasses the synthesis, structure, and properties of inorganic compounds and the design and construction of new crystalline materials. He has shown that organic and inorganic molecules can be stitched together into extended porous structures to make metal–organic frameworks, zeolitic imidazolate frameworks, and covalent organic frameworks.

ACKNOWLEDGMENTS

We gratefully acknowledge Prof. Y.-B. Zhang (ShanghaiTech University), Dr. H. Furukawa, and Mr. C. Diercks for their valuable input and proof-reading. Financial support for MOF research in the laboratories of O.M.Y. is provided by BASF SE (Ludwigshafen, Germany); U.S. Department of Defense, Defense Threat Reduction Agency Grant HDTRA 1-12-1-0053; and U.S. Department of Energy, Office of Science, Office of Basic Energy Sciences, Energy Frontier Research Center grant DE-SC0001015.

REFERENCES

- (1) Yaghi, O. M.; O'Keeffe, M.; Ockwig, N. W.; Chae, H. K.; Eddadoudi, M.; Kim, J. Reticular Synthesis and the Design of New Materials. *Nature* **2003**, *423*, 705–714.
- (2) Ockwig, N. W.; Delgado-Friedrichs, O.; O'Keeffe, M.; Yaghi, O. M. Reticular Chemistry: Occurrence and Taxonomy of Nets and Grammar for the Design of Frameworks. *Acc. Chem. Res.* **2005**, *38*, 176–182.
- (3) Zhou, H.-C.; Long, J. R.; Yaghi, O. M. Introduction to Metal–Organic Frameworks. *Chem. Rev.* **2012**, *112*, 673–674.
- (4) Zhou, H.-C.; Kitagawa, S. Metal–Organic Frameworks (MOFs). *Chem. Soc. Rev.* **2014**, *43*, 5415–5418.
- (5) Furukawa, H.; Cordova, K. E.; O'Keeffe, M.; Yaghi, O. M. The Chemistry and Applications of Metal–Organic Frameworks. *Science* **2013**, *341*, 1230444.
- (6) Li, M.; Li, D.; O'Keeffe, M.; Yaghi, O. M. Topological Analysis of Metal–Organic Frameworks with Polytopic Linkers and/or Multiple Building Units and the Minimal Transitivity Principle. *Chem. Rev.* **2014**, *114*, 1343–1370.
- (7) O'Keeffe, M.; Yaghi, O. M. Deconstructing the Crystal Structures of Metal–Organic Frameworks and Related Materials into Their Underlying Nets. *Chem. Rev.* **2012**, *112*, 675–702.
- (8) Cohen, S. M. Postsynthetic Methods for the Functionalization of Metal–Organic Frameworks. *Chem. Rev.* **2012**, *112*, 970–1000.
- (9) Evans, J. D.; Sumbly, C. J.; Doonan, C. J. Post-Synthetic Metalation of Metal–Organic Frameworks. *Chem. Soc. Rev.* **2014**, *43*, 5933–5951.
- (10) Deria, P.; Mondloch, J. E.; Karagiari, O.; Bury, W.; Hupp, J. T.; Farha, O. K. Beyond Post-Synthesis Modification: Evolution of Metal–Organic Frameworks via Building Block Replacement. *Chem. Soc. Rev.* **2014**, *43*, 5896–5912.
- (11) Deng, H.; Doonan, C. J.; Furukawa, H.; Ferreira, R. B.; Towne, J.; Knobler, C. B.; Wang, B.; Yaghi, O. M. Multiple Functional Groups of Varying Ratios in Metal–Organic Frameworks. *Science* **2010**, *327*, 846–850.
- (12) Zhang, Y.-B.; Furukawa, H.; Ko, N.; Nie, W.; Park, H. J.; Okajima, S.; Cordova, K. E.; Deng, H.; Kim, J.; Yaghi, O. M. Introduction of Functionality, Selection of Topology, and Enhancement of Gas Adsorption in Multivariate Metal–Organic Framework-177. *J. Am. Chem. Soc.* **2015**, *137*, 2641–2650.
- (13) Gascon, J.; Corma, A.; Kapteijn, F.; Llabrés i Xamena, F. X. Metal Organic Framework Catalysis: Quo vadis? *ACS Catal.* **2014**, *4*, 361–378.
- (14) Liu, J.; Chen, L.; Cui, H.; Zhang, J.; Zhang, L.; Su, C.-Y. Applications of Metal–Organic Frameworks in Heterogeneous Supramolecular Catalysis. *Chem. Soc. Rev.* **2014**, *43*, 6011–6061.
- (15) Zhang, T.; Lin, W. Metal–Organic Frameworks for Artificial Photosynthesis and Photocatalysis. *Chem. Soc. Rev.* **2014**, *43*, 5982–5993.
- (16) Yoon, M.; Srirambalaji, R.; Kim, K. Homochiral Metal–Organic Frameworks for Asymmetric Heterogeneous Catalysis. *Chem. Rev.* **2012**, *112*, 1196–1231.
- (17) Lee, J. Y.; Farha, O. K.; Roberts, J.; Scheidt, K. A.; Nguyen, S. T.; Hupp, J. T. Metal–Organic Framework Materials as Catalysts. *Chem. Soc. Rev.* **2009**, *38*, 1450–1459.
- (18) Sumida, K.; Rogow, D. L.; Mason, J. A.; McDonald, T. M.; Bloch, E. D.; Herm, Z. R.; Bae, T.-H.; Long, J. R. Carbon Dioxide Capture in Metal–Organic Frameworks. *Chem. Rev.* **2012**, *112*, 724–781.
- (19) Suh, M. P.; Park, H. J.; Prasad, T. K.; Lim, D.-W. Hydrogen Storage in Metal–Organic Frameworks. *Chem. Rev.* **2012**, *112*, 782–835.
- (20) Wu, H.; Gong, Q.; Olson, D. H.; Li, J. Commensurate Adsorption of Hydrocarbons and Alcohols in Microporous Metal Organic Frameworks. *Chem. Rev.* **2012**, *112*, 836–868.
- (21) Li, J.-R.; Sculley, J.; Zhou, H.-C. Metal–Organic Frameworks for Separations. *Chem. Rev.* **2012**, *112*, 869–932.
- (22) Decoste, J. B.; Peterson, G. W. Metal–Organic Frameworks for Air Purification of Toxic Chemicals. *Chem. Rev.* **2014**, *114*, 5695–5727.
- (23) Burtch, N. C.; Jasuja, H.; Walton, K. S. Water Stability and Adsorption in Metal–Organic Frameworks. *Chem. Rev.* **2014**, *114*, 10575–10612.
- (24) Qiu, S.; Xue, M.; Zhu, G. Metal–Organic Framework Membranes: From Synthesis to Separation Applications. *Chem. Soc. Rev.* **2014**, *43*, 6116–6140.
- (25) He, Y.; Zhou, W.; Qian, G.; Chen, B. Methane Storage in Metal–Organic Frameworks. *Chem. Soc. Rev.* **2014**, *43*, 5657–5678.
- (26) Férey, G.; Millange, F.; Morcrette, M.; Serre, C.; Doublet, M.-L.; Grenèche, J.-M.; Tarascon, J.-M. Mixed-Valence Li/Fe-Based Metal–Organic Frameworks with Both Reversible Redox and Sorption Properties. *Angew. Chem., Int. Ed.* **2007**, *46*, 3259–3263.
- (27) Yoon, M.; Suh, K.; Natarajan, S.; Kim, K. Proton Conduction in Metal–Organic Frameworks and Related Modularly Built Porous Solids. *Angew. Chem., Int. Ed.* **2013**, *52*, 2688–2700.
- (28) Choi, K. M.; Jeong, H. M.; Park, J. H.; Zhang, Y.-B.; Kang, J. K.; Yaghi, O. M. Supercapacitors of Nanocrystalline Metal–Organic Frameworks. *ACS Nano* **2014**, *8*, 7451–7457.
- (29) Fujita, M.; Kwon, Y. J.; Washizu, S.; Ogura, K. Preparation, Clathration Ability, and Catalysis of a Two-Dimensional Square Network Material Composed of Cadmium(II) and 4,4'-Bipyridine. *J. Am. Chem. Soc.* **1994**, *116*, 1151–1152.
- (30) Chen, B.; Eddaoudi, M.; Reineke, T. M.; Kampf, J. W.; O'Keeffe, M.; Yaghi, O. M. Cu₂(ATC) 6H₂O: Design of Open Metal Sites in Porous Metal–Organic Crystals (ATC: 1,3,5,7-adamantane tetracarboxylate). *J. Am. Chem. Soc.* **2000**, *122*, 11559–11560.
- (31) Chui, S. S. Y.; Lo, S. M. F.; Charmant, J. P. H.; Orpen, A. G.; Williams, I. D. A Chemically Functionalizable Nanoporous Material [Cu₃(TMA)₂(H₂O)₃]_n. *Science* **1999**, *283*, 1148–1150.
- (32) Férey, G.; Mellot-Draznieks, C.; Serre, C.; Millange, F.; Dutour, J.; Surblé, S.; Margiolaki, I. A Chromium Terephthalate-Based Solid with Unusually Large Pore Volumes and Surface Area. *Science* **2005**, *309*, 2040–2042.
- (33) Bauer, S.; Serre, C.; Devic, T.; Horcajada, P.; Marrot, J.; Férey, G.; Stock, N. High-Throughput Assisted Rationalization of the Formation of Metal Organic Frameworks in the Iron(III) Aminoterephthalate Solvothermal System. *Inorg. Chem.* **2008**, *47*, 7568–7576.
- (34) Serra-Crespo, P.; Ramos-Fernandez, E. V.; Gascon, J.; Kapteijn, F. Synthesis and Characterization of an Amino Functionalized MIL-101(Al): Separation and Catalytic Properties. *Chem. Mater.* **2011**, *23*, 2565–2572.
- (35) Schlichte, K.; Kratzke, T.; Kaskel, S. Improved Synthesis, Thermal Stability and Catalytic Properties of the Metal–Organic Framework Compound Cu₃(BTC)₂. *Microporous Mesoporous Mater.* **2004**, *73*, 81–88.
- (36) Henschel, A.; Gedrich, K.; Kraehnert, R.; Kaskel, S. Catalytic Properties of MIL-101. *Chem. Commun.* **2008**, 4192–4194.
- (37) Alaerts, L.; Séguin, E.; Poelman, H.; Thibault-Starzyk, F.; Jacobs, P. A.; De Vos, D. E. Probing the Lewis Acidity and Catalytic Activity of the Metal–Organic Framework [Cu₃(btc)₂] (BTC = Benzene-1,3,5-tricarboxylate). *Chem.—Eur. J.* **2006**, *12*, 7353–7363.
- (38) Vandichel, M.; Vermoortele, F.; Cottenie, S.; De Vos, D. E.; Waroquier, M.; Van Speybroeck, V. Insight in the Activity and Diastereoselectivity of Various Lewis Acid Catalysts for the Citronellal Cyclization. *J. Catal.* **2013**, *305*, 118–129.
- (39) Cirujano, F. G.; Llabrés i Xamena, F. X.; Corma, A. MOFs as Multifunctional Catalysts: One-Pot Synthesis of Menthol from Citronellal over a Bifunctional MIL-101 Catalyst. *Dalton Trans.* **2012**, *41*, 4249–4254.

- (40) Hwang, Y. K.; Hong, D.-Y.; Chang, J.-S.; Jhung, S. H.; Seo, Y.-K.; Kim, J.; Vimont, A.; Daturi, M.; Serre, C.; Férey, G. Amine Grafting on Coordinatively Unsaturated Metal Centers of MOFs: Consequences for Catalysis and Metal Encapsulation. *Angew. Chem., Int. Ed.* **2008**, *47*, 4144–4148.
- (41) Hartmann, M.; Fischer, M. Amino-Functionalized Basic Catalysts with MIL-101 Structure. *Microporous Mesoporous Mater.* **2012**, *164*, 38–43.
- (42) Kim, J.; Bhattacharjee, S.; Jeong, K.-E.; Jeong, S.-Y.; Ahn, W.-S. Selective Oxidation of Tetralin over a Chromium Terephthalate Metal Organic Framework, MIL-101. *Chem. Commun.* **2009**, 3904–3906.
- (43) Maksimchuk, N. V.; Timofeeva, M. N.; Melgunov, M. S.; Shmakov, A. N.; Chesalov, Y. A.; Dybtsev, D. N.; Fedin, V. P.; Kholdeeva, O. A. Heterogeneous Selective Oxidation Catalysts Based on Coordination Polymer MIL-101 and Transition Metal-Substituted Polyoxometalates. *J. Catal.* **2008**, *257*, 315–323.
- (44) Maksimchuk, N. V.; Kovalenko, K. A.; Fedin, V. P.; Kholdeeva, O. A. Heterogeneous Selective Oxidation of Alkenes to α,β -Unsaturated Ketones over Coordination Polymer MIL-101. *Adv. Synth. Catal.* **2010**, *352*, 2943–2948.
- (45) Corma, A.; Garcia, H.; Llabrés i Xamena, F. X. Engineering Metal Organic Frameworks for Heterogeneous Catalysis. *Chem. Rev.* **2010**, *110*, 4606–4655.
- (46) Farrusseng, D.; Aguado, S.; Pinel, C. Metal–Organic Frameworks: Opportunities for Catalysis. *Angew. Chem., Int. Ed.* **2009**, *48*, 7502–7513.
- (47) Olah, G. A.; Prakash, G. K. S.; Molnár, Á.; Sommer, J. *Superacid Chemistry*, 2nd ed.; John Wiley & Sons, Inc.: New York, 2009; Chapter 1, p 27.
- (48) Corma, A. Inorganic Solid Acids and Their Use in Acid-Catalyzed Hydrocarbon Reactions. *Chem. Rev.* **1995**, *95*, 559–614.
- (49) Furukawa, H.; Müller, U.; Yaghi, O. M. “Heterogeneity within Order” in Metal–Organic Frameworks. *Angew. Chem., Int. Ed.* **2015**, *54*, 3417–3430.
- (50) Wang, Z.; Cohen, S. M. Postsynthetic Modification of Metal–Organic Frameworks. *Chem. Soc. Rev.* **2009**, *38*, 1315–1329.
- (51) Tanabe, K. K.; Cohen, S. M. Postsynthetic Modification of Metal–Organic Frameworks—A Progress Report. *Chem. Soc. Rev.* **2011**, *40*, 498–519.
- (52) Salomon, W.; Roch-Marchal, C.; Mialane, P.; Pouschmeyer, P.; Serre, C.; Haouas, M.; Taulelle, F.; Yang, S.; Ruhlmann, L.; Dolbecq, A. Immobilization of Polyoxometalates in the Zr-Based Metal Organic Framework UiO-67. *Chem. Commun.* **2015**, *51*, 2972–2975.
- (53) Herron, N.; Stucky, G. D.; Tolman, C. A. The Reactivity of Tetracarboxylnickel Encapsulated in Zeolite X. A Case History of Intrazeolite Coordination Chemistry. *Inorg. Chim. Acta* **1985**, *100*, 135–140.
- (54) Ponomareva, V. G.; Kovalenko, K. A.; Chupakhin, A. P.; Dybtsev, D. N.; Shutova, E. S.; Fedin, V. P. Imparting High Proton Conductivity to a Metal–Organic Framework Material by Controlled Acid Impregnation. *J. Am. Chem. Soc.* **2012**, *134*, 15640–15643.
- (55) Ponomareva, V. G.; Kovalenko, K. A.; Chupakhin, A. P.; Shutova, E. S.; Fedin, V. P. CsHSO₄—Proton Conduction in a Crystalline Metal–Organic Framework. *Solid State Ionics* **2012**, *225*, 420–423.
- (56) Ono, Y. In *Perspectives in Catalysis*; Thomas, J. M., Zamarava, K. I., Eds.; Blackwell: London, 1992; p 341.
- (57) Misono, M. Heterogeneous Catalysis by Heteropoly Compounds of Molybdenum and Tungsten. *Catal. Rev. Sci. Eng.* **1988**, *29*, 269–321.
- (58) Kozhevnikov, I. V. Catalysis by Heteropoly Acids and Multicomponent Polyoxometalates in Liquid-Phase Reactions. *Chem. Rev.* **1998**, *98*, 171–198.
- (59) Hagrman, D.; Hagrman, P. J.; Zubietta, J. Solid-State Coordination Chemistry: The Self-Assembly of Microporous Organic–Inorganic Hybrid Frameworks Constructed from Tetrapyrrolylporphyrin and Bimetallic Oxide Chains or Oxide Clusters. *Angew. Chem., Int. Ed.* **1999**, *38*, 3165–3168.
- (60) Du, D.-Y.; Qin, J.-S.; Li, S.-L.; Su, Z.-M.; Lan, Y.-Q. Recent Advances in Porous Polyoxometalate-Based Metal–Organic Framework Materials. *Chem. Soc. Rev.* **2014**, *43*, 4615–4632.
- (61) Juan-Alcañiz, J.; Gascon, J.; Kapteijn, F. Metal–Organic Frameworks as Scaffolds for the Encapsulation of Active Species: State of the Art and Future Perspectives. *J. Mater. Chem.* **2012**, *22*, 10102–10118.
- (62) Wei, M.; He, C.; Hua, W.; Duan, C.; Li, S.; Meng, Q. A Large Protonated Water Cluster H⁺(H₂O)₂₇ in a 3D Metal–Organic Framework. *J. Am. Chem. Soc.* **2006**, *128*, 13318–13319.
- (63) Sun, C.-Y.; Liu, S.-X.; Liang, D.-D.; Shao, K.-Z.; Ren, Y.-H.; Su, Z.-M. Highly Stable Crystalline Catalysts Based on Microporous Metal–Organic Framework and Polyoxometalates. *J. Am. Chem. Soc.* **2009**, *131*, 1883–1888.
- (64) Juan-Alcañiz, J.; Ramos-Fernandez, E. V.; Lafont, U.; Gascon, J.; Kapteijn, F. Building MOF Bottles around Phosphotungstic Acid Ships: One-Pot Synthesis of Bifunctional Polyoxometalate-MIL-101 Catalysts. *J. Catal.* **2010**, *269*, 229–241.
- (65) Canioni, R.; Roch-Marchal, C.; Sécheresse, F.; Horcajada, P.; Serre, C.; Hardi-Dan, M.; Férey, G.; Grenèche, J.-M.; Lefebvre, F.; Chang, J.-S.; et al. Stable Polyoxometalate Insertion within the Mesoporous Metal Organic Framework MIL-100(Fe). *J. Mater. Chem.* **2011**, *21*, 1226–1233.
- (66) Micek-Ilnicka, A.; Gil, B. Heteropolyacid Encapsulation into the MOF: Influence of Acid Particles Distribution on Ethanol Conversion in Hybrid Nanomaterials. *Dalton Trans.* **2012**, *41*, 12624–12629.
- (67) Juan-Alcañiz, J.; Goesten, M. G.; Ramos-Fernandez, E. V.; Gascon, J.; Kapteijn, F. Towards Efficient Polyoxometalate Encapsulation in MIL-100(Cr): Influence of Synthesis Conditions. *New J. Chem.* **2012**, *36*, 977–987.
- (68) Wang, H.; Chen, C.; Wu, Z.; Que, Y.; Feng, Y.; Wang, W.; Wang, L.; Guan, G.; Liu, X. Encapsulation of Heteropolyanion-Based Ionic Liquid within the Metal–Organic Framework MIL-100(Fe) for Biodiesel Production. *ChemCatChem* **2015**, *7*, 441–449.
- (69) Corma, A. State of the Art and Future Challenges of Zeolites as Catalysts. *J. Catal.* **2003**, *216*, 298–312.
- (70) Chaplais, G.; Simon-Masseron, A.; Porcher, F.; Lecomte, C.; Bazer-Bachi, D.; Bats, N.; Patarin, J. IM-19: A New Flexible Microporous Gallium Based-MOF Framework with Pressure- and Temperature-Dependent Openings. *Phys. Chem. Chem. Phys.* **2009**, *11*, 5241–5245.
- (71) Rosi, N. L.; Kim, J.; Eddaoudi, M.; Chen, B.; O’Keeffe, M.; Yaghi, O. M. Rod Packings and Metal–Organic Frameworks Constructed from Rod-Shaped Secondary Building Units. *J. Am. Chem. Soc.* **2005**, *127*, 1504–1518.
- (72) Ravon, U.; Savonnet, M.; Farrusseng, D.; Simon-Masseron, A.; Chaplais, G.; Bazer-Bachi, D.; Bats, N.; Lecomte, V. FR 0805536, 2008.
- (73) Ravon, U.; Savonnet, M.; Aguado, S.; Domine, M. E.; Farrusseng, D. Engineering of Coordination Polymers for Shape Selective Alkylation of Large Aromatics and the Role of Defects. *Microporous Mesoporous Mater.* **2010**, *129*, 319–329.
- (74) Ravon, U.; Chaplais, G.; Chizallet, C.; Seyyedi, B.; Bonino, F.; Bordiga, S.; Bats, N.; Farrusseng, D. Investigation of Acid Centers in MIL-53(Al, Ga) for Brønsted-Type Catalysis: In Situ FTIR and Ab Initio Molecular Modeling. *ChemCatChem* **2010**, *2*, 1235–1238.
- (75) Loiseau, T.; Serre, C.; Huguenard, C.; Fink, G.; Taulelle, F.; Henry, M.; Bataille, T.; Férey, G. A Rationale for the Large Breathing of the Porous Aluminum Terephthalate (MIL-53) Upon Hydration. *Chem.—Eur. J.* **2004**, *10*, 1373–1382.
- (76) Tian, A. X.; Lin, X. L.; Liu, X. J.; Ying, J.; Wang, X. L. Hydroxyl- and Chloro-Bridges as “Structural Assistants” in the Construction of Two New Keggin-Based 3D Frameworks. *RSC Adv.* **2013**, *3*, 17188–17194.
- (77) Whitfield, T. R.; Wang, X.; Liu, L.; Jacobson, A. J. Metal–Organic Frameworks Based on Iron Oxide Octahedral Chains Connected by Benzenedicarboxylate Dianion. *Solid State Sci.* **2005**, *7*, 1096–1103.
- (78) Qian, J.; Jiang, F.; Yuan, D.; Wu, M.; Zhang, S.; Zhang, L.; Hong, M. Highly Selective Carbon Dioxide Adsorption in a Water-Stable Indium–Organic Framework Material. *Chem. Commun.* **2012**, *48*, 9696–9698.
- (79) Ren, G.; Liu, S.; Ma, F.; Wei, F.; Tang, Q.; Yang, Y.; Liang, D.; Li, S.; Chen, Y. A 9-Connected Metal–Organic Framework with Gas Adsorption Properties. *J. Mater. Chem.* **2011**, *21*, 15909.

- (80) D'Vries, R. F.; de la Pena-O'shea, V. A.; Snejko, N.; Iglesia, M.; Gutierrez-Puebla, E.; Monge, M. Á. H_3O_2 Bridging Ligand in a Metal–Organic Framework. Insight into the Aqua-Hydroxo \leftrightarrow Hydroxyl Equilibrium: A Combined Experimental and Theoretical Study. *J. Am. Chem. Soc.* **2013**, *135*, 5782–5792.
- (81) Cavka, J. H.; Jakobsen, S.; Olsbye, U.; Guillou, N.; Lamberti, C.; Bordiga, S.; Lillerud, K. P. A New Zirconium Inorganic Building Brick Forming Metal Organic Frameworks with Exceptional Stability. *J. Am. Chem. Soc.* **2008**, *130*, 13850–13851.
- (82) Horcajada, P.; Surblé, S.; Serre, C.; Hong, D.-Y.; Seo, Y.-K.; Chang, J.-S.; Grenèche, J.-M.; Margiolaki, I.; Férey, G. Synthesis and Catalytic Properties of MIL-100(Fe), an Iron(III) Carboxylate with Large Pores. *Chem. Commun.* **2007**, 2820–2822.
- (83) Aguirre-Díaz, L. M.; Gándara, F.; Iglesias, M.; Snejko, N.; Gutiérrez-Puebla, E.; Monge, M. Á. Tunable Catalytic Activity of Solid Solution Metal–Organic Frameworks in One-Pot Multicomponent Reactions. *J. Am. Chem. Soc.* **2015**, *137*, 6132–6135.
- (84) Vimont, A.; Goupil, J.-M.; Lavalley, J.-C.; Daturi, M.; Surblé, S.; Serre, C.; Millange, F.; Férey, G.; Audebrand, N. Investigation of Acid Sites in a Zeotypic Giant Pores Chromium(III) Carboxylate. *J. Am. Chem. Soc.* **2006**, *128*, 3218–3227.
- (85) Volklinger, C.; Leclerc, H.; Lavalley, J.-C.; Loiseau, T.; Férey, G.; Daturi, M.; Vimont, A. Infrared Spectroscopy Investigation of the Acid Sites in the Metal–Organic Framework Aluminum Trimesate MIL-100(Al). *J. Phys. Chem. C* **2012**, *116*, 5710–5719.
- (86) Wang, Z. *Comprehensive Organic Name Reactions and Reagents*; John Wiley & Sons, Inc.: New York, 2010; p 1131.
- (87) Vimont, A.; Leclerc, H.; Maugé, F.; Daturi, M.; Lavalley, J.-C.; Surblé, S.; Serre, C.; Férey, G. Creation of Controlled Bronsted Acidity on a Zeotypic Mesoporous Chromium(III) Carboxylate by Grafting Water and Alcohol Molecules. *J. Phys. Chem. C* **2007**, *111*, 383–388.
- (88) Derouault, J.; Dziembowska, T.; Forel, M. T. Infrared and Raman Investigation of the Liquid Addition Compounds $\text{BF}_3\text{-CH}_3\text{OH}$ and $\text{BF}_3\text{-2CH}_3\text{OH}$. *J. Mol. Struct.* **1978**, *47*, 59–63.
- (89) DeCoste, J. B.; Demasky, T. J.; Katz, M. J.; Farha, O. K.; Hupp, J. T. A UiO-66 Analogue with Uncoordinated Carboxylic Acids for the Broad-Spectrum Removal of Toxic Chemicals. *New J. Chem.* **2015**, *39*, 2396–2399.
- (90) Katz, M. J.; Brown, Z. J.; Colon, Y. J.; Siu, P. W.; Scheidt, K. A.; Snurr, R. Q.; Hupp, J. T.; Farha, O. K. A Facile Synthesis of UiO-66, UiO-67 and Their Derivatives. *Chem. Commun.* **2013**, *49*, 9449–9451.
- (91) Furukawa, H.; Gándara, F.; Zhang, Y.-B.; Jiang, J.; Queen, W. L.; Hudson, M. R.; Yaghi, O. M. Water Adsorption in Porous Metal–Organic Frameworks and Related Materials. *J. Am. Chem. Soc.* **2014**, *136*, 4369–4381.
- (92) Jiang, J.; Gándara, F.; Zhang, Y.-B.; Na, K.; Yaghi, O. M.; Klempner, W. G. Superacidity in Sulfated Metal–Organic Framework-808. *J. Am. Chem. Soc.* **2014**, *136*, 12844–12847.
- (93) Hammett, L. P.; Deyrup, A. J. A Series of Simple Basic Indicators. I. The Acidity Functions of Mixtures of Sulfuric and Perchloric Acids with Water. *J. Am. Chem. Soc.* **1932**, *54*, 2721–2739.
- (94) Biswas, S.; Zhang, J.; Li, Z.; Liu, Y.-Y.; Grzywa, M.; Sun, L.; Volkmer, D.; Van Der Voort, P. Enhanced Selectivity of CO_2 over CH_4 in Sulphonate-, Carboxylate- and Iodo-Functionalized UiO-66 Frameworks. *Dalton Trans.* **2013**, *42*, 4730–4737.
- (95) Ragon, F.; Campo, B.; Yang, Q.; Martineau, C.; Wiersum, A. D.; Lago, A.; Guillerm, V.; Hemsley, C.; Eubank, J. F.; Vishnuvarthan, M.; et al. Acid-Functionalized UiO-66(Zr) MOFs and Their Evolution after Intra-Framework Cross-Linking: Structural Features and Sorption Properties. *J. Mater. Chem. A* **2015**, *3*, 3294–3309.
- (96) Qin, C.; Wang, X.; Carlucci, L.; Tong, M.; Wang, E.; Hu, C.; Xu, L. From Arm-Shaped Layers to a New Type of Polythreaded Array: A Two Fold Interpenetrated Three-Dimensional Network with a Rutile Topology. *Chem. Commun.* **2004**, 1876–1877.
- (97) Li, J.; Ma, C.; He, G.; Qiu, L. Polymeric Frameworks Constructed from Zn with Benzenetricarboxylic Acid Ligands and Monodentate 4,4'-Bipyridine: Hydrothermal Synthesis, Crystal Structures and Luminescence. *J. Coord. Chem.* **2008**, *61*, 251–261.
- (98) Wang, L.; Yang, M.; Shi, Z.; Chen, Y.; Feng, S. Two-Dimensional Metal–Organic Framework Constructed from 4,4'-Bipyridine and 1,2,4-Benzenetricarboxylate: Synthesis, Structure and Magnetic Properties. *J. Solid State Chem.* **2005**, *178*, 3359–3365.
- (99) Morris, W.; Doonan, C. J.; Yaghi, O. M. Postsynthetic Modification of a Metal–Organic Framework for Stabilization of a Hemiaminal and Ammonia Uptake. *Inorg. Chem.* **2011**, *50*, 6853–6855.
- (100) Van Humbeck, J. F.; McDonald, T. M.; Jing, X.; Wiers, B. M.; Zhu, G.; Long, J. R. Ammonia Capture in Porous Organic Polymer Densely Functionalized with Brønsted Acid Groups. *J. Am. Chem. Soc.* **2014**, *136*, 2432–2440.
- (101) Foo, M. L.; Horike, S.; Fukushima, T.; Hijikata, Y.; Kubota, Y.; Takata, M.; Kitagawa, S. Ligand-Based Solid Solution Approach to Stabilisation of Sulphonic Acid Groups in Porous Coordination Polymer $\text{Zr}_6\text{O}_4(\text{OH})_4(\text{BDC})_6(\text{UiO}-66)$. *Dalton Trans.* **2012**, *41*, 13791–13794.
- (102) Akiyama, G.; Matsuda, R.; Sato, H.; Takata, M.; Kitagawa, S. Cellulose Hydrolysis by a New Porous Coordination Polymer Decorated with Sulfonic Acid Functional Groups. *Adv. Mater.* **2011**, *23*, 3294–3297.
- (103) Juan-Alcañiz, J.; Gielisse, R.; Lago, A. B.; Ramos-Fernandez, E. V.; Serra-Crespo, P.; Devic, T.; Guillou, N.; Serre, C.; Kapteijn, F.; Gascon, J. Towards Acid MOFs—Catalytic Performance of Sulfonic Acid Functionalized Architectures. *Catal. Sci. Technol.* **2013**, *3*, 2311–2318.
- (104) Zhou, Y.-X.; Chen, Y.-Z.; Hu, Y.; Huang, G.; Yu, S.-H.; Jiang, H.-L. MIL-101- SO_3H : A Highly Efficient Brønsted Acid Catalyst for Heterogeneous Alcoholysis of Epoxide under Ambient Conditions. *Chem.—Eur. J.* **2014**, *20*, 14976–14980.
- (105) Olchowka, J.; Volklinger, C.; Henry, N.; Loiseau, T. Synthesis, Structural Characterization, and Dehydration Analysis of Uranyl Zinc Mellitate, $(\text{UO}_2)_2\text{Zn}(\text{H}_2\text{O})_4(\text{H}_2\text{mel}) \cdot 2\text{H}_2\text{O}$. *Eur. J. Inorg. Chem.* **2013**, 2109–2114.
- (106) Li, X.; Wang, Y.; Ma, Z.; Zhang, R.; Zhao, J. Synthesis and Characterization of Two 3-D Polymeric Lanthanide Complexes Constructed from 1,2,4,5-Benzenetetracarboxylic Acid. *J. Coord. Chem.* **2010**, *63*, 1029–1037.
- (107) Sanselme, M.; Grenèche, J.-M.; Riou-Cavellec, M.; Férey, G. The First Ferric Carboxylate with a Three-Dimensional Hydrid Open-Framework (MIL-82): Its Synthesis, Structure, Magnetic Behavior and Study of Its Dehydration by Mössbauer Spectroscopy. *Solid State Sci.* **2004**, *6*, 853–858.
- (108) Zhang, L.-P.; Ma, J.-F.; Yang, J.; Pang, Y.-Y.; Ma, J.-C. Series of 2D and 3D Coordination Polymers Based on 1,2,3,4-Benzenetetracarboxylate and N-Donor Ligands: Synthesis, Topological Structures, and Photoluminescent Properties. *Inorg. Chem.* **2010**, *49*, 1535–1550.
- (109) Yan, S.-X.; Zhao, D.; Li, T.; Wang, R.; Meng, X.-R. Syntheses, Structures, and Properties of Four Cu(II) Complexes Containing 2-(1H-Imidazol-1-methyl)-1H-benzimidazole Ligand. *J. Coord. Chem.* **2012**, *65*, 945–957.
- (110) Cao, R.; Sun, D.; Liang, Y.; Hong, M.; Tatsumi, K.; Shi, Q. Syntheses and Characterization of Three-Dimensional Channel-like Polymeric Lanthanide Complexes Constructed by 1,2,4,5-Benzenetetracarboxylic Acid. *Inorg. Chem.* **2002**, *41*, 2087–2094.
- (111) Volklinger, C.; Loiseau, T.; Guillou, N.; Férey, G.; Haouas, M.; Taulelle, F.; Elkaim, E.; Stock, N. High-Throughput Aided Synthesis of the Porous Metal–Organic Framework-Type Aluminum Pyromellitate, MIL-121, with Extra Carboxylic Acid Functionalization. *Inorg. Chem.* **2010**, *49*, 9852–9862.
- (112) Wang, J.; Lin, Z.; Ou, Y.-C.; Yang, N.-L.; Zhang, Y.-H.; Tong, M.-L. Hydrothermal Synthesis, Structures, and Photoluminescent Properties of Benzenepentacarboxylate Bridged Networks Incorporating Zinc(II)–Hydroxide Clusters or Zinc(II)–Carboxylate Layers. *Inorg. Chem.* **2008**, *47*, 190–199.
- (113) Lalonde, M. B.; Getman, R. B.; Lee, J. Y.; Roberts, J. M.; Sarjeant, A. A.; Scheidt, K. A.; Georgiev, P. A.; Embs, J. P.; Eckert, J.; Farha, O. K.; et al. A Zwitterionic Metal–Organic Framework with Free Carboxylic Acid Sites that Exhibits Enhanced Hydrogen Adsorption Energies. *CrystEngComm* **2013**, *15*, 9408–9414.

- (114) Gagnon, K. J.; Perry, H. P.; Clearfield, A. Conventional and Unconventional Metal–Organic Frameworks Based on Phosphonate Ligands: MOFs and UMOFs. *Chem. Rev.* **2012**, *112*, 1034–1054.
- (115) Shimizu, G. K. H.; Vaidyanathan, R.; Taylor, J. M. Phosphonate and Sulfonate Metal Organic Frameworks. *Chem. Soc. Rev.* **2009**, *38*, 1430–1449.
- (116) Ingleson, M. J.; Barrio, J. P.; Bacsa, J.; Dickinson, C.; Park, H.; Rosseinsky, M. J. Generation of a Brønsted Acid Site in a Chiral Framework. *Chem. Commun.* **2008**, 1287–1289.
- (117) Vermoortele, F.; Ameloot, R.; Alaerts, L.; Matthesen, R.; Carlier, B.; Ramos Fernandez, E. V.; Gascon, J.; Kapteijn, F.; De Vos, D. E. Tuning the Catalytic Performance of Metal–Organic Frameworks in Fine Chemistry by Active Site Engineering. *J. Mater. Chem.* **2012**, *22*, 10313–10321.
- (118) Britt, D.; Lee, C.; Uribe-Romo, F.; Furukawa, H.; Yaghi, O. M. Ring-Opening Reactions within Porous Metal–Organic Frameworks. *Inorg. Chem.* **2010**, *49*, 6387–6389.
- (119) Gadzikwa, T.; Farha, O. K.; Mulfort, K. L.; Hupp, J. T.; Nguyen, S. T. A Zn-Based, Pillared Paddlewheel MOF Containing Free Carboxylic Acids via Covalent Post-Synthesis Elaboration. *Chem. Commun.* **2009**, 3720–3722.
- (120) Tanabe, K. K.; Cohen, S. M. Engineering a Metal–Organic Framework Catalyst by Using Postsynthetic Modification. *Angew. Chem., Int. Ed.* **2009**, *48*, 7424–7427.
- (121) Kucera, F.; Jancar, J. Homogeneous and Heterogeneous Sulfonation of Polymers: A Review. *Polym. Eng. Sci.* **1998**, *38*, 783–792.
- (122) Burrows, A. D.; Frost, C. G.; Mahon, M. F.; Richardson, C. Sulfur-Tagged Metal–Organic Frameworks and Their Post-Synthetic Oxidation. *Chem. Commun.* **2009**, 4218–4220.
- (123) Phang, W. J.; Jo, H.; Lee, W. R.; Song, J. H.; Yoo, K.; Kim, B.; Hong, C. S. Superprotonic Conductivity of a UiO-66 Framework Functionalized with Sulfonic Acid Groups by Facile Postsynthetic Oxidation. *Angew. Chem., Int. Ed.* **2015**, *54*, 5142–5146.
- (124) Goesten, M. G.; Juan-Alcañiz, J.; Ramos-Fernandez, E. V.; Gupta, K. B. S. S.; Stavitski, E.; van Bekkum, H.; Gascon, J.; Kapteijn, F. Sulfation of Metal–Organic Frameworks: Opportunities for Acid Catalysis and Proton Conductivity. *J. Catal.* **2011**, *281*, 177–187.
- (125) Brozek, C. K.; Dincă, M. Cation Exchange at the Secondary Building Units of Metal–Organic Frameworks. *Chem. Soc. Rev.* **2014**, *43*, 5456–5467.
- (126) Han, Y.; Li, J.-R.; Xie, Y.; Guo, G. Substitution Reactions in Metal–Organic Frameworks and Metal–Organic Polyhedra. *Chem. Soc. Rev.* **2014**, *43*, 5952–5981.
- (127) Wilmer, C. E.; Farha, O. K.; Yildirim, T.; Eryazici, I.; Krungleviciute, V.; Sarjeant, A. A.; Snurr, R. Q.; Hupp, J. T. Gram-Scale, High-Yield Synthesis of a Robust Metal–Organic Framework for Storing Methane and Other Gases. *Energy Environ. Sci.* **2013**, *6*, 1158–1163.
- (128) Karagiari, O.; Vermeulen, N. A.; Klet, R. C.; Wang, T. C.; Moghadam, P. Z.; Al-Juaid, S. S.; Stoddart, J. F.; Hupp, J. T.; Farha, O. K. Functionalized Defects through Solvent-Assisted Linker Exchange: Synthesis, Characterization, and Partial Postsynthesis Elaboration of a Metal–Organic Framework Containing Free Carboxylic Acid Moieties. *Inorg. Chem.* **2015**, *54*, 1785–1790.
- (129) Barin, G.; Krungleviciute, V.; Gutov, O.; Hupp, J. T.; Yildirim, T.; Farha, O. K. Defect Creation by Linker Fragmentation in Metal–Organic Frameworks and Its Effects on Gas Uptake Properties. *Inorg. Chem.* **2014**, *53*, 6914–6919.
- (130) Walling, C. The Acid Strength of Surfaces. *J. Am. Chem. Soc.* **1950**, *72*, 1164–1168.
- (131) Benesi, H. A. Acidity of Catalyst Surfaces. I. Acid Strength from Colors of Adsorbed Indicators. *J. Am. Chem. Soc.* **1956**, *78*, 5490–5494.
- (132) Klodnig, W. F. Use of Hammett Indicators for Acidity Measurements in Zeolites. *J. Phys. Chem.* **1979**, *83*, 765–766.
- (133) Chen, F. R.; Coudurier, G.; Joly, J. F.; Védrine, J. C. Superacid and Catalytic Properties of Sulfated Zirconia. *J. Catal.* **1993**, *143*, 616–626.
- (134) Zang, Y.; Shi, J.; Zhang, F.; Zhong, Y.; Zhu, W. Sulfonic Acid-Functionalized MIL-101 as a Highly Recyclable Catalyst for Esterification. *Catal. Sci. Technol.* **2013**, *3*, 2044–2049.
- (135) Chen, S.-Y.; Yokoi, T.; Tang, C.-Y.; Jang, L.-Y.; Tatsumi, T.; Chan, J. C. C.; Cheng, S. Sulfonic Acid-Functionalized Platelet SBA-15 Materials as Efficient Catalysts for Biodiesel Synthesis. *Green Chem.* **2011**, *13*, 2920–2930.
- (136) Deeba, M.; Hall, W. K. The Measurement of Catalyst Acidity. I. Titration Measurements. *J. Catal.* **1979**, *60*, 417–429.
- (137) (a) Fameth, W. E.; Gorte, R. J. Methods for Characterizing Zeolite Acidity. *Chem. Rev.* **1995**, *95*, 615–635.
- (138) Gao, Z.; Chen, J.; Hua, W.; Tang, Y. Characterization of Solid Superacidity by *n*-Alkane Isomerization Reactions at Low Temperature. *Stud. Surf. Sci. Catal.* **1994**, *90*, 507–518.
- (139) Derouane, E. G.; Védrine, J. C.; Ramos Pinto, R.; Borges, P. M.; Costa, L.; Lemos, M. A. N. D. A.; Lemos, F.; Ramôa Ribeiro, F. The Acidity of Zeolites: Concepts, Measurements and Relation to Catalysis: A Review on Experimental and Theoretical Methods for the Study of Zeolite Acidity. *Catal. Rev. Sci. Eng.* **2013**, *55*, 454–515.
- (140) Kunkeler, P.; van der Waal, J.; Bremmer, J.; Zuurdeeg, B.; Downing, R.; van Bekkum, H. Application of Zeolite Titanium Beta in the Rearrangement of α -Pinene Oxide to Campholenic Aldehyde. *Catal. Lett.* **1998**, *53*, 135–138.
- (141) Corma, A.; García, H. Lewis Acids: From Conventional Homogeneous to Green Homogeneous and Heterogeneous Catalysis. *Chem. Rev.* **2003**, *103*, 4307–4365.
- (142) Vermoortele, F.; Vandichel, M.; Van de Voorde, B.; Ameloot, R.; Waroquier, M.; Van Speybroeck, V.; De Vos, D. E. Electronic Effects of Linker Substitution on Lewis Acid Catalysis with Metal–Organic Frameworks. *Angew. Chem., Int. Ed.* **2012**, *51*, 4887–4890.
- (143) Vermoortele, F.; Bueken, B.; Le Bars, G.; Van de Voorde, B.; Vandichel, M.; Houthoofd, K.; Vimont, A.; Daturi, M.; Waroquier, M.; Van Speybroeck, V.; et al. Synthesis Modulation as a Tool To Increase the Catalytic Activity of Metal–Organic Framework: The Unique Case of UiO-66(Zr). *J. Am. Chem. Soc.* **2013**, *135*, 11465–11468.
- (144) Ameloot, R.; Vermoortele, F.; Hofkens, J.; Schryver, F. C. D.; De Vos, D. E.; Roeffraers, M. B. J. Three-Dimensional Visualization of Defects Formed during the Synthesis of Metal–Organic Frameworks: A Fluorescence Microscopy Study. *Angew. Chem., Int. Ed.* **2013**, *52*, 401–405.
- (145) Comelli, N. A.; Ponzi, E. N.; Ponzi, M. I. α -Pinene Isomerization to Camphene: Effect of Thermal Treatment on Sulfated Zirconia. *Chem. Eng. J.* **2006**, *117*, 93–99.
- (146) Ecomier, M. A.; Wilson, K.; Lee, A. F. Structure–Reactivity Correlations in Sulphated-Zirconia Catalysts for the Isomerization of α -Pinene. *J. Catal.* **2003**, *215*, 57–65.
- (147) van der Waal, J. C.; van Bekkum, H.; Vital, J. M. The Hydration and Isomerization of α -Pinene over Zeolite Beta. A New Coupling Reaction Between α -Pinene and Ketones. *J. Mol. Catal. A* **1996**, *105*, 185–192.
- (148) Rachwalik, R.; Olejniczak, Z.; Jiao, J.; Huang, J.; Hunger, M.; Sulikowski, B. Isomerization of α -Pinene over Dealuminated Ferrierite-Type Zeolites. *J. Catal.* **2007**, *252*, 161–170.
- (149) Auroux, A. Acidity and Basicity: Determination by Adsorption Microcalorimetry. *Mol. Sieves* **2008**, *6*, 45–152.
- (150) Mekki-Rarrada, A.; Auroux, A. *Thermal Methods, in Characterization of Solid Materials and Heterogeneous Catalysis, from Structure to Surface Reactivity*; Che, M., Védrine, J. C., Eds., Wiley-VCH, Weinheim, Germany, 2012; p 747.
- (151) Rodríguez-González, L.; Hermes, F.; Bertmer, M.; Rodríguez-Castellón, E.; Jiménez-López, A.; Simon, U. The Acid Properties of H-ZSM-5 as Studied by NH_3 -TPD and ^{27}Al -MAS-NMR Spectroscopy. *Appl. Catal., A* **2007**, *328*, 174–182.
- (152) Niwa, M.; Katada, N. New Method for the Temperature-Programmed Desorption (TPD) of Ammonia Experiment for Characterization of Zeolite Acidity: A Review. *Chem. Rec.* **2013**, *13*, 432–455.

- (153) Saha, D.; Deng, S. Ammonia Adsorption and Its Effects on Framework Stability of MOF-5 and MOF-177. *J. Colloid Interface Sci.* **2010**, *348*, 615–620.
- (154) Petit, C.; Bandoz, T. J. Enhanced Adsorption of Ammonia on Metal–Organic Framework/Graphite Oxide Composites: Analysis of Surface Interaction. *Adv. Funct. Mater.* **2010**, *20*, 111–118.
- (155) Guo, X.; Zhu, G.; Li, Z.; Sun, F.; Yang, Z.; Qiu, S. A Lanthanide Metal–Organic Framework with High Thermal Stability and Available Lewis-Acid Metal Sites. *Chem. Commun.* **2006**, 3172–3174.
- (156) Matsushashi, H.; Arata, K. Temperature Programmed Desorption of Argon for Evaluation of Surface Acidity of Solid Superacids. *Chem. Commun.* **2000**, 387–388.
- (157) Kubelková, L.; Nováková, J. Temperature –Programmed Desorption and Conversion of Acetone and Diethyl Ketone Preadsorbed on HZSM-5. *Zeolites* **1991**, *11*, 822–826.
- (158) Lercher, J. A.; Gründling, C.; Eder-Mirth, G. Infrared Studies of the Surface Acidity of Oxides and Zeolites Using Adsorbed Probe Molecules. *Catal. Today* **1996**, *27*, 353–376.
- (159) Lok, B. M.; Marcus, B. K.; Angell, C. L. Characterization of Zeolite Acidity. II. Measurement of Zeolite Acidity by Ammonia Temperature Programmed Desorption and FTIR. Spectroscopy Techniques. *Zeolites* **1986**, *6*, 185–194.
- (160) Wakabayashi, F.; Kondo, J. N.; Domen, K.; Hirose, C. FT-IR Studies of the Interaction between Zeolitic Hydroxyl Groups and Small Molecules. 3. Adsorption of Oxygen, Argon, Nitrogen, and Xenon on H-ZSM-5 at Low Temperatures. *J. Phys. Chem.* **1996**, *100*, 4154–4159.
- (161) Nakamoto, K. *Infrared and Raman Spectra of Inorganic and Coordination Compounds: Part B: Applications in Coordination, Organometallic, and Bioinorganic Chemistry*, 6th ed.; John Wiley & Sons, Inc.: New York, 2009; Chapter 1, p 132.
- (162) Hadjiivanov, K. I.; Vayssilov, G. N. Characterization of Oxide Surfaces and Zeolites by Carbon Monoxide as an IR Probe Molecule. *Adv. Catal.* **2002**, *47*, 307–511.
- (163) Braga, D.; Grepioni, F. Hydrogen-Bonding Interactions with the CO Ligand in the Solid State. *Acc. Chem. Res.* **1997**, *30*, 81–87.
- (164) Zecchina, A.; Bordiga, S.; Spoto, G.; Marchese, L.; Petrin, G.; Leofanti, G.; Padovan, M. Silicalite Characterization. 2. IR Spectroscopy of the Interaction of Carbon Monoxide with Internal and External Hydroxyl Groups. *J. Phys. Chem.* **1992**, *96*, 4991–4997.
- (165) Lavalley, J.-C.; Jolly-Feaugas, S.; Janin, A.; Saussey, J. In Situ Fourier Transform Infrared Studies of Active Sites and Reaction Mechanisms in Heterogeneous Catalysis: Hydrocarbon Conversion on H-Zeolites. *Mikrochim. Acta Suppl.* **1997**, *14*, 51–56.
- (166) Cairon, O.; Thomas, K.; Chambellan, A.; Chevreau, T. Acid-Catalyzed Benzene Hydroconversion Using Various Zeolites: Brønsted Acidity, Hydrogenation and Side-Reactions. *Appl. Catal., A* **2003**, *238*, 167–183.
- (167) Oliviero, L.; Vimont, A.; Lavalley, J.-C.; Romero, S.; Sarría, F.; Gaillard, M.; Mauge, F. 2,6-Dimethylpyridine as a Probe of the Strength of Brønsted Acid Sites: Study on Zeolites. Application to Alumina. *Phys. Chem. Chem. Phys.* **2005**, *7*, 1861–1869.
- (168) Cairon, O.; Thomas, K.; Chevreau, T. FTIR Studies of Unusual OH Groups in Steamed HNaY Zeolites: Preparation and Acid Properties. *Microporous Mesoporous Mater.* **2001**, *46*, 327.
- (169) Pelmenschikov, A. G.; van Santen, R. A.; Jänchen, J.; Meijer, E. CD₃CN as a Probe of Lewis and Brønsted Acidity of Zeolites. *J. Phys. Chem.* **1993**, *97*, 11071–11074.
- (170) Adeeva, V.; de Haan, J. W.; Jänchen, J.; Lei, G. D.; Schünemann, V.; van de Ven, L. J. M.; Sachtler, W. M. H.; van Santen, R. A. Acid Sites in Sulfated and Metal-Promoted Zirconium Dioxide Catalysts. *J. Catal.* **1995**, *151*, 364–372.
- (171) Nakamoto, K. *Infrared and Raman Spectra of Inorganic and Coordination Compounds: Part B: Applications in Coordination, Organometallic, and Bioinorganic Chemistry*, 6th ed.; John Wiley & Sons, Inc.: New York, 2009; Chapter 1, p 84.
- (172) Nakamoto, K. *Infrared and Raman Spectra of Inorganic and Coordination Compounds: Part B: Applications in Coordination, Organometallic, and Bioinorganic Chemistry*, 6th ed.; John Wiley & Sons, Inc.: New York, 2009; Chapter 1, p 62.
- (173) Fournler, M.; Thouvenot, R.; Rocchiccioli-Deltcheff, C. Catalysis by Polyoxometalates. *J. Chem. Soc. Faraday Trans.* **1991**, *87*, 349–356.
- (174) Klinowski, J. In *Solid State NMR Spectroscopy*; Blackwell Science Ltd.: Oxford, UK, 2002; p 437.
- (175) Li, H.; Eddaoudi, M.; O’Keeffe, M.; Yaghi, O. M. Design and Synthesis of an Exceptionally Stable and Highly Porous Metal–Organic Framework. *Nature* **1999**, *402*, 276–279.
- (176) Yang, L.; Naruke, H.; Yamase, T. A Novel Organic/Inorganic Hybrid Nanoporous Material Incorporating Keggin-Type Polyoxometalates. *Inorg. Chem. Commun.* **2003**, *6*, 1020–1024.
- (177) Horcajada, P.; Serre, C.; Vallet-Regí, M.; Sebban, M.; Taulelle, F.; Férey, G. Metal–Organic Frameworks as Efficient Materials for Drug Delivery. *Angew. Chem.* **2006**, *118*, 6120–6124.
- (178) Volkringer, C.; Meddouri, M.; Loiseau, T.; Guillou, N.; Marrot, J.; Férey, G.; Haouas, M.; Taulelle, F.; Audebrand, N.; Latroche, M. The Kagomé Topology of the Gallium and Indium Metal–Organic Framework Types with a MIL-68 Structure: Synthesis, XRD, Solid-State NMR Characterizations, and Hydrogen Adsorption. *Inorg. Chem.* **2008**, *47*, 11892–11901.
- (179) Habib, H. A.; Hoffmann, A.; Huppe, H. A.; Steinfeld, G.; Janiak, C. Crystal Structure Solid-State Cross Polarization Magic Angle Spinning ¹³C NMR Correlation in Luminescent d¹⁰ Metal–Organic Frameworks Constructed with the 1,2-Bis(1,2,4-triazol-4-yl)ethane Ligand. *Inorg. Chem.* **2009**, *48*, 2166–2180.
- (180) Stallmach, F.; Gröger, S.; Künzel, V.; Kärger, J.; Yaghi, O. M.; Hesse, M.; Müller, U. NMR Studies on the Diffusion of Hydrocarbons on the Metal–Organic Framework Material MOF-5. *Angew. Chem., Int. Ed.* **2006**, *45*, 2123–2126.
- (181) Chen, J. J.; Kong, X.; Sumida, K.; Manupillai, M. A.; Long, J. R.; Reimer, J. A. Ex Situ NMR Relaxometry of Metal–Organic Frameworks for Rapid Surface-Area Screening. *Angew. Chem., Int. Ed.* **2013**, *52*, 12043–12046.
- (182) Kong, X.; Deng, H.; Yan, F.; Kim, J.; Swisher, J. A.; Smit, B.; Yaghi, O. M.; Reimer, J. A. Mapping of Functional Groups in Metal–Organic Frameworks. *Science* **2013**, *341*, 882–885.
- (183) Kong, X.; Scott, E.; Ding, W.; Mason, J. A.; Long, J. R.; Reimer, J. A. CO₂ Dynamics in a Metal–Organic Framework with Open Metal Sites. *J. Am. Chem. Soc.* **2012**, *134*, 14341–14344.
- (184) Lin, L.-C.; Kim, J.; Kong, X.; Scott, E.; McDonald, T. M.; Long, J. R.; Reimer, J. A.; Smit, B. Understanding CO₂ Dynamics in Metal–Organic Frameworks with Open Metal Sites. *Angew. Chem., Int. Ed.* **2013**, *52*, 4410–4413.
- (185) Lieder, C.; Opelt, S.; Dyballa, M.; Henning, H.; Klemm, E.; Hunger, M. Adsorbate Effect on AlO₄(OH)₂ Centers in the Metal–Organic Framework MIL-53 Investigated by Solid-State NMR Spectroscopy. *J. Phys. Chem. C* **2010**, *114*, 16596–16602.
- (186) Jänchen, J.; van Wolput, J. H. M. C.; van de Ven, L. J. M.; de Haan, J. W.; van Santen, R. A. FTIR spectroscopic and 1H MAS NMR Studies of the Influence of Lattice Chemistry and Structure on Brønsted Acidity in Zeolites. *Catal. Lett.* **1996**, *39*, 147–152.
- (187) Huang, J.; Jiang, Y.; Reddy Marthala, V. R.; Wang, W.; Sulikowski, B.; Hunger, M. In Situ 1H MAS NMR Investigation of the H/D Exchange of Alkylaromatic Hydrocarbons on Zeolites H-Y, La, Na-Y, and H-ZSM-5. *Microporous Mesoporous Mater.* **2007**, *99*, 86–90.
- (188) Hunger, M. Brønsted Acid Sites in Zeolites Characterized by Multinuclear Solid-State NMR Spectroscopy. *Catal. Rev. Sci. Eng.* **1997**, *39*, 345–393.
- (189) Zheng, A.; Huang, S.-J.; Liu, S.-B.; Deng, F. Acid Properties of Solid Acid Catalysts Characterized by Solid-State ³¹P NMR of Adsorbed Phosphorous Probe Molecules. *Phys. Chem. Chem. Phys.* **2011**, *13*, 14889–14901.
- (190) Ferm, M.; Hellsten, S. Trends in Atmospheric Ammonia and Particulate Ammonium Concentrations in Sweden and Its Cause. *Atmos. Environ.* **2012**, *61*, 30–39.
- (191) Sutton, M. A.; Erisman, J. W.; Dentener, F.; Möller, D. Ammonia in the Environment: From Ancient Times to the Present. *Environ. Pollut.* **2008**, *156*, 583–604.

- (192) Liu, X.; Zhang, Y.; Han, W.; Tang, A.; Shen, J.; Cui, Z.; Vitousek, P.; Erisman, J. W.; Goulding, K.; Christie, P.; Fangmeier, A.; Zhang, F. Enhanced Nitrogen Deposition over China. *Nature* **2013**, *494*, 459–462.
- (193) *Permissible Exposure Limits for Chemical Contaminants*; Cal/OSHA: Oakland, CA; http://www.dir.ca.gov/title8/5155stable_ac1.html (accessed on April 12, 2015).
- (194) Britt, D.; Tranchemontagne, D.; Yaghi, O. M. Metal–Organic Frameworks with High Capacity and Selectivity for Harmful Gases. *Proc. Natl. Acad. Sci. U. S. A.* **2008**, *105*, 11623–11627.
- (195) Glover, T. G.; Peterson, G. W.; Schindler, B. J.; Britt, D.; Yaghi, O. M. MOF-74 Building Unit Has a Direct Impact on Toxic Gas Adsorption. *Chem. Eng. Sci.* **2011**, *66*, 163–170.
- (196) Petit, C.; Huang, L.; Jagiello, J.; Kevin, J.; Gubbins, K. E.; Bandoz, T. J. Toward Understanding Reactive Adsorption of Ammonia on Cu-MOF/Graphite Oxide Nanocomposites. *Langmuir* **2011**, *27*, 13043–13051.
- (197) Petit, C.; Bandoz, T. J. Synthesis, Characterization, and Ammonia Adsorption Properties of Mesoporous Metal–Organic Framework (MIL(Fe))–Graphite Oxide Composites: Exploring the Limits of Material Fabrication. *Adv. Funct. Mater.* **2011**, *21*, 2108–2117.
- (198) Spanopoulos, I.; Xydia, P.; Malliakas, C. D.; Trikalitis, P. N. A Straight Forward Route for the Development of Metal–Organic Frameworks Functionalized with Aromatic –OH Groups: Synthesis, Characterization, and Gas (N₂, Ar, H₂, CO₂, CH₄, NH₃) Sorption Properties. *Inorg. Chem.* **2013**, *52*, 855–862.
- (199) Yu, D.; Ghosh, P.; Snurr, R. Q. Hierarchical Modeling of Ammonia Adsorption in Functionalized Metal–Organic Frameworks. *Dalton Trans.* **2012**, *41*, 3962–3973.
- (200) Jasuja, H.; Peterson, G. W.; Decoste, J. B.; Browe, M. A.; Walton, K. S. Evaluation of MOFs for Air Purification and Air Quality Control Applications: Ammonia Removal from Air. *Chem. Eng. Sci.* **2015**, *124*, 118–124.
- (201) Kim, K. C.; Yu, D.; Snurr, R. Q. Computational Screening of Functional Groups for Ammonia Capture in Metal–Organic Frameworks. *Langmuir* **2013**, *29*, 1446–1456.
- (202) Kreuer, K. D.; Weppner, W.; Rabenau, A. Vehicle Mechanism, a New Model for the Interpretation of Conductivity of Fast Proton Conductors. *Angew. Chem., Int. Ed. Engl.* **1982**, *21*, 208–209.
- (203) van Grothuss, C. J. D. Sur la décomposition de l'eau et des corps qu'elle tient en dissolution à l'aide de l'électricité galvanique. *Ann. Chim.* **1806**, *58*, 54–73.
- (204) Ueki, T.; Watanabe, M. Macromolecules in Ionic Liquids: Progress, Challenges, and Opportunities. *Macromolecules* **2008**, *41*, 3739–3749.
- (205) Mauritz, K. A.; Moore, R. B. State of Understanding of Nafion. *Chem. Rev.* **2004**, *104*, 4535–4585.
- (206) Kreuer, K.-D. Proton Conductivity: Materials and Applications. *Chem. Mater.* **1996**, *8*, 610–641.
- (207) Shimizu, G. K. H.; Taylor, J. M.; Kim, S. Proton Conduction with Metal–Organic Frameworks. *Science* **2013**, *341*, 354–355.
- (208) Ramaswamy, P.; Wong, N. E.; Shimizu, G. K. H. MOFs as Proton Conductors—Challenges and Opportunities. *Chem. Soc. Rev.* **2014**, *43*, 5913–5932.
- (209) Sadakiyo, M.; Yamada, T.; Kitagawa, H. Rational Designs for Highly Proton-Conductive Metal–Organic Frameworks. *J. Am. Chem. Soc.* **2009**, *131*, 9906–9907.
- (210) Sadakiyo, M.; Yamada, T.; Honda, K.; Matsui, H.; Kitagawa, H. Control of Crystalline Proton-Conducting Pathways by Water-Induced Transformations of Hydrogen-Bonding Networks in a Metal–Organic Framework. *J. Am. Chem. Soc.* **2014**, *136*, 7701–7707.
- (211) Sadakiyo, M.; Yamada, T.; Kitagawa, H. Proton Conductivity Control by Ion Substitution in a Highly Proton-Conductive Metal–Organic Framework. *J. Am. Chem. Soc.* **2014**, *136*, 13166–13169.
- (212) Phang, W. J.; Lee, W. R.; Yoo, K.; Ryu, D. W.; Kim, B.; Hong, C. S. pH-Dependent Proton Conducting Behavior in a Metal–Organic Framework Material. *Angew. Chem.* **2014**, *126*, 8523–8527.
- (213) Dybtsev, D. N.; Ponomareva, V. G.; Aliev, S. B.; Chupakhin, A. P.; Gallyamov, M. R.; Moroz, N. K.; Kolesov, B. A.; Kovalenko, K. A.; Shutova, E. S.; Fedin, V. P. High Proton Conductivity and Spectroscopic Investigation of Metal–Organic Framework Materials Impregnated by Strong Acids. *ACS Appl. Mater. Interfaces* **2014**, *6*, 5161–5167.
- (214) Dupuis, A.-C. Proton Exchange Membranes for Fuel Cells Operated at Medium Temperatures: Materials and Experimental Techniques. *Prog. Mater. Sci.* **2011**, *56*, 289–327.
- (215) Shigematsu, A.; Yamada, T.; Kitagawa, H. Wide Control of Proton Conductivity in Porous Coordination Polymers. *J. Am. Chem. Soc.* **2011**, *133*, 2034–2036.
- (216) Yamada, T.; Shirai, Y.; Kitagawa, H. Synthesis, Water Adsorption, and Proton Conductivity of Solid-Solution-Type Metal–Organic Frameworks Al(OH)(bdc-OH)_x(bdc-NH₂)_{1-x}. *Chem.—Asian J.* **2014**, *9*, 1316–1320.
- (217) Li, Z.; He, G.; Zhao, Y.; Cao, Y.; Wu, H.; Li, Y.; Jiang, Z. Enhanced Proton Conductivity of Proton Exchange Membranes by Incorporating Sulfonated Metal–Organic Frameworks. *J. Power Sources* **2014**, *262*, 372–379.
- (218) Hurd, J. A.; Vaidhyanathan, R.; Thangadurai, V.; Ratcliffe, C. I.; Moudrakovski, I. L.; Shimizu, G. K. H. Anhydrous Proton Conduction at 150 °C in a Crystalline Metal–Organic Framework. *Nat. Chem.* **2009**, *1*, 705–710.
- (219) Taylor, J. M.; Mah, R. K.; Moudrakovski, I. L.; Ratcliffe, C. I.; Vaidhyanathan, R.; Shimizu, G. K. H. Facile Proton Conduction via Ordered Water Molecules in a Phosphonate Metal–Organic Framework. *J. Am. Chem. Soc.* **2010**, *132*, 14055–14057.
- (220) Colodrero, R. M. P.; Olivera-Pastor, P.; Losilla, E. R.; Hernández-Alonso, D.; Aranda, M. A. G.; León-Reina, L.; Rius, J.; Demadis, K. D.; Moreau, B.; Villemin, D.; et al. High Proton Conductivity in a Flexible, Cross-Linked, Ultramicroporous Magnesium Tetrakisphosphate Hybrid Framework. *Inorg. Chem.* **2012**, *51*, 7689–7698.
- (221) Taylor, J. M.; Dawson, K. W.; Shimizu, G. K. H. A Water-Stable Metal–Organic Framework with Highly Acidic Pores for Proton-Conducting Applications. *J. Am. Chem. Soc.* **2013**, *135*, 1193–1196.
- (222) Kim, S.; Dawson, K. W.; Gelfand, B. S.; Taylor, J. M.; Shimizu, G. K. H. Enhancing Proton Conduction in a Metal–Organic Framework by Isomorphous Ligand Replacement. *J. Am. Chem. Soc.* **2013**, *135*, 963–966.
- (223) Colodrero, R. M. P.; Papathanasiou, K. E.; Stavgiannoudaki, N.; Olivera-Pastor, P.; Losilla, E. R.; Aranda, M. A. G.; León-Reina, L.; Sanz, J.; Sobrados, I.; Choquesillo-Lazarte, D.; et al. Multifunctional Luminescent and Proton-Conducting Lanthanide Carboxyphosphonate Open-Framework Hybrids Exhibiting Crystalline-to-Amorphous-to-Crystalline Transformations. *Chem. Mater.* **2012**, *24*, 3780–3792.
- (224) Costantino, F.; Donnadio, A.; Casciola, M. Survey on the Phase Transitions and Their Effect on the Ion-Exchange and on the Proton-Conduction Properties of a Flexible and Robust Zr Phosphonate Coordination Polymer. *Inorg. Chem.* **2012**, *51*, 6992–7000.
- (225) Baranov, A. I.; Shuvalov, L. A.; Shchagina, N. M. Superior Conductivity and Phase Transitions in CsHSO₄ and CsHSeO₄ Crystals. *JETP Lett.* **1982**, *36*, 459–462.
- (226) Li, Z.; He, G.; Zhang, B.; Cao, Y.; Wu, H.; Jiang, Z.; Zhou, T. Enhanced Proton Conductivity of Nafion Hybrid Membrane under Different Humidities by Incorporating Metal–Organic Frameworks with High Phytic Acid Loading. *ACS Appl. Mater. Interfaces* **2014**, *6*, 9799–9807.
- (227) Wee, L. H.; Bonino, F.; Lamberti, C.; Bordiga, S.; Martens, J. A. Cr-MIL-101 Encapsulated Keggin Phosphotungstic Acid as Active Nanomaterial for Catalysing the Alcoholysis of Styrene Oxide. *Green Chem.* **2014**, *16*, 1351–1357.
- (228) Khder, A. E. R. S.; Hassan, H. M. A.; El-Shall, M. S. Metal–Organic Frameworks with High Tungstophosphoric Acid Loading as Heterogeneous Acid Catalysts. *Appl. Catal., A* **2014**, *487*, 110–118.
- (229) Bromberg, L.; Hatton, T. A. Aldehyde–Alcohol Reactions Catalyzed under Mild Conditions by Chromium(III) Terephthalate Metal Organic Framework (MIL-101) and Phosphotungstic Acid Composites. *ACS Appl. Mater. Interfaces* **2011**, *3*, 4756–4764.
- (230) Zhang, Y.; Degirmenci, V.; Li, C.; Hensen, E. J. M. Phosphotungstic Acid Encapsulated in Metal–Organic Framework as

Catalysts for Carbohydrate Dehydration to 5-Hydroxymethylfurfural. *ChemSusChem* **2011**, *4*, 59–64.

(231) Janssens, N.; Wee, L. H.; Bajpe, S.; Breyneart, E.; Kirschhock, C. E. A.; Martens, J. A. Recovery and Reuse of Heteropolyacid Catalyst in Liquid Reaction Medium through Reversible Encapsulation in $\text{Cu}_3(\text{BTC})_2$ Metal–Organic Framework. *Chem. Sci.* **2012**, *3*, 1847–1850.

(232) Liang, D.-D.; Liu, S.-X.; Ma, F.-J.; Wei, F.; Chen, Y.-G. A Crystalline Catalyst Based on a Porous Metal–Organic Framework and 12-Tungstosilicic Acid: Particle Size Control by Hydrothermal Synthesis for the Formation of Dimethyl Ether. *Adv. Synth. Catal.* **2011**, *353*, 733–742.

(233) Bromberg, L.; Su, X.; Hatton, T. A. Heteropolyacid-Functionalized Aluminum 2-Aminoterephthalate Metal–Organic Frameworks as Reactive Aldehyde Sorbents and Catalysts. *ACS Appl. Mater. Interfaces* **2013**, *5*, 5468–5477.

(234) Ramos-Fernandez, E. V.; Pieters, C.; van der Linden, B.; Juan-Alcañiz, J.; Serra-Crespo, P.; Verhoeven, M. W. G. M.; Niemantsverdriet, H.; Gascon, J.; Kapteijn, F. Highly Dispersed Platinum in Metal Organic Framework NH_2 -MIL-101(Al) Containing Phosphotungstic Acid—Characterization and Catalytic Performance. *J. Catal.* **2012**, *289*, 42–52.

(235) Chen, J.; Wang, S.; Huang, J.; Chen, L.; Ma, L.; Huang, X. Conversion of Cellulose and Cellobiose into Sorbitol Catalyzed by Ruthenium Supported on a Polyoxometalate/Metal–Organic Framework Hybrid. *ChemSusChem* **2013**, *6*, 1545–1555.

(236) Wang, S.; Chen, J.; Chen, L. Selective Conversion of Cellulose into Ethylene Glycol over Metal–Organic Framework-Derived Multifunctional Catalysts. *Catal. Lett.* **2014**, *144*, 1728–1734.

(237) Luo, Q.-X.; Ji, M.; Lu, M.-H.; Hao, C.; Qiu, J.-S.; Li, Y.-Q. Organic Electron-Rich *N*-Heterocyclic Compound as a Chemical Bridge: Building a Brønsted Acidic Ionic Liquid Confined in MIL-101 Nanocages. *J. Mater. Chem. A* **2013**, *1*, 6530–6534.

(238) Ravon, U.; Domine, M. E.; Gaudillere, C.; Desmartin-Chomel, A.; Farrusseng, D. MOFs as Acid Catalysts with Shape Selectivity Properties. *New J. Chem.* **2008**, *32*, 937–940.

(239) Nguyen, L. T. L.; Nguyen, C. V.; Dang, G. H.; Le, K. K. A.; Phan, N. T. S. Towards Applications of Metal–Organic Frameworks in Catalysis: Friedel–Crafts Acylation Reaction over IRMOF-8 as an Efficient Heterogeneous Catalyst. *J. Mol. Catal. A* **2011**, *349*, 28–35.

(240) Položij, M.; Rubeš, M.; Čejka, J.; Nachtigall, P. Catalysis by Dynamically Formed Defects in a Metal–Organic Framework Structure: Knoevenagel Reaction Catalyzed by Copper Benzene-1,3,5-tricarboxylate. *ChemCatChem* **2014**, *6*, 2821–2824.

(241) Lescouet, T.; Chizallet, C.; Farrusseng, D. The Origin of the Activity of Amine-Functionalized Metal–Organic Frameworks in the Catalytic Synthesis of Cyclic Carbonates from Epoxide and CO_2 . *ChemCatChem* **2012**, *4*, 1725–1728.

(242) Herbst, A.; Khutia, A.; Janiak, C. Brønsted Instead of Lewis Acidity in Functionalized MIL-101Cr MOFs for Efficient Heterogeneous (nano-MOF) Catalysis in the Condensation Reaction of Aldehyde with Alcohols. *Inorg. Chem.* **2014**, *53*, 7319–7333.

(243) Toyao, T.; Fujiwaki, M.; Horiuchi, Y.; Matsuoka, M. Applications of an Amino-Functionalised Metal–Organic Framework: An Approach to a One-Pot Acid-Base Reaction. *RSC Adv.* **2013**, *3*, 21582–21587.

(244) Hasan, Z.; Jun, J. W.; Jhung, S. H. Sulfonic Acid-Functionalized MIL-101(Cr): An Efficient Catalyst for Esterification of Oleic Acid and Vapor-Phase Dehydration of Butanol. *Chem. Eng. J.* DOI:10.1016/j.cej.2014.09.025.

(245) Chen, J.; Li, K.; Chen, L.; Liu, R.; Huang, X.; Ye, D. Conversion of Fructose into 5-Hydroxymethylfurfural Catalyzed by Recyclable Sulfonic Acid-Functionalized Metal–Organic Frameworks. *Green Chem.* **2014**, *16*, 2490–2499.

(246) Garibay, S. J.; Wang, Z.; Cohen, S. M. Evaluation of Heterogeneous Metal–Organic Framework Organocatalysts Prepared by Postsynthetic Modification. *Inorg. Chem.* **2010**, *49*, 8086–8091.

(247) McGuirk, C. M.; Katz, M. J.; Stern, C. L.; Sarjeant, A. A.; Hupp, J. T.; Farha, O. K.; Mirkin, C. A. Turning on Catalysis: Incorporation of a

Hydrogen-Bond-Donating Squaramide Moiety into a Zr Metal–Organic Framework. *J. Am. Chem. Soc.* **2015**, *137*, 919–925.

(248) Luan, Y.; Qi, Y.; Jin, Z.; Peng, X.; Gao, H.; Wang, G. Synthesis of a Flower-Like Zr-Based Metal–Organic Framework and Study of Its Catalytic Performance in the Mannich Reaction. *RSC Adv.* **2015**, *5*, 19273–19278.

(249) Luan, Y.; Zheng, N.; Qi, Y.; Yu, J.; Wang, G. Development of a SO_3H -Functionalized UiO-66 Metal–Organic Framework by Postsynthetic Modification and Studies of Its Catalytic Activities. *Eur. J. Inorg. Chem.* **2014**, 4268–4272.

(250) Li, B.; Leng, K.; Zhang, Y.; Dynes, J. J.; Wang, J.; Hu, Y.; Ma, D.; Shi, Z.; Zhu, L.; Zhang, D.; et al. Metal–Organic Framework Based upon the Synergy of a Brønsted Acid Framework and Lewis Acid Centers as a Highly Efficient Heterogeneous Catalyst for Fixed-Bed Reactions. *J. Am. Chem. Soc.* **2015**, *137*, 4243–4248.

(251) Evans, O. R.; Ngo, H. L.; Lin, W. Chiral Porous Solids Based on Lamellar Lanthanide Phosphonates. *J. Am. Chem. Soc.* **2001**, *123*, 10395–10396.

(252) Zheng, M.; Liu, Y.; Wang, C.; Liu, S.; Lin, W. Cavity-Induced Enantioselectivity Reversal in a Chiral Metal–Organic Framework Brønsted Acid Catalyst. *Chem. Sci.* **2012**, *3*, 2623–2627.